Combination of hydro-geophysical methods for delineation of characteristic structures in subsoil

Inauguraldissertation

zur
Erlangung der Würde eines Doktors der Philosophie
vorgelegt der
Philosophisch-Naturwissenschaftlichen Fakultät
der Universität Basel

von
Daniel Altdorff
aus Erlabrunn / Deutschland

Basel, 2012

Genehmigt von der Philosophisch-Naturwissenschaftlichen Fakultät

auf Antrag von

Prof. Dr. Peter Huggenberger
Angewandte und Umweltgeologie
Universtität Basel

Associate Prof. Dr. Anthony L. Endres
Department of Earth & Environmental Sciences
University of Waterloo / Canada

Basel, den 15.11 2011

Prof. Dr. Martin Spiess
Dekan

Acknowledgements

The present thesis resulted from my research work during the years 2008 to 2011 at the Helmholtz Centre for Environmental Research – UFZ / Germany and the Department of Environmental Sciences, University of Basel /Switzerland.
At first I wane thank both of my supervisors, Dr. Peter Dietrich head of the Department Monitoring and Exploration Technologies at UFZ and Prof. Dr. Peter Huggenberger, Professor and Head of the Department of Applied and Environmental Geology at the University of Basel for supporting my work during the whole PhD duration. Both Peters were always present to discuss special items, to advance and to encourage me. Both understands it ´to guide without pressure´.
Sincere thanks to Dr. Anthony L. Endres, Associate Professor at the Department of Earth & Environmental Sciences, University of Waterloo / Canada for his acceptance to be the co-referent of this thesis.
Special thanks are addressed to Dr. Steffen Popp-Hofmann, staff member of the Department Monitoring and Exploration Technologies for his support during the field works as well as for the close cooperation and fruitful discussions. Many thanks are addressed to Dr. Steffen Zacharias from the Department Monitoring and Exploration Technologies for his constructive help with statistical questions and the critical discussions towards the improvement of the results. Many thanks to the Simon Kögler from the UFZ Leipzig and to David Sauer from the University Potsdam for supporting the field work several times. I also like to thank the student assistants Marcus Jenderka from the University Leipzig / Germany for helping from time to time in several odds and ends.
I would also like to thank Dr. Jannis Epting from the Department of Environmental Sciences / University of Basel for the constructive cooperation during the years as well as for his advices in administrative issues.

Especially thanks to all members of the Department Monitoring and Exploration Technologies at the UFZ and the Department of Applied and Environmental Geology of the University Basel for the supporting, motivation and discussion throughout my PhD time.

I also acknowledge the Helmholtz research platform MOSAIC (model-driven site assessment, information & control) for providing the technical equipment.

TABLE OF CONTENTS

Part III - Detection of ancient active channel zones using hydrogeophysical methods: An approach to more effective channel restoration

64

Abstract

All terrestrial environmental processes involve the soil including hydrological, geological, meteorological, ecological and anthropological factors. The stress on natural soils increases significantly with agricultural and urban land use as a consequence of the world‘s growing population. This leads among others to deforestation and soil sealing and consequently to the decrease of natural habitats and resources. Thus, protection and preservation of soil and the maintaining and avoiding of negative affects from land-use change marks is a challenge for the policy, agricultural economics, and the geosciences.

A perspective for maintaining and avoiding extensive and destructive land use is given by the optimization of current land use. Therefore reliable information of soil and subsoil properties are needed. However, direct analysis of crucial soil properties, e. g. grain size or soil moisture is still time consuming and costly, and provides only single point information. But in particular soil data for medium and large-scale areas are needed for the assessment of soil development and future-oriented planning.

Proximal soil sensing techniques (PSS) offers an opportunity for obtaining data from medium and large–scale areas time and cost efficient. However, all PSS methods response only indirectly to the relevant soil properties and could be affected by several soil properties. Hence, a recent challenge is the improvement of PSS data evaluation and interpretation.

The presented PhD thesis addresses the improvement of data evaluation and interpretation of the PSS methods electromagnetic induction (EMI) and gamma spectrometry (GS) at three different test sites and three different problems. For each problem an individual adjusted approach was develop, applied and critical discussed.

In *Part I* the study consider the moisture distribution at a land slide affected hill slope in Austria by means of EMI. The presented study monitored the temporal, spatial and vertical behavior of soil-moisture distribution at a previously identified dynamic slope area over a period of nine month. By the assumption of relative temporal stability of soil properties, seasonal changes in measured electric conductivity (EC) should originate from soil moisture content. This study also faces the challenge of shifts in absolute EC values resulting from different calibration situation or different EMI devices and provides an opportunity for comparability of different EC data. By this approach an delineation of soil moisture pattern was successful derived. *Part I* also explores the visualization of temporal changes in three-dimensional subsurface data.

Part II focuses the problem of synthesis and simplification of multilayered input data of a floodplain in Central Germany towards a clear delineation of surface. This study tackle the problem by a K-means cluster algorithm in order to generate a 2dimensional map from the test site that includes the main characteristics from divergent input data. However do the generated cluster partitions really reflect the main characteristics of soil properties? Hence, this study also addressed on the reliability of such cluster maps by validation of independent soil properties such as grain-size, thickness of soil layers, and the color. The results show that not all partitions can be confirmed by independent soil samples; one of three clusters significantly differs from the others, the other two clusters could not confirmed by the considered parameters.

Part III investigates a floodplain of a low-mountain river in Switzerland in order to detect the ancient active stream channels (AAC). This part is subdivided into two approaches; first a 3D subsurface model as a result from the iterative inversion of predicted EMI values was generated.

Thereby various electric conductivity maps (EC) were generated by forward modeling and compared with the corresponding measured data. The study use the best fitted input data for the generation of the 3D model. In a second approach a K-means cluster map for the floodplain surface was generated that combines the main characteristics from multilayered subsurface data by synthesis and simplification analogue to *Part II*. The obtained cluster characterizes different soil conditions, which are indicative for the delineation of AAC.
Although developed under specific site conditions all demonstrated approaches offers portability and should be applied in other applications.

Introduction

1. Motivation / Problems and approaches

All terrestrial environmental processes involve the soil including hydrological, geological, meteorological, ecological and anthropological factors. The stress on natural soils increases significantly with agricultural and urban land use as a consequence of the world‘s growing population (approx. 1.6Mill humans per week, Helmholtz Statistic 2011). This leads among others to deforestation and soil sealing and consequently to the decrease of natural habitats and resources. Thus, the protection and preservation of soils along with prevention measures in land-use scenarios is a challenge for the policy, agricultural economics, and the geosciences (Huisman et al. 2008). Although most countries still have reserves, soil is a finite resource and needs a consideration as most precious and threatened resource (Banwart 2011), and all planning concepts should rely on sustainable land-use scenarios.

A perspective for maintaining and avoiding extensive and destructive land use is given by the optimization of current land use, e. g. by reutilization of anthropogenic modified soils and agriculturally site-specific crop management (SSCM) (Pringle et al. 2003, Green et al. 2007). Therefore reliable and detailed spatial and temporal information of relevant soil and subsoil properties are needed that allow an adaptive land-use management, for example the adjustment of fertilizer and pesticide applications (Green and Erskine 2004, Behrens et al. 2005, Behrens and Scholten 2006). Relevant soil properties in terms of agriculture and land management options are for example bulk density, soil moisture, soil texture, and organic carbon content due to its strong relation to environmental soil processes (e. g., Rawls et al. 1991, Tamari et al. 1996, Schaap and Bouten 1996, Schaap et al. 1998, Pachepsky et al. 1996, 1999, Minasny et al. 1999, Wosten et al. 2001, Western et al. 2002, Pachepsky and Rawls 2004, Parajka et al. 2006, Mahmood and Vivoni 2008, Deng et al. 2009) In addition, reliable soil data in adequate temporal resolution provide essential information for predicting effects of climatic and environmental change on soil conditions. Hence, the investigation of soil properties has become a key issue in soil and geosciences (Lin 2003, Carrolla and Oliver 2005, Behrens and Scholten 2006, Corwin et al. 2006, Hartemink and McBratney 2008, Behrens et al. 2009, Brocca et al. 2009, Eggleton et al. 2009, Zacharias et al. 2009, Minasny et al 2010).

However, direct analysis of crucial soil properties, e. g. grain size or soil moisture by soil sampling is still time consuming and costly, and provides only single point information. In addition, direct soil information are mostly available only for small-scale areas, but precise soil data are also needed for medium and large-scale areas (up to several square kilometers) for the assessment of soil development and future-oriented planning. Prediction of soil conditions over large scales e. g., by upscaling is complex due to the heterogeneity of soil properties and this issue has been addressed in discussions since more than a decade (McKenzie et al 2008). Hence, methods are needed for time and cost efficient acquisition of soil and subsoil data from medium and large-scale areas.

Proximal soil sensing techniques (PSS) are an opportunity for obtaining data from medium and large–scale areas that allow a time and cost efficient characterization of soils and subsoils (Hubbard and Rubin 2003, Pellegrin and Wannemaker 2005, Becht et al. 2006, Lambot et al 2006, Steelman & Endres 2009, Viscarra Rossel et al. 2011, McBratney et al. 2011, Hura et al. 2011). PSS started in the early 20century by using a dynamometer for mechanical resistivity and spreads (Sudduth 2011). Since then, PSS has been enhanced and represents nowadays a highly developed sensing technology. The principle of PSS is the measurement of easily recordable physical variables, which are representative for specific soil properties, the so-called proxy values. Relatively easy obtainable proxies are for example the electric conductivity, the gamma decay or different color spectrums. Proxies are typically obtainable from surface and do not need an engagement in soil structure by probe taking.

A widespread application area for PSS methods is in hydrological and hydrogeological questions due to the complexity for obtaining direct hydrological related data, e. g. for investigation of soil moisture (Huth and Poulton 2007, Wagner et al. 2008, Martinez et al. 2010) riverbed investigation (Kim et al. 2002) groundwater distribution information (Belaval et al. 2003, Manheim et al. 2004, Taniguchi et al. 2007, Nyquist et al. 2008) or investigations of ground water table (Loheide et al. 2005, Abdu et al. 2008, Buchanan and Triantafilis 2009). Two common and established PSS methods capable for hydrological and hydrogeological questions are electromagnetic induction (EMI) (McNeil 1980, Lesch et al. 2005, Triantafilis and Lesch 2005, Pellergin and Wannamaker 2005, Wong et al. 2006, Hayley 2007, Martinez et al. 2011) and gamma spectrometry (GS) (Bierwirth et al. 1996, Wong and Haper 1999, Taylor et al. 2002, Pracilio et al 2006, Viscarra Rossel et al. 2007, Altdorff and Dietrich 2011) due to the significant relation between the obtained geophysical parameters apparent electric conductivity (EC) and natural gamma decay (DC). These parameters are in significant relation to several relevant soil properties, e. g. soil moisture and clay content (e. g., Hedley et al. 2004, Pracilio et al. 2006,

Martinez et al. 2010). Both methods are able to record high precision soil data in combination with the use of Global Positioning System (GPS) for simultaneous spatial allocation of sampling points. This simultaneous spatial allocation allows a new dimension of soil data acquiring e. g., by car-borne surveys. This facilitates a parallel and multiple data collection e. g., parallel EC and gamma ray recording. Also it increases as a result the amount and quality of data on the one hand. On the other hand, while GPS connected EMI and GS recordings and its combination delivers more precise and multidimensional results, also the interpretation becomes often more complicated and usually requires the output of dissimilar maps. In addition, EMI and GS response only indirectly to the relevant soil properties (a problem of PSS methods in generally). Hence, new approaches and analysis tools for multidimensional data are needed, which is a recent challenge in soil science. In particular, the improvement of the reliability of PSS results towards the solution of specific questions is an addressed question.

The presented PhD thesis addresses the improvement of data evaluation and interpretation of the proximal soil sensing methods electromagnetic induction (EMI) and gamma spectrometry (GS) at three different test sites and three different problems. All demonstrated studies deal with the delineation of characteristic structures in the subsoil, the subsequent data analysis as well as with the critical interpretation towards an assessment of soils as scientific base for future oriented land-use recommendations.
The thesis addresses in particular the following questions:

(1) How can the comparability of the absolute EMI values assured and shifts of data ranges excluded?
(2) Is a delineation of soil moisture and its spatial and temporal distribution with EMI possible?
(3) Are EMI and GS results able to delineate similar soil characteristics from the same test site?
(4) How can multidimensional subsurface data are combined towards a 2dimensional test site mapping and do the generated partitions really reflect the main characteristics of soil properties?
(5) Can an EMI forward modeling approach predict the measured EMI values and the structure of four different investigation depths with just one model?
(6) Is a reliable 3dimensional delineation of significant structures in subsurface possible by EMI and GS data only?

The presented studies discuss these questions by means of practical examples and leads to a distinct conclusion.

2. Methodology

In the following section a short introduction into the measuring principles of EMI and GS is given for a better understanding of the demonstrated approaches.

Electromagnetic induction (EMI)

EMI is based on the difference of electric properties of soil material. A two coils system in the measuring device generates and receives electromagnetic fields; thereby one coil generates a primary electromagnetic field and stimulates the conductor in the subsoil. The electric properties of the subsurface material respond to primary electromagnetic field and engendered a weak secondary field, which overlays the primary electric field. The second coil receives the primary and secondary fields. In dependency of electric soil properties, the secondary field varies in its intensity: the higher conductive the soil material the higher measured apparent conductivity. A description of the technical details is given in Knödel et al. (2005).

EMI devices differ in its maximum exploration depth, which is controlled by the coil distance, the coil configuration, and measuring frequency. In generally, larger coil distances increase the exploration depth, but also the coil configuration has an influence on the investigation depth. The investigation depth or pseudo depth (PD) is an integral signal and means that 3/4 of original signal originates from the area from PS to the surface (in an ideally homogeneous subsoil) (McNeill 1980). There are two common coil configurations, the horizontal position φ_H, where the coils axis are arranged parallel to the ground and the vertical position φ_V where the coils axis stand orthogonal to the ground surface. Figure 1 shows two different PD with relatively responses for horizontal and vertical configuration on example of the EM38 device (Geonics Limited). While the PD of φ_H is maximum 0.75m, the PD of the φ_V reaches up to 1.5m. It demonstrates the PD of the vertical mode is always approx. two times higher then the horizontal mode (McNeil 1980)

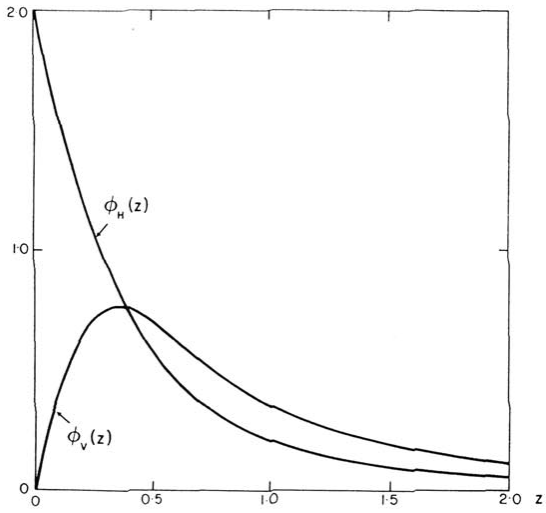

Figure 1 comparison of relative responses for vertical and horizontal modes, x-axis depth [m], y-axis sensitivity [%] (McNeill 1980)

However the obtained electric conductivity signal (EC) is an integral signal that responds to several soil properties, e. g. clay content, moisture content, bulk density and grain size. Thus making an allocation to one of these qualities can be difficult (Rein et el. 2004, Mojid 2007). Nevertheless, EMI is an established tool for subsoil characterization since several decades and offers a bought range of application possibilities. A frequent application of EMI technology is the detection of clay minerals due to its relatively high electric conductivity in contrast to the background. Thus a number of studies postulate a positive correlation of clay with the EC signal (e.g. Bierwirth et al. 1996, Hedley et al. 2004, Triantaflis & Lesch 2005, Pracilio et al. 2006, Mojid et al. 2007, Weller et al 2007). Other studies use EMI for characterizing of a sanitary landfill McNeil (1980), investigation of soil-moisture pattern (Kachanoski et al. 1988, Mojid et al. 2007) or considered the soil texture with EMI (Cockx et al. 2007). Hedley et al. (2004) found a relation between the EC signal and the cation-exchange capacity, Abdu et al. (2008) predicted the water holding capacity with EMI devices and Robinson et al. (2009) used EMI for crop prediction.

In this thesis the ground conductivity meters EM38DD and EM31MK (Geonics Limited, Mississauga, Ontario Canada) come to apply in both horizontal and vertical coil configurations and obtain integral investigation depths between 0.75m and 6m

Gamma-ray spectrometry (GS)

Measuring principle of the gamma spectrometry is based on the natural decay of radioactive elements in rocks and soils and its ability to emit electromagnetic waves with discrete energies (IAEA 2003, Viscarra Rossel et al. 2007). The radiance is scaled by the distance and power of the emitted particle in alpha, beta and gamma – last one has the highest energies (up to several MeV) and the largest outrange with reach up to approx 30cm from subsoil (IAEA 2003). Signals related to potassium (range of 1.370–1.570 MeV), uranium (range of 1.660–1.860 MeV) and thorium (range of 2.410–2.810 MeV) as well as the total count (range of 0.4–2.810 MeV) (Figure 2) .

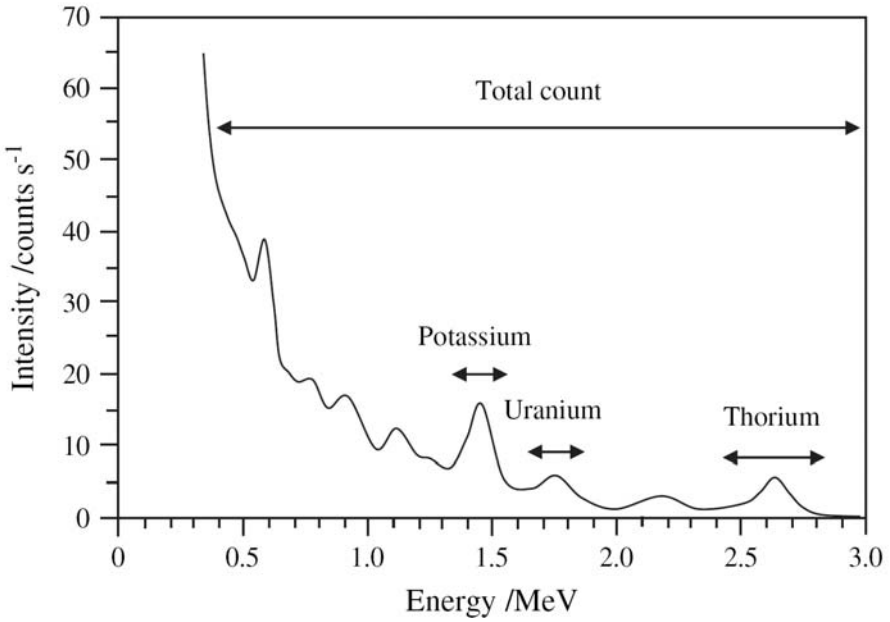

Figure 2 Typical gamma-ray spectrum and position of the element peaks for potassium, uranium, thorium, and total count (Viscarra Rossel et al. 2007)

The emitted discrete energies enable an allocation to the corresponding elements. This allows a detector at the surface the counting the impacts from the emitted energy. A gamma detector contains a piezoelectric crystal and a high sensitive recording device. If a gamma particle hits the crystal during the survey, the stimulated crystal generates a measurable electric impulse. In relation to the discrete gamma energies the triggered impulse is higher or lower and allowed a subsequently allocation from the recorded data to the elements - see more details in *´Guidelines for radioelement mapping using gamma ray spectrometry data´* (IAEA 2003).

In soil science usually the elements potassium, uranium, thorium will extract and considered (Minty et al. 1997, Viscarra Rossel et al. 2006, Viscarra Rossel et al. 2007, Buchanan and Triantafilis 2009). These elements stand in a close context to defined soil components because it's chemical configuration. GS was original developed for commodity prospection and comes to

applying in soil science since almost more then two decades (e.g. Dickson et al. 1996, Cook et al. 1996, Dickson & Scott 1997, Wilford et al. 1997, Buchanan and Triantafilis 2009). Darnley & Ford (1987) derived from the gamma signal information of parent material of soils. Other studied postulates correlations from GS signal with clay content (Worg & Haper 1999, Taylor et al. 2002, Pracilio et al.2006, Viscarra Rossel et al. 2007) Bierwirth et al. (1997) investigates hydrological infiltration beds in soil using gamma spectrometry, Viscarra Rossel et al. (2006) found a correlation of gamma signal with the pH values in soil and Wong et al. (2008) postulates correlation of the GS signal with soil texture.

In the presented studies of this thesis a GSCar gamma spectrometer (GF Instruments / Czech Republic) with 512 5.66 keV channels and a total measuring range from 100 keV to 3 MeV was used.

3. Thesis organization

The presented thesis is divided into three parts, each representing a standalone article including corresponding references.
Due to the thematically overlapping slightly reiteration within this thesis might be possible.

In *Part I* consider a land slide affected hill slope in Vorarlberg / Austria. The creeping landslide at this very inhomogeneous area is triggered by precipitation infiltration and its corresponding changes in vadose zone moisture distribution (Schneider, 1999, Lindenmaier et al. 2005, Wienhöfer et al. 2011). The shear zone is located in a depth between 8m and 11m and is observable at the surface (Schneider, 1999). Reliable information of spatial soil moisture distribution and its associated dynamics is fundamental to any investigation or assessment of the landslide processes. However obtaining reliable information on spatial moisture dynamics over the field scale remains a challenge (Parajka et al 2006, Abdu et al. 2008, Wagner et al. 2008, Brocca et al. 2009).
Thus, apparent electric conductivity data from EMI was used from individual depth intervals up to 6m as proxy for soil moisture investigation due to the (dependent) relationship between moisture and electric soil conditions. The presented study in *Part I* monitored the temporal, spatial and vertical behavior of soil-moisture distribution at a previously identified dynamic slope

area over a period of nine month (Lindenmaier et al. 2005) (Figure 3). By the assumption of relative temporal stability of soil properties, seasonal changes in measured EC should originate from soil moisture content.

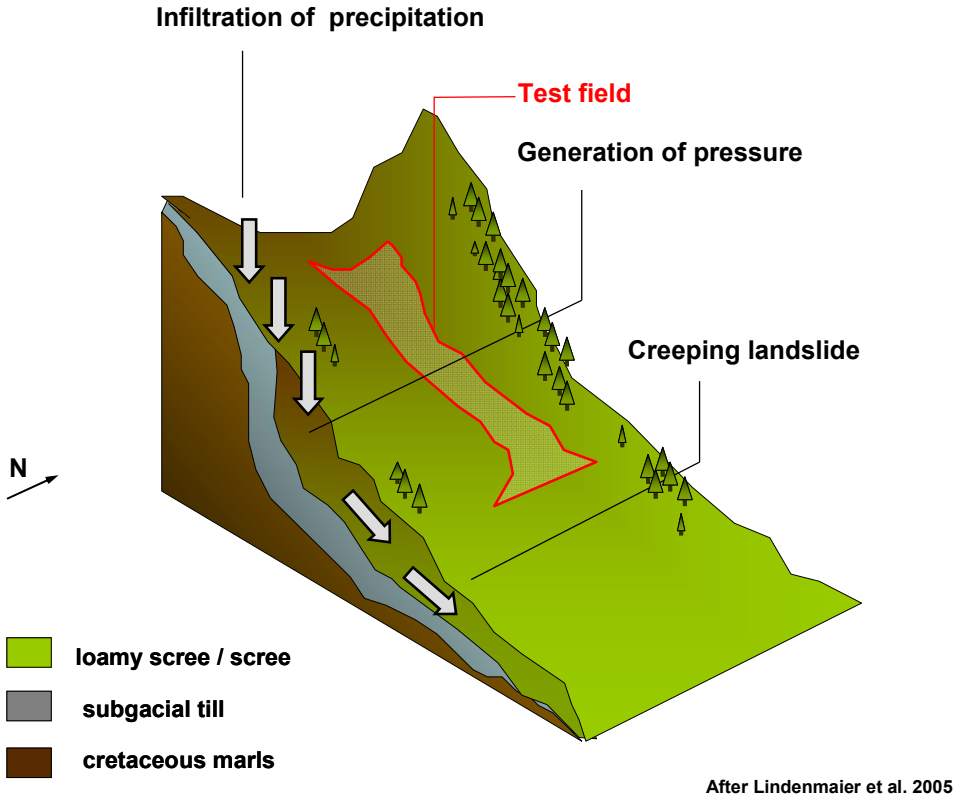

Figure 3 Schematic figure of the landslide affected hill; due to infiltration of precipitation without subjacent drainage a lateral pressure is generated that triggers the landslide in relation to the soil moisture, by means of an EMI monitoring of moisture distribution a delineation of areas with different soil-moisture dynamics is possible

This study also face the challenge of shifts in absolute EC values due to different calibration situation or different EMI devices and provide one opportunity for comparability of different EC data. *Part I* also explores the visualization of temporal changes in three-dimensional subsurface data.

In *Part II* focus on the delineation of different soil properties of a medium scale floodplain (approx. 50,000m²) in Central Germany from multidimensional input data (Figure 4). As

mentioned the demand for reliable high-precision maps of soil and subsoil properties has increased over the past years. These multidimensional data sets can lead to multilayered and complex maps of parameters which are only indirectly related to soil properties and soil functions. However, in applications usually just one clear elementary map is required. *Part II* of the thesis therefore addresses the problem of simplification and synthesis of multidimensional subsurface data for the generation of a 2D map. While the development of survey methods and its combination delivers more precise and multidimensional results, also the interpretation becomes often more complex and usually leads to multilayered maps. For example, the use of different survey methods (e.g. EMI and GS) results in different maps because the different methods measure various physical variables, which can be related to one single soil property in variable manner. But the real world application of land use and further investigation approaches usually demands a clear and elementary partitioning of the surface, for example in terms of agricultural issues. Therefore, a synthesis and simplification of information from different input maps are required (Figure 4).

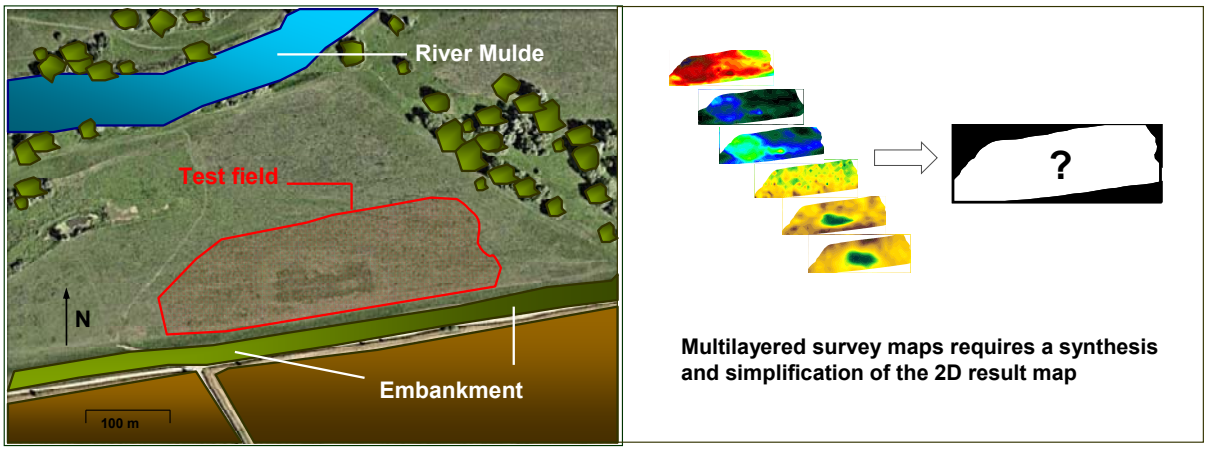

Figure 4 The studied floodplain with the test field (enclosed with red line on the left side) and a schematic figure of the motivation for the simplification and synthesis of multilayered subsurface data for generation of a 2D map (right side)

The study tackle the problem of synthesis by a K-means cluster algorithm in order to generate a 2dimensional map from the test site that includes the main characteristics from divergent input data. However do the generated cluster partitions really reflect the main characteristics of soil properties? Hence, this study focuses on the reliability of such cluster maps by a critical evaluation of the generated partitions. Therefore, independent soil properties such as grain-size characteristics, thickness of soil layers, and the color of randomly taken soil samples were

compared with its cluster allocation. If the generated cluster partitioning reflects the main characteristics of the soil, the chosen properties should significantly correlate with the cluster allocation.

In *Part III* deals with the problem of river restoration and applied restoration measures. Since the positive effects from river restoration to several environmental processes have become aware, methods for effective restoration are required. This study investigates a floodplain of a low-mountain river in Switzerland in order to detect the ancient active stream channels (AAC) as basis for river restoration measures (Figure 5).

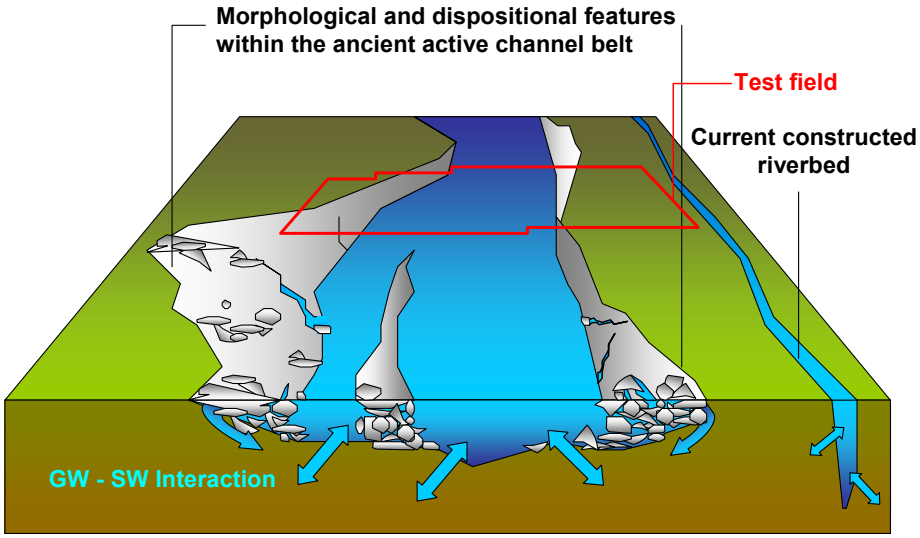

Figure 5 Schematic figure of the investigated floodplain: ancient active river channel (AAC) with geomorphological units developed in the transition between high and low flow (middle) current riverbed (left) with increasing ground floor and location of test field (red line)

This part is subdivided into two approaches; first a 3D subsurface model as a result from the iterative inversion of predicted EMI values was generated. Thereby various electric conductivity maps (EC) were generated by forward modelling and compared with the corresponding maps from measured data. The geological input parameters were varying until the predicted EC maps fit to the real EC values. Subsequently, the study use the best fitted input data for the generation of the 3D model. In a second approach a K-means cluster map for the floodplain surface was generated that combines the main characteristics from multilayered subsurface data by synthesis

and simplification analogue to *Part III*. The obtained cluster should characterize different soil conditions, which are indicative for the delineation of ancient active channel zones.

References

Abdu, H., D. A. Robinson, et al. 2008. Geophysical imaging of watershed subsurface patterns and prediction of soil texture and water holding capacity. Water Resources Research 44.

Altdorff, D., Dietrich, P., 2011. Combination of electromagnetic induction (EMI) and gamma-spectrometry using K-means clustering: A study for evaluation of site partitioning. Journal of Plant Nutrition and Soil Science, in press.

Belaval M, Lane JW Jr, Lesmes DP, Kineke GC (2003) Continuous-resistivity profiling for coastal groundwater investigations: three case studies. In: Proceedings to the Symposium in the Application of Geophysics to Engineering and Environmental Problems (SAGEEP), 6–10 April 2003, San Antonio, TX, Environmental and Engineering Geophysics Society, Denver

Banwart, S., 2011. Save our soils. Nature, 474(7350):151-152.

Becht, A., Appel, E., Dietrich, P. 2006. Analysis of multi-offset GPR data: a case study in a coarse-grained gravel aquifer Near Surface Geophysics 4 (4), 227 – 240

Behrens, T. H. Förster et al. 2005. Digital soil mapping using artificial neural networksJournal of Plant Nutrition and Soil Science Volume 168, Issue 1, pages 21–33

Behrens, T and T. Scholten. 2006. Digital soil mapping in Germany—a review J. Plant Nutr. Soil Sci. 2006, 169, 434–443

Behrens T., O. Schneider, et al. 2009. Analysis on pedodiversity and spatial subset representativity - the German soil map 1:1,000,000. Journal of Plant Nutrition and Soil Science, 172:91 – 100.

Bierwirth, P. Gessler P et al. 1996. Empirical investigation of airborne gamma-ray images as an indicator of soil properties Wagga Wagga, NSW. AGSO Record

Bierwirth, P., S. Hardy, P. Wilson, S. Philip, D. Smith, I. Heiner, and M. Grundy. 1997. Integrating gamma-radiometrics into landscape modelling of soil attributes: Results of an ACLEP exchange. Australian Collaborative Land Evaluation

Program. CSIRO Canberra, Australia 6, no. 4: 15–18.

Brocca, L., F. Melone , et. al. 2009. Soil moisture temporal stability over experimental areas in Central Italy. Geoderma. Volume 148, Issues 3-4, 364-374

Buchanan, S., and J. Triantafilis. 2009. Mapping water table depth using geophysical and environmental variables. Ground Water 47:80-96.

Caroll, Z.L and. Oliver M.A. 2005. Exploring the spatial relations between soil physical properties and apparent electrical conductivity. Geoderma Volume 128, Issues 3-4, Pages 354-374

Cockx, L., M., Van Meirvenne, and De Vos, B.: Using the EM38DD Soil sensor to delineate clay lenses in a sandy forest soil, Soil Sci Soc Am J, 71(4), 1314-1322, 2007.

Cook, S.E., Corner, R.J., Groves, P.R. & Grealish, G.J. 1996. Use of airborne gamma radiometric data for soil mapping. Australian Journal of Soil Research, 34, 183–194.

Darnley, A.G. & Ford, K.L. 1987. Regional airborne gamma-ray surveys: a review. In: Exploration ’87 (ed. G.D. Garland), pp. 229–240. Third Decennial International Conference on Geophysical and Geochemical Exploration for Minerals and Groundwater. Special Volume 3. Geological Survey of Canada, Ontario, Canada.

Deng H. Y. MingYe et al. 2009 Quantification of uncertainty in pedotransfer function-based parameter estimation for unsaturated flow modeling WATER RESOURCES RESEARCH, VOL. 45, W04409, doi:10.1029/2008WR007477

Dickson, B.L., Fraser, S.J. & Kinsey-Henderson, A. 1996. Interpreting aerial gamma-ray surveys utilising geomorphological and weathering models. Journal of Geochemical Exploration, 57, 75–88.

Dickson, B.L. & Scott, K.M. 1997. Interpretation of aerial gammaray surveys: adding the geochemical factors. AGSO. Journal of Australian Geology and Geophysics, 17, 187–200.

Dietrich, P., Fechner, T. et al., 1998. A intergated hydrogeophysical approach to subsurface characterizon. in: Herbert, M and Kovar, K. Groundwater Quality: Remediation and Protection, IAHS Publication, 250, ISSN 0144-7815:513-520.

Eggleton, P., Inward, K., Smith, J., Jones, D.T., Sherlock, E., 2009. A six year study of earthworm (Lumbricidae) populations in pasture woodland in southern England shows their responses to soil temperature and soil moisture. Soil Biology & Biochemistry 41, 1857– 1865.

Falloon PD, Harrison R, Betts R. 2006. Impact of land use change on climate in HadGEM1. European Geosciences Union General Assembly, Vol 8. Geophysical Research Abstracts; 2006b. p. 01425. Vienna, Austria, 02–07 April 2006.

Green R. T. and R. H. Erskine 2004. Measurement, scaling, and topographic analyses of spatial crop yield and soil water content. Hydrol. Process. 18, 1447–1465

Green T. R, J. D. Salas, A. Martinez and R. H. Erskinea. 2007. Relating cropnext term yield to topographic attributes using Spatial Analysis Neural Networks and regression. Geoderma, 139(1-2):23 – 37.

Hayley K, L. R. Bentley 2007. Low temperature dependence of electrical resistivity: Implications for near surface geophysical monitoring GEOPHYSICAL RESEARCH LETTERS, VOL. 34, L18402, 5 PP.,:10.1029/ GL03112

Hedley, C.B., I.Y. Yule, et al. 2004. Rapid identification of soil textural and management zones using electromagnetic induction sensing of soils. Australian Journal of Soil Research 42:389-400.

Helmholtz Statistic 2011, http://de.statista.com/statistik/daten/studie/1816/umfrage/zuwachs-der-weltbevoelkerung/ Accessed October 2011

Hubbard S. YRubin 2000 Hydrogeological parameter estimation using. Journal of Contaminant Hydrology 45_2000.3–34 geophysical data: a review of selected techniques

Huisman J.A., L. Breuer, H. Bormann, et al. 2009 Assessing the impact of land use change on hydrology by ensemble modeling (LUCHEM) III: Scenario analysis Advances in Water Resources 32 159–170

Hura T, Hura K, Grzesiak M. 2011. Soil Drought Applied During the Vegetative Growth of Triticale Modifies the Physiological and Biochemical Adaptation to Drought During the Generative Development. Journal of Agronomy and Crop Science Volume: 197 Issue: 2 Pages: 113-123

Huth N.I., and P.L. Poulton 2007. An electromagnetic induction method for monitoring variation in soil moisture in agroforestry systems. Australian Journal of Soil Research 45: 63–72.

Internatrional Atomic Energy Agency, 2003. Guidelines for radioelement mapping using gamma ray spectrometry data. ISBN: 92–0–108303–3.

Kachanoski, R. G., Gregorich, E. G., and van Wesenbeeck, I. J.: Estimating spatial variations of soil water content using noncontacting electromagnetic inductive methods, Canadian Journal of Soil Scienes, 68, 715-722, 1988.

Kim, J.-H., Yi, M.-J., Song, Y., Cho, S.-J. Chung, S.-H., and Kim, K.-S., 2002a, DC resistivity survey to image faults beneath a riverbed: Symposium on the Application of Geophysics to Engineering and Environmental Problems(SAGEEP), 13IDA10.

Knödel, K. H. Krummel, G. Lange. 2005.Handbuch zur Erkundung des Untergrundes von Deponien und Altlasten: Band 3: Geophysik Springer Berlin Heidelberg; Auflage: 2., überarb. Aufl. Deutsch ISBN-10: 3540222758

Lambot, S., Weihermüller, L., Huisman J.A., et al. 2006, Analysis of air-launched ground-penetrating radar techniques to measure the soil surface water content WATER RESOURCES RESEARCH, VOL. 42, W11403, doi:10.1029/2006WR005097

Lesch, S.M., Corwin, D.L., Robinson, D.A., 2005. Apparent soil electrical conductivity mapping as an agricultural management tool in arid zone soils. Computers and Electronics in Agriculture 46, Issue 1, 351-378.

Lin, H., 2003. Hydropedology: Bridging Disciplines, Scales, and Data. Vadose Zone Journal 2, 1– 11.

Lindenmaier, F. Zehe, E. et al., 2005. Process identification at a slow-moving landslide in the Voralberg Alps. Hydrological Processess, 19(8):1635 – 1651.

McBratney A.B., B. Minasny, et al. Removing the effect of soil moisture from NIR diffuse reflectance spectra for prediction of soil carbon. The Second Global Workshop on Proximal Soil Sensing – Montreal 2011 / 108

McKenzie NJ., Grundy, MJ., Webster R., and Ringrose-Voase AJ, 2008. Guidelines for Surveying Soil and Land Resources, 37 p.

McNeil, J. D. 1980. Electromagnetic terrain conductivity measurment at low induction numbers.Geonics. Ltd., Technical Note TN-6.

Mahmood T H. and E. R. Vivoni 2008. Evaluation of distributed soil moisture simulations through field observations during the North American monsoon in Redondo Creek, New Mexico. Ecohydrol. 1, 271–287

Manheim FT, Krantz DE, Bratton JF (2004) Studying ground water under Delmarva coastal bays using electrical resistivity. Ground Water 42(7):1052–1068

Martinez G., K. Vanderlinden, et al. 2010. Field-scale soil moisture patter mapping using electromagnetic induction. Vadose Zone J. 9: 871–881.

Minasny, B., A. B. McBratney, and K. Bristow 1999 , Comparison of different approaches to the development of pedotransfer function for water-retention curves, Geoderma, 93 3– 4 , 225– 253, doi:10.1016/ S0016-7061 99 00061-0.

Minasny, B, A.B. McBratney and A.E. Hartemink 2010 Global pedodiversity, taxonomic distance, and the World Reference Base. Geoderma 155: 132-139

Minty, B.: Fundamentals of airborne gamma-ray spectrometry, AGSO Journal of Australian Geology & Geophysics, 17(2), 39-50, 1997.

Mojid, M.A., D.A. Rose, et al. 2007. A model incorporating the diffuse double layer to predict the electrical conductivity of bulk soil. European Journal of Soil Science 58:560-572.

Nyquist J.E., Freyer, P.A., Toran L. (2008) Stream Bottom Resistivity Tomography to Map Ground Water Discharge, Ground water Vol. 46, No. 4, pages 561–569

Pachepsky, Y. A., D. Timmlin, and G. Varallyay 1996 , Artificial neural networks to estimate soil water retention from easily measurable data, Soil Sci. Soc. Am. J., 60 3 , 727–733.

Pachepsky, Y. A., W. J. Rawls, and D. J. Timlin 1999 , The current status of pedotransfer functions: Their accuracy, reliability, and utility in fieldand regional-scale modeling in Assessment of Non-point Source Pollution in the Vadose Zone, Geophys. Monogr. Ser., vol. 108, edited by D. L. Corwin, K. Loague, and T. R. Ellsworth, pp. 223 – 234, AGU, Washington, D. C.

Pellerin, L., Wannamaker P. E., 2005, Multi-dimensional electromagnetic modeling and inversion with application to near-surface earth investigations. Computers and Electronics in Agriculture 46 71–102

Pracilio, G., M.L. Adams, et al., 2006. Determination of spatial distribution patterns of clay and plant available potassium contents in surface soils at the farm scale using high resolution gamma ray spectrometry. Plant and Soil, 282:67 – 82.

Pracilio, G., Adams, M.L., Smettem, K.R.J., and Harper, R.J. 2006.: Determination of spatial distribution patterns of clay and plant available potassium contents in surface soils at the farm scale using high resolution gamma ray spectrometry, Plant and Soil, 282, 67-82,

Parajka , V. Naeimi et al. 2006. Assimilating scatterometer soil moisture data into conceptual hydrologic models at the regional scale, Hydrol. Earth Syst. Sci., 10, 353–368, 2006

Pringle M.J., A.B. McBratney, B.M. Whelana and J.A. Taylora. 2003. A preliminary approach to assessing the opportunity for site-specific crop managementnext term in a field, using yield monitor data. Agricultural Systems, 76(1):273 – 292.

Rawls, W. J., T. J. Gish, and D. L. Brakensiek 1991 , Estimating soil water retention from soil physical properties and characteristics, in Advances in Soil Science, vol. 16, edited by B. A. Stewart, pp. 213– 234, Springer, New York.

Rein A., R. Hoffmann, P. Dietrich 2004. Influence of natural time-dependent variations of electrical conductivity on DC resistivity measurements. Journal of Hydrology 285 215–232

Robinson, N.J., Rampant, P. C., et al., 2009. Advances in precision agriculture in south-eastern australia. Ii. Spatio-temporal prediction of crop yield using terrain derivatives and proximally sensed data. Crop and Pasture Science, 60:859 – 869.

Schaap, M. G., and W. Bouten 1996 , Modeling water retention curves of sandy soils using neural networks, Water Resour. Res., 32 10 , 3033– 3040, doi:10.1029/96WR02278.

Schaap, M. G., and F. L. Leij 1998 , Database-related accuracy and uncertainty of pedotransfer functions, Soil Sci., 163 10 , 765– 779, doi:10.1097/00010694-199810000-00001.

Schneider, U., 1999. Geotechnische Untersuchungen, satellitengestütze (GPS) Bewegungsanalysen und Standsicherheitsüberlegungen an einem Kriechhang in Ebnit, Voralberg. University of Karlsruhe.

Steelman, C M., Endres, A. L. 2009, Evolution of high-frequency ground-penetrating radar direct ground wave propagation during thin frozen soil layer development Cold Regions Science and Technology 57 116–122

Taylor, M.J., Smettem K., 2002. Relationships between soil properties and high-resolution radiometrics, central eastern Wheatbelt, Western Australia. Exploration Geophysics, 33(2):95 – 102.

Tamari, S., J. H. M. Wosten, and J. C. Ruiz-Suarez 1996 , Testing an artificial neural network for predicting soil hydraulic conductivity, Soil Sci. Soc. Am. J., 60 6 , 1732– 1741.

Taniguchi M, Tomotoshi I, Burnett WC, Wattayakorn G (2007) Evaluating ground water-sea water interactions via resistivity and seepage meters. Ground Water 45(6):729–735

Triantafilis, J., Lesch, S. M., 2005. Mapping clay content variation using electromagnetic induction techniques. Computers and Electronics in Agriculture 46:203-237.

Viscarra Rossel R.A., H. J. Taylor et al. 2007. Multivariate calibration of hyperspectral γ-ray energy spectra for proximal soil sensing. European Journal of Soil Science, Volume 58, Issue 1, pages 343–353

Viscarra Rossel R.A., Chappell, A. et al. 2011. On the soil information content of visible–near infrared reflectance spectra European Journal of Soil Science Special Issue: Pedometrics Volume 62, Issue 3, pages 442–453

Wagner W., C. Pathe, et al. 2008. Temporal Stability of Soil Moisture and Radar Backscatter Observed by the Advanced Synthetic Aperture Radar (ASAR). Sensors 8: 1174-1197.

Weller, U., Zipprich, M., Sommer, M., Castell, W.Z., Wehrhan, M., 2007. Mapping clay content across boundaries at the landscape scale with electromagnetic induction. Soil Science Society of America Journal 71, 1740-1747.

Western A, B. Rodger and G. Bölsch 2002. SCALING OF SOILMOISTURE: Annu. Rev. Earth Planet. Sci. 2002. 30:149–80 DOI: 10.1146/annurev.earth.30.091201.140434

Wienhöfer, J., Lindenmaier, F., 2011. Challenges in Understanding the Hydrologic Controls on the Mobility of Slow-Moving Landslides. Vadose Zone Journal, 10(2):496 – 511.

Wilford, J.R., Bierwirth, P.N. & Craig, M.A. 1997. Application of airborne gamma-ray spectrometry in soil/regolith mapping and applied geomorphology. AGSO Journal of Australian Geology and Geophysics, 17, 201–216.

Wong, M.T.F., and R.J. Harper. 1999. Use of on-ground gamma-ray spectrometry to measure plant-available potassium and other topsoil attributes. Australian Journal of Soil Research 37:267-277.

Wong, M.T.F., S. Asseng, et al. 2006. A flexible approach to managing variability in grain yield and nitrate leaching at within-field to farm scales. Precision Agriculture 7:405-417.

Wong, M. T. F., Asseng, S., et al., 2008. Mapping subsoil acidity and shallow soil across a field with information from yield maps, geophysical sensing and the grower. Precision Agriculture, 9:3 – 15.

Wong, M. T. F., Oliver, Y. M., et al., 2009. Gamma-radiometric assessment of soil depth across a landscape not measurable using electromagnetic surveys. Soil Science Society of America Journal, 73:1261 – 1267

Wong, M.T.F. & Harper, R.J. 1999. Use of on-ground gammaray spectrometry to measure plant-available potassium and other topsoil attributes. Australian Journal of Soil Research, 37, 267–277.

Wosten, J. H. M., Y. A. Pachepsky, and W. J. Rawls 2001 , Pedotransferfunctions: Bridging the gap between available basic soil data and missing soil hydraulic characteristics, J. Hydrol., 251 3–4 , 123–150, doi:10.1016/S0022-1694 01 00464-4.

Zacharias, S., D. Altdorff et al., 2009. Hydropedology and Pedotransfer Functions. in E.J. van Henten, D. Goense et al: Precision agriculture ´09. Wageningen Academic Publishers, pp. 545-550.

PART I

Spatial and temporal soil moisture observation at a landslide affected Alpine hillside using electromagnetic induction (EMI)

Daniel Altdorff[1] *& Peter Dietrich*[1]*,*

[1] *UFZ Leipzig, Departement Monitoring- and Exploration Technologies, Permoserstraße 15, 04318 Leipzig, Germany*

Subbmitted manusrcibt for Geoderma Special Issue: Proximal Soil Sensing
Submitting date: 08/11/2011 Manuscript Number: GEODER7004

Spatial and temporal soil moisture observation at a landslide affected Alpine hillside using electromagnetic induction (EMI)

Daniel Altdorff[1] & Peter Dietrich[1],

[1] UFZ Leipzig, Departement Monitoring- and Exploration Technologies, Permoserstraße 15, 04318 Leipzig, Germany

Abstract

Spatial and temporal soil moisture dynamics play a major role in landslide affected areas. Landslide activity is largely controlled by pore pressure changes in response to rising groundwater levels, which can be related to changes in vadose zone moisture distribution. While knowledge of soil moisture conditions is of utmost importance to the prediction of landslides, it is difficult to obtain reliable information over the field-scale. A possibility of filling that information gap is the indirect mapping of soil moisture by electromagnetic induction (EMI), due to the relationship between moisture and electric soil conditions. However the fact that EMI data can vary in its absolute data ranges by other influences hindered a direct comparison of survey data in order to explore its changes.

This study uses spatial and temporary EMI measurements to delineate moisture patterns over a heterogeneous, landslide-affected hill slope. By means of discovering this pattern and its dynamic changes, resulting in the derivation of zones of potential higher and lower land slide vulnerability is possible.

As such, we investigate the temporal, spatial and vertical behavior of moisture distribution over a nine-month period; EMI measurements include four different integral depths: 0.75 m, 1.5 m, 3 m, and 6 m. We tackle the problem of comparability by normalization of the obtained EMI data. To separate the dynamic moisture signal from the geological signal, we subtract the temporal values from the mean values and delineate any relative changes at each depth. From the standard deviations obtained from the temporal maps, we identify areas of higher and lower dynamic soil moisture changes. To reveal the relationship between soil moisture and topography, we use high-resolution aspect, slope, and altitude data in comparable format. A two-layer system could be indentified: one upper more dynamic layer which is associated with hill altitude and a deeper, more stationary layer with a different structure. Slope and aspect have only marginal influence on the moisture pattern.

The approach developed in this study was able to identify moisture dynamics over larger scales and with complex accessibility problems. In addition, it allows for the visualization of temporal changes in three-dimensional subsurface data.

Key words: soils moisture pattern, EMI monitoring and normalization, landslide, proximal soil sensing, visualizing temporal changes

1. Introduction

Spatial and temporal soil moisture dynamics play a major role in landslide affected areas and their associated forecast (Flageollet et al. 1999, Bogaard & Van Asch 2002, Malet et al. 2004, Talebi et al. 2007, Chambers et al. 2010). The risk of landslide activity is expected to increase, due to the effects of climate change, e.g. expected increase in extreme natural events and due to intensified land use across mountainous areas and resultant changes of soil properties, in particular the moisture content. Several studies demonstrated the critical role of spatial soil moisture distribution in combination with hill slope stability, specifically the water content of the upper centimetres (Nyberg 1996, Crave & Gascuel-Odoux 1997, Van Asch et al. 2001). In general, the risk of landslides increases with increasing soil water content. However landslide processes show complex mechanical and fluid interactions and several studies also highlights some contradictory cases, due to negative feedback (Iverson 2005, Van Asch 2009). In any case, obtaining reliable information of spatial soil moisture distribution and its associated dynamics is fundamental to any investigation or assessment of landslide processes. (Crave and Gascuel-Odoux, 1997, Famiglietti et al., 1998, Wienhöfer et al. 2009).

Although several soil moisture measurement strategies have been developed over the last few decades, obtaining reliable information on spatial moisture dynamics over the field scale remains a challenge (Parajka et al 2006, Abdu et al. 2008, Wagner et al. 2008, Brocca et al. 2009, 2010).

A possibility for filling this information gap is the mapping of soil moisture by means of geophysical properties, e.g. from the electric conductivity measured by electromagnetic induction (EMI), due to the (dependent) relationship between moisture and electric soil conditions (Dietrich 1999, Brevik et al. 2006, Wong et al. 2006, Buchanan & Triantafilis 2009, Chambers et al. 2010). EMI has been an established tool for subsurface characterization for several decades (McNeil 1980, Triantafilis and Lesch 2005, Robinson et al. 2009, Wong et al 2009). It has the capacity to non-invasively map over larger spatial areas with low operation costs. The method is easy to apply and can be automated to collect georeferenced data. However, one of the challenges with this method is that it records an integrated electrical conductivity (EC) value, and includes the effects of clay and mineral properties, porosity and water content; hence, making an allocation to one of these qualities, in this case oil moisture, can be difficult (Rein et el. 2004, Mojid 2007, Buchanan & Triantafilis 2009). Despite the fact that several EMI studies attest a positive correlation of electric conductivity with soil moisture (Brevik 2006, Wong 2006, Huth & Poulton 2007), a generalization is not feasible due to the multiplicity of affecting properties, as long as other potential variables remain unknown.

Given the relative temporal stability of soil properties, seasonal changes in measured EC signal will be due to changing moisture conditions within the soil. Thus, the comparison of different EMI maps presents a potential opportunity to explore changes in soil moisture and to identify more hydrologically active locations (Abdu et al. 2008). Robinson et al. (2009) identified zones of water depletion and accumulation in a tropical deltaic soil by the subtraction of different EMI surveys. Similar to this study, Martinez et al. (2010) applied a procedure for deriving the moisture content at an agricultural test field. Both studies postulated a significant effect of precipitation upon the measured EC contrast. However, a simple determination of water content from EC, before and after periods of rainfall for areas with higher precipitation levels, is difficult because of the lack of a dry reference day. This is particularly true if the temporal sampling interval is larger than the frequency of rain events. Even if significant wet and dry periods are identified, the

distribution of water within heterogeneous soils can only partly be explained by the time distribution and rate of precipitation input (Price & Bauer 1983). Takagi and Lin (2011) showed that soil moisture variability in hills increases exponentially with increasing catchment-wide wetness due to subsurface lateral flows. Kampf (2011) demonstrated by means of a hypothetical hillslope and real precipitation data that simulations show a nonlinear increase in subsurface stormflow with increasing initial storage. In addition, the resident time of the water within heterogeneous, cohesive soils is difficult to assess and cannot be correlated with the magnitude or frequency of such precipitation events. The schematic diagram in Figure 1 shows the precipitation and evapotranspiration processes on a homogeneous soil in comparison with heterogeneous soil on a hill slope.

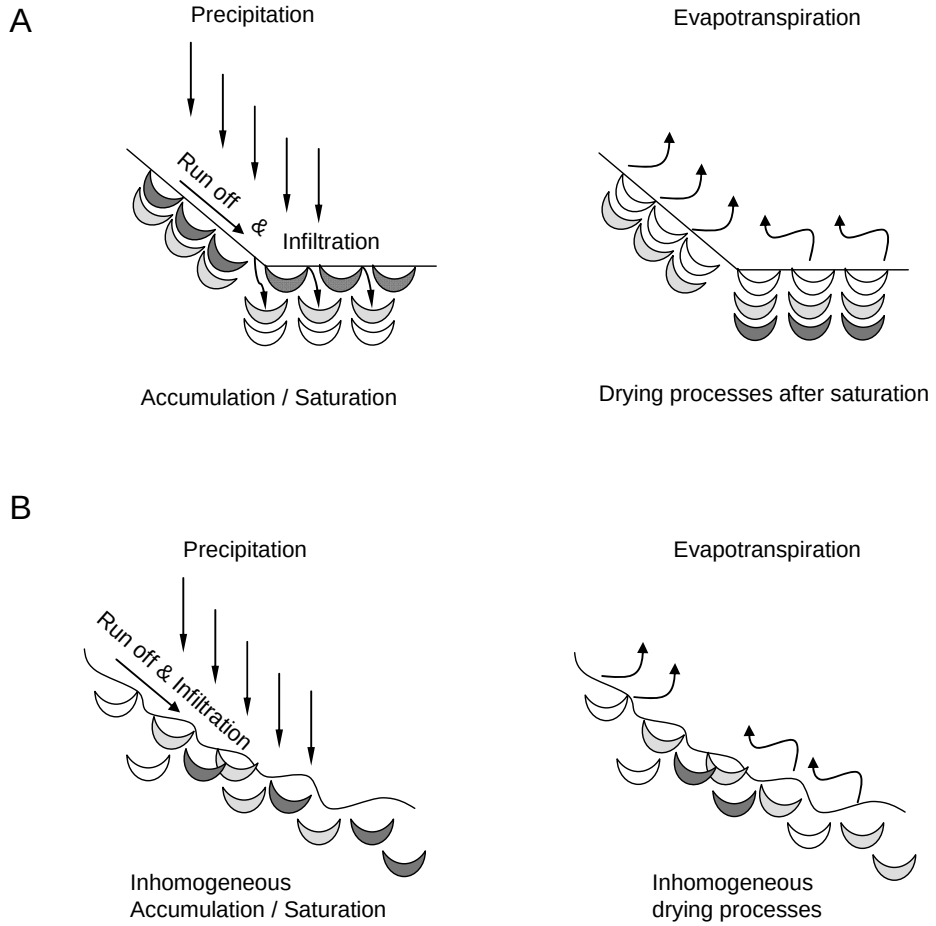

Figure 1: Schematic diagram of precipitation and evapotranspiration processes at an homogeneous (A) and inhomogeneous soil (B) on a hill slope; the levels of gray reflex the lever of saturation: dark grey means saturated, white means dry

While infiltration and drying in homogeneous soils occurs in a more linear fashion, it should be noted that these processes occur at a variable rate within heterogeneous soils, and therefore, a direct correspondence of measured EC values to rain events is difficult.

In all cases, the main challenge is the separation of the dynamic, moisture-induced signal from the static geological background signal.
We use EMI to investigate the dynamic moisture pattern for a heterogeneous, landslide-effected Alpine soil during a nine-months monitoring period under different weather conditions (wet to dry). Landslides at this hill slope usually occur in the upper few meters and are triggered by changes in moisture conditions (Schneider, 1999, Lindenmaier et al. 2005, Wienhöfer et al. 2009). Thus, our surveys will focus on the moisture distribution within this zone. In comparison to other studies, we investigate the temporal, horizontal and vertical behaviour of moisture distribution over a nine-month monitoring period for four different investigation depths: 0.75 m, 1.5 m, 3 m, and 6 m. However, the fact that EMI data can vary in its absolute data ranges as a result of other influences hindered a direct comparison and its use for further calculations. Therefore we normalized the obtained EMI data and, eliminating the need for shifts in absolute values. To separate the geological signal from the dynamic moisture signal, we subtract the temporal value from the mean values. For this purpose, we use discretion and normalize all EC values to the same dimensionless data range, in order to adjust for any differences in absolute data ranges. We also use the standard deviation of all depths to identify any layers of higher or lower dynamic moisture variability. For our investigation of the relationship between soil moisture and topographic data, we use a digital elevation model to represent general aspect, slope, and altitude data in a comparable format.
This study focuses on the development of an investigation method of dynamic changes in soil moisture for sites with a dimension of several thousand square meters and/or with challenging accessibility. In addition, the method aims to address the issue of location optimization for future measurements / instrumentations.

2. Materials and Methods

2.1 Study area

General setting

The Heumoeser slope test site belongs to the Vorarlberg Alps and is a rainfall-triggered land slide area located 10 km east of the city of Dornbirn (north-western Austria). The whole investigative area extends to a total of 1800 m x 600 m, with elevations between 1360 m and 940 m. Landslide events were first recorded since the mid 1960´s and from the 1990´s onwards, the area was the subject of various investigation approaches. Thereby, a resultant movement velocity of up to 15cm per year with higher rates in spring and summer was observed, and the shear zone identified at an approximate depth of between 5 and 11 m (Schneider, 1999). Further investigations show a verifiable dependency of slope stability in combination with rainfall (Schneider, 1999, Lindenmaier et al. 2005, Wienhöfer et al. 2009) which could be resolve into several discrete rupture episodes. The topsoil material consists of very heterogeneous loamy scree and glacial till, with high silt/clay content and glacial components of varying size from the surrounding bedrock. The bedrock basement consists of layered upper cretaceous marls with a main tectonic fault direction of NW–SE and a secondary direction of NE-SW (Schneider 1999).

Test site

For the definition of an intensive test field, we use the hydrotopic delineation method of Lindenmaier et al. (2005) that divides the slope into 4 different local hydrotopes, as a result of combination with available vegetation, topography, slope, and geological data. Thereby we selected an area within the most dynamic north-western part, which is characterized by highly variable relief and small-scale features, such as bulging and plane areas that may be attributed to soil creep. Soil in this area is very cohesive and has stagnic properties that indicate low infiltration capacities (Lindenmaier et al. 2005). The test field extends over an area of approximately 7500 m², with an altitude ranging from 1050 m to 1100 m above sea level (asl). In general, the hillslopes have a strike of N-S and dip towards the east with a maximum slope of 26°. The test site is naturally bordered in N and S by coniferous forest. South, several meters from the test site border, the altitude rises up to approx. 1250 m asl with slope up to 50°. Due to the amount of natural springs and the high annual precipitation (long-term average 2155 mm, Wienhöfer et al 2009), the vegetation is ample, filled with grassland in summer, varying with in respect to the heterogeneities of the soil.

2.2 Soil Samples

In late July, twelve soil probes were taken within the test field and grain size analyses were performed in the laboratory. The probes were taken by a Pürckhauer soil probe up to a depth of 1m, randomly distributed in the test field (Figure 2).

Figure 2 Satellite photo with contour lines and test field (grey) with raw data distribution from EMI survey, in this case March (dark grey line), the location of the soil samples (black crosses) as well as the location of the FDR transect (double arrow)

The sediments were divided into an upper (0 - 0.60 m) and a lower horizon (0.60 – 1 m). For grain size analysis, a SEDIMAT 4- 12 (UGT / Germany) is used, according the German standard DIN ISO 11277.

2.3 FDR

For validation of results, we attempt to utilize Frequency-Domain-Response (FDR) data. FDR is a common method for indentifying the volume moisture content, based on the distinctions in dielectric permittivity from water relative properties to soil matrix properties (Jones et al. 2005, Bittelli et al. 2008). However, measurement with dielectric permittivity is only a proxy and limited by several conditions, in particular by a very high electric conductive soil matrix, e.g. with high clay content (Blonquist, Jr. et al. 2005, Bogena et al 2007).

In this study, the FDR data was monitored along an approx. 8 m transect during the summer months (late July to mid Sep.) The transect was located in the middle of the test site in an area where sharp changes were recorded in the uppermost EC data from previous surveys (Figure2 and 7). Two different types of Frequency-Domain-Response (FDR) loggers were used, five ThetaProbes ML2x FD (UMS/Germany) and two 5TM Soil Moisture-Probes (DECAGON / Pullman, WA USA), therefore seven in total, all buried at a depth of 15 cm.

2.4 EMI survey and database

For EMI monitoring, we used EM38DD and EM31MK2 devices (Geonics Limited, Mississauga, Ontario Canada) in horizontal and vertical dipole coil configurations. Thereby we obtained the following integral values related to pseudo depths (PD) of 0.75 m - EM38 horizontal (EM38h), 1.5 m - EM38vertical mode (EM38v), 3 m - EM31vertical mode (EM31h) and 6 m - EM31vertical mode (EM31v). The PD means two-thirds of the response signal originates from the soil above (McNeil 1980). Both EMI units were connected with a DGPS system and were used manually at a height of approx. 20cm (Em38) and approx. 35 cm (Em31). Surveys were collected at walking speed depending on the topographic conditions, approx. 2-3 km/h. The track distance was approx. 5 m and the recording frequency was 5 Hz for both instruments. In six separate field survey dates, we collected 24 data sets with approximately 200.000 total DGPS allocated point data (approx. 8400 each), evenly distributed over the test field, an example of raw data distribution is seen in Figure 2. The surveys took place between March and October 2010.

EC values are highly sensitive to outside influences, such as temperature, solar radiation, and battery voltage; consequently, device calibration is complex and reproducibility of absolute data is rendered difficult, despite regular calibration (Domsch 2004, Pellerin & Wannamaker 2005, Hayley et al. 2007, Abdu et al 2008, Santos & Porsani 2011). This limits the scope of the informational value of the results, in particular for monitoring studies. These drawbacks are well known in the geosciences community and still in discussion; on the European scale the European Committee for Standardization currently devise a schedule for standardization of EMI near surface survey (CEN 2010).

In this study we calibrated the devices according to the manual and at the same calibration point (except March); nevertheless the data ranges vary significantly for each measuring mode, in

particular the Em38h data from the upper soil (see Figure3 for measured absolute min/max values, evident outliers <0.5% of the total data points are already removed).

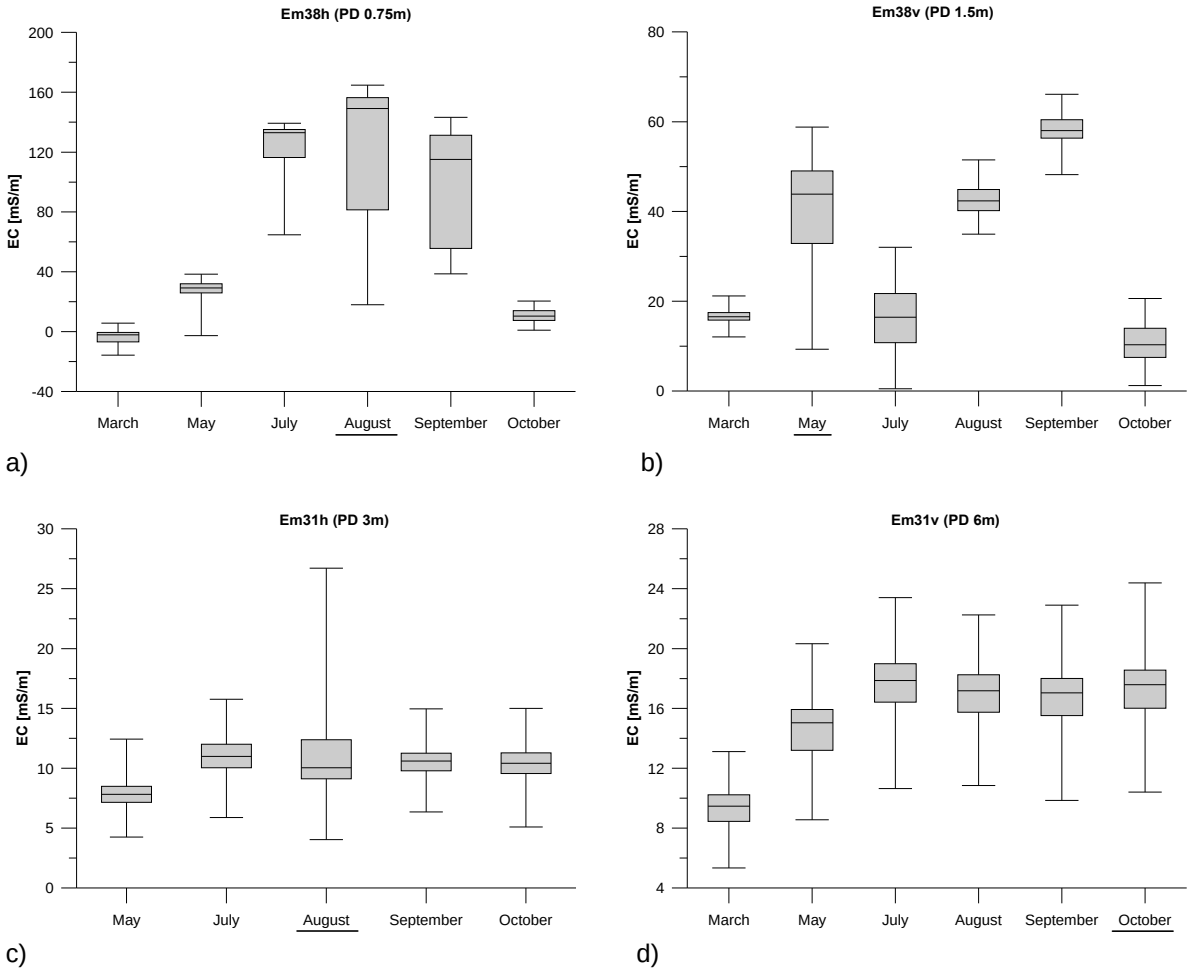

Figure3: Box and whisker plots of EC for different survey dates and investigation depths (evident outliers already removed), whiskers indicate the total range (widest spread month underlined), top and the bottom of the box show the 25th and 75th percentiles, and the line inside the box is the median value; a) Em38h, b) Em38v, c) Em31h and d) Em31v

These differences underlie the problems of absolute values as further calculations with the absolute values will not lead to useful results being obtained.

Comparing the maps is possible based upon working with normalized, discrete relative data. Therefore, we first filtered the raw data with approx. 5 – 95 % from whole range, in order to avoid an overweighting of values in the subsequently normalized data sets. Then we interpolated all data by means of variogram analyses and block Kriging to obtain a separate EC map for each measuring day and investigation depth. Subsequently, we rasterize all maps to the same grid size (1x1m) and obtain a matrix with identical coordinates (*x; y*) and their corresponding EC values. Now we normalize all EC values to a comparable data range with 0.00 as the smallest value to 1

as the biggest value, subsequently also referred to as σ. This maintained the relation in data range and allowed visualization with identical scaling to take place, as well as further calculations.
Similar to the EC data, we prepared the altitude, the aspect and the slope of the data sets without normalizing the data ranges.

2.5 EMI data analysis

For each of the four investigation depths, we use the arithmetic mean $\overline{\sigma}$ from the (dimensionless) values to visualize the geological structure without the dynamic signal (Figure4).

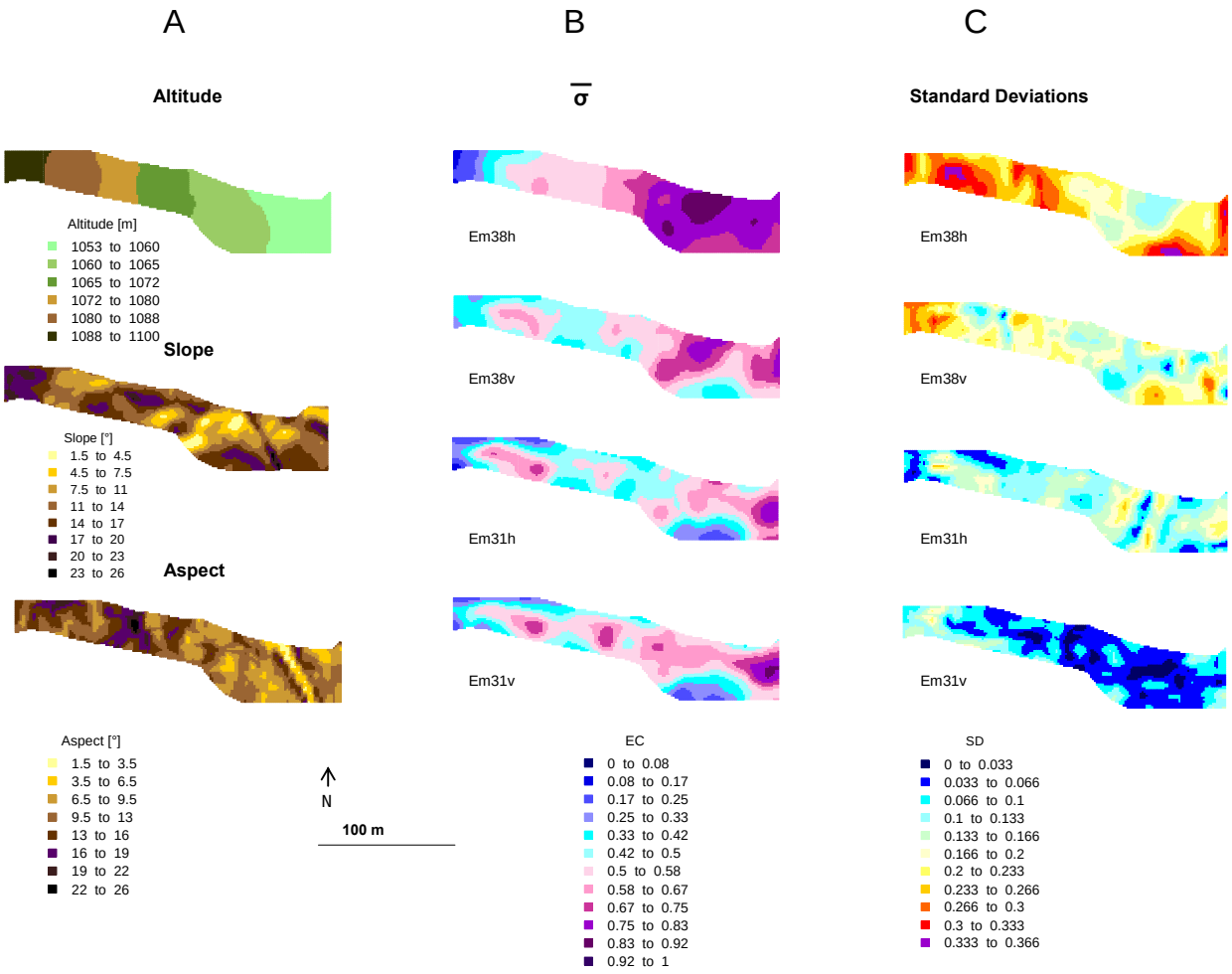

Figure4: A – topographical data, B – EC mean value (dimensionless), and C – standard deviation of each investigation depth

Then we subtract the mean value $\overline{\sigma}$ from the day value n σ_n to highlight the seasonal changes (*SC*) ($SC = \sigma_n - \overline{\sigma}$). Subsequently, we divide the results of *SC* by the mean value $\overline{\sigma}$ to delineate the relative changes (*RC*) and for further contrast ($RC = (\sigma_n - \overline{\sigma}) / \overline{\sigma}$). For a small amount of data, $\overline{\sigma}$ is zero, thus the corresponding RC values are omitted (division by zero). In addition, the data range of *RC* is partly extreme, due to a very small $\overline{\sigma}$ for these data points.

Furthermore, we calculate the standard deviation (*SD*) from each investigation depth. Precipitation data is provided from the Stadt Dornbirn (Vorarlberger Landesregierung 2010). The meteorological station is located approximately 500m from the test field. Due to local conditions, a representative constant groundwater table is non-existent.

3. Results and Discussion

3.1 Soil samples

The results of the soil samples confirm the assumption of very loamy and cohesive soil. Table 1 shows the results of the grain size [vol %] analysis of the upper soil, split into depths of 0- 0.60 m and 0.60 - 1 m, as well their corresponding min/max and mean values.

Table 1: grain size [vol %] of the soil samples taken in two different depths [cm] with min/max values

SS #	clay 0-60	silt 0-60	sand 0-60	clay 60-100	silt 60-100	sand 60-100
1	20,67	57,62	21,71	43,36	49,04	7,60
2	33,34	45,69	20,97	36,00	47,00	17,00
3	22,86	56,47	20,67	41,32	44,52	14,17
4	25,67	51,48	22,85	25,67	51,48	22,85
5	42,21	42,52	15,27	42,21	42,52	15,27
6	33,73	51,72	14,55	34,14	51,49	14,37
7	37,39	50,90	11,71	45,38	37,19	17,43
8	42,84	45,93	11,24	42,84	45,93	11,24
9	43,56	41,52	14,92	45,63	40,25	14,11
10	29,89	53,38	16,73	29,71	50,91	19,38
11	19,57	49,97	30,46	18,76	64,96	16,28
Min	19,57	41,52	11,24	18,76	37,19	7,60
Max	43,56	57,62	30,46	45,63	64,96	22,85
Mean	33,34	50,90	16,73	41,32	47,00	15,27

Generally, both depths have very high clay and silt content; however a distinct difference between the upper and the lower sediments is not observable in this data, apart from slightly lower clay content in the upper centimetre. Furthermore, no spatial correlation appears in this data; despite the relatively small number of sample points, results from the probes clearly illustrate the inhomogeneous conditions of the site.

3.2 FDR

The data collected in September showed the soil around the transect to be completely saturated, as the majority of the FDR probes were located under water. Results obtained show very high

conductivity (<0.5dS/m) with a marginal dynamic over the whole monitoring distance (>0.02dS/m) leading to implausible moisture content (< 53%) and an unlikely dynamic variation in moisture (lesser then 1% vol). This indicates an error, presumably induced due to the very high clay content. This problem occurs when the conductivity of the soil is very high which affects the measured high frequency wave. The results show FDR measurement is not suitable for soil moisture measuring at this test site, consequently we did not include the FDR data in our further approaches and investigation.
In the following section, we focus on identifying moisture patterns in general, without quantitative interpretations.

3.3 EMI

Despite calibrating the devices according to the manual; the data ranges vary for each measuring mode. Generally, the range decreases with investigation depth. It was not possible to define a preferential month for the widest ranges. A noticeable and striking find is the negative EC values obtained in the Em38h values. These negative values can occur if the calibration point, the point where the instrument was set to zero, has a higher conductivity than some parts of the test field. The negative values in the results underlie the problem of comparing absolute values and the demand for normalization. In addition to the negative values, note the decrease in absolute values for the Em38h between Sept and Oct, as an example of relative changes of values. Therefore, we work further with normalized EC data. The attempt to directly combine EC data with precipitation data is always difficult and does not lead to distinct conclusion in this study. Although a general indication for a relationship exists, this precludes the temporal precipitation distribution of the test site and lacks a “dry reference day”, due to continual rain events (Figure 5).

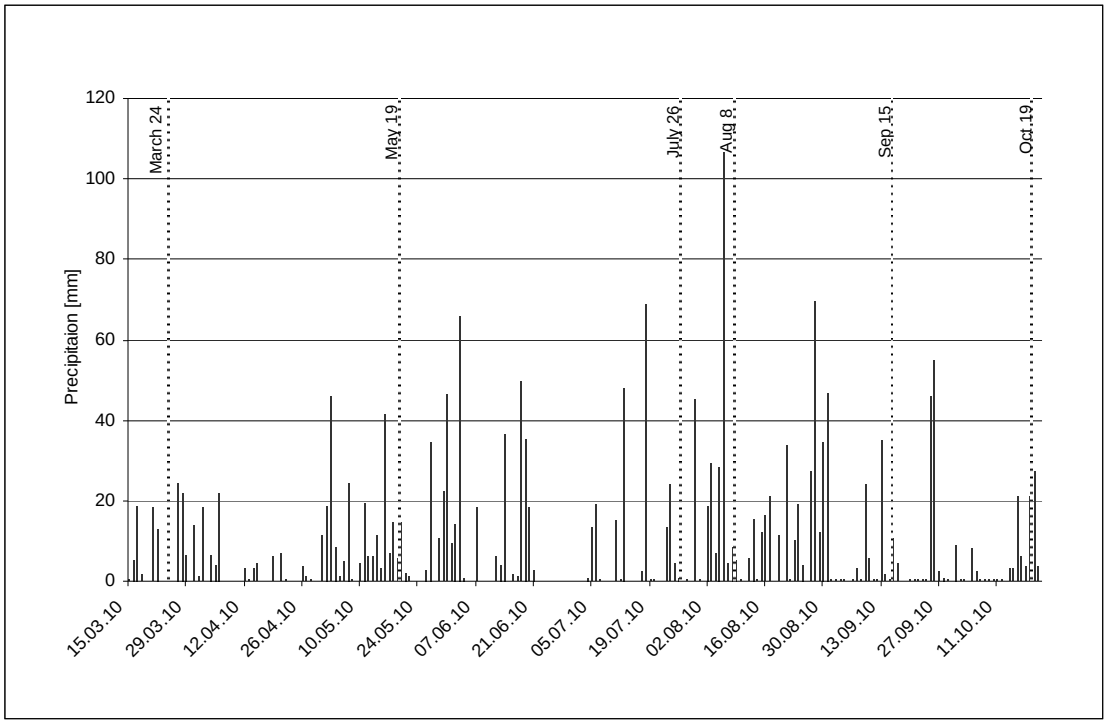

Figure 5: precipitation during the monitoring period with survey data (after Amt der Vorarlberger Landesregierung 2010)

Even if the precipitation was clearly divided into wet and dry periods, the resident time of the water in the soil would remain unknown and, particularly for glacial till and silt layers, the resident time is usually longer than seasonal precipitation variability. A tracer test in the same hydrotope, approx. 50 m distance from the test site, was aborted after three hours without visible percolation of salt tracer in a 1 m³ excavation. Furthermore, a heterogeneous soil matrix distribution and complex evapotranspiration processes make a direct allocation of the moisture movement to the precipitation events unfeasible (see schematic diagram in Figure1).

3.4 Spatial results

The mean values of EC in Figure4b show clear patterns of areas with higher and lower conductivity. In general, the eastern area is more conductive in all maps, particularly in the upper region. The values decrease with PD of 3m (Em31h) and slightly increase in the lowermost part (Em31v), probably due to reaching the saturated zone. Regarding the structure of the EC distribution, a two-layer system could be detected with different orientations: one upper with E-W orientated pattern and one deeper, with S-N orientated pattern represented by the uppermost signal (Em38h) and the lowest signal (Em31v). The different investigation depth reflects the contrast of the layers. Note that the Em31h integrative signal is still affected by the upper layer but lower structures dominate the signal. By assuming the structure of the mean values may reflect the geological situation; the higher conducted areas presumably contain regions with thicker local glacial till or clay layers.

When comparing EC data with topographical information (Figure4a), a relation of altitude and the uppermost maps is apparent, whilst the deeper maps seem more affected by the aspect, in particular the Em38v map. Figure 6 shows the combination of all variables vs. each other.

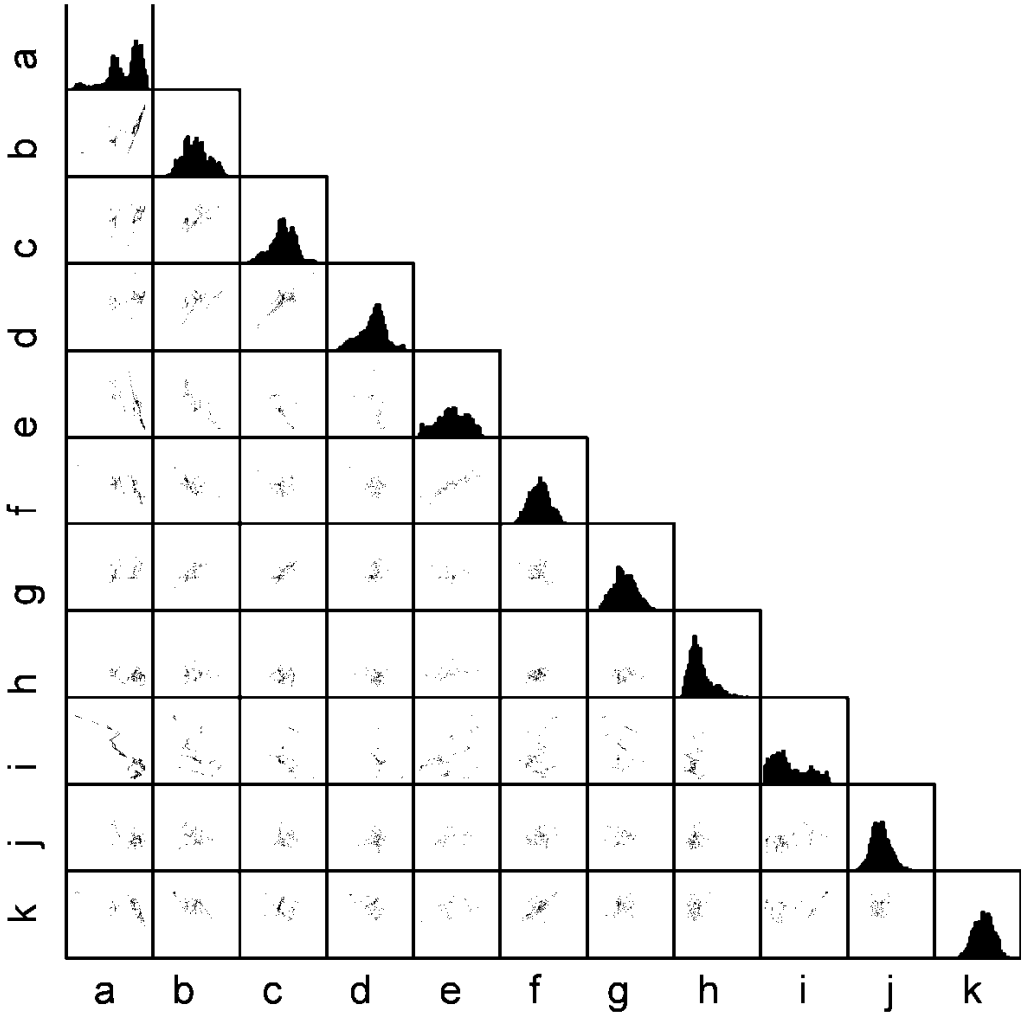

Figure6: Plots of the variables: mean (*a* -Em38h; *b* – Em38v; *c* – Em31h; *d* – Em31v) standard deviation *SD* (*e* - Em38h; *f* – Em38v; *g* – Em31h; *h* – Em31v) and topographic data (*i* – altitude; *j* – slope; *k* – aspect)

The bar charts in the uppermost cells contain the data value distribution, e.g. unimodal for the aspect and more bimodal for the Em38mean. The other boxes highlight the relationship of two variables respectively. Besides a linear trend of the mean values of Em38v, Em31h and Em31v, a negative linear relationship of altitude and all EC mean values, fading with depth, is visible. However, other variables, including the aspect, are contrary to expectations. This gives reason to the assumption that the altitude direction controls the upper layer's moisture dynamic.

3.5 Temporal results

Temporal maps of investigation depths vary in data range and EC distribution (Figure 3). Except in March we calibrate at the same calibration point; apparently in March a higher conductive location then the test field was used. Note furthermore, the decreasing of absolute values in

Em38h between Sept and Oct as example for relative changes of data ranges that demands normalization for further proceedings.
Despite the fact temperature also vary with seasons, the differences during a field day was marginal and could be neglected; the majority of the signal contrast originates from changes in soil moisture.
To delineate dynamic areas, we use the standard deviation (*SD*) from all surveys over the complete monitoring period. The *SD* of maps is an appropriated indicator for moisture dynamic areas.
Regarding Figure4c, the division in an upper, more dynamic moisture area and a deeper, stationary layer is identifiable with an observable, clear decrease in dynamic moisture region area with depth. This graduation is normal and reflects the reliability of the results. It is interesting that some higher dynamic areas in the upper layer correspond with special lower areas in the lower maps, e.g. in the SE of the site. These zones could be related to the altitude
data, however the plots in Figure6 did not contain spatial information that show unordinary dependencies with changing orientations on very small scales response to these areas.
For a more detailed analysis, we consider the temporal changes of the upper and lower layer. From four available investigation depths, we perform in depth analysis upon the top Em38h (PD 0.75m) and lowermost Em31v signal (PD 6m), only due to its significance concerning layer deviation.
Analogous to the mean data, the Em38h data (PD 0.75m) shows a visibly E-W pattern with intensive and sharp contrasts (Figure7a).

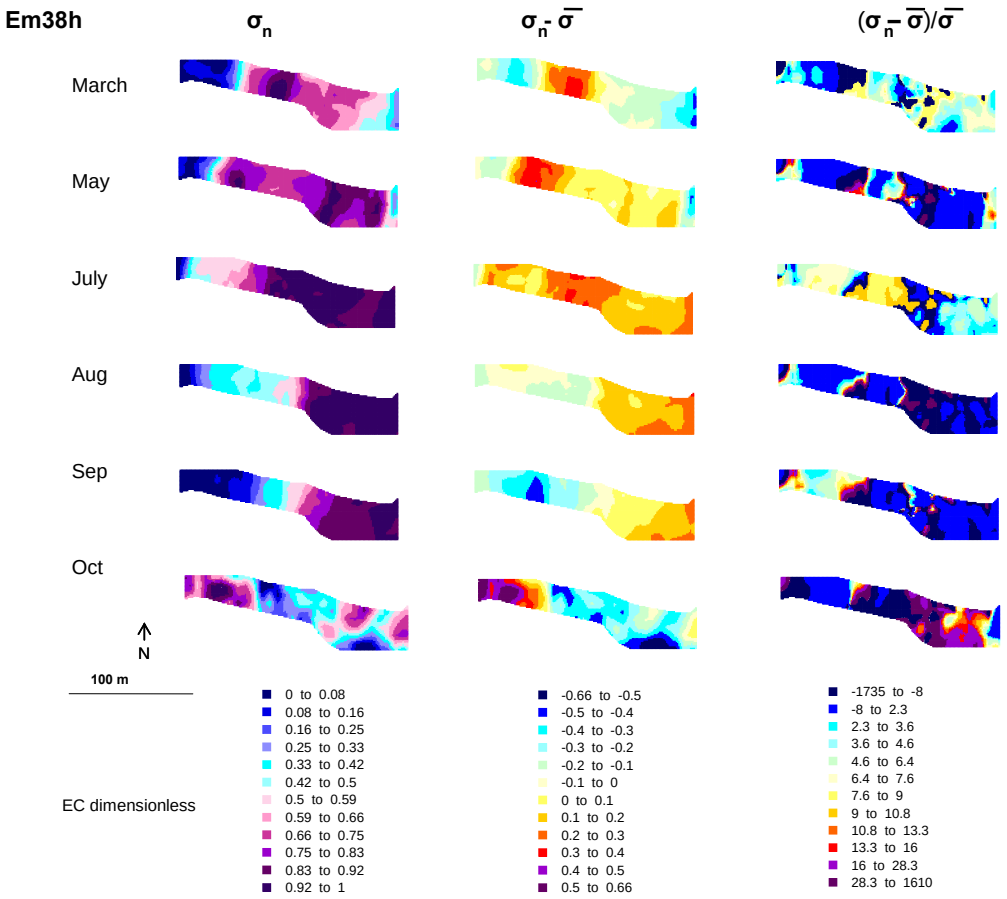

Figure7: Em38h (PD 0.75m) A - temporal data (dimensionless), B – seasonal change, and C – relative changes

In general, the higher areas are located in the eastern part, predominantly in warmer months. The difference maps in Figure7b highlight zones of temporal change, with an intensive contrast observed in obtained results for March, May and October. Of interest is the dislocation of depletion and accumulation zones, in particular between Sept and Oct. The maps of relative changes in Figure 7c describe areas with a higher dynamic variability. These areas are independent from depletion and accumulation and move only slightly over time. Comparing topographical data, dynamic motion predominantly takes place according to the E-W altitude (compare Figure4a). We interpret these changes in the upper layer as soil moisture movement downwards, dependent upon the slope.

In the lower part of Em31v data (PD 6m), the situation is different, with all maps showing a similar and more stationary EC distribution (Figure8a).

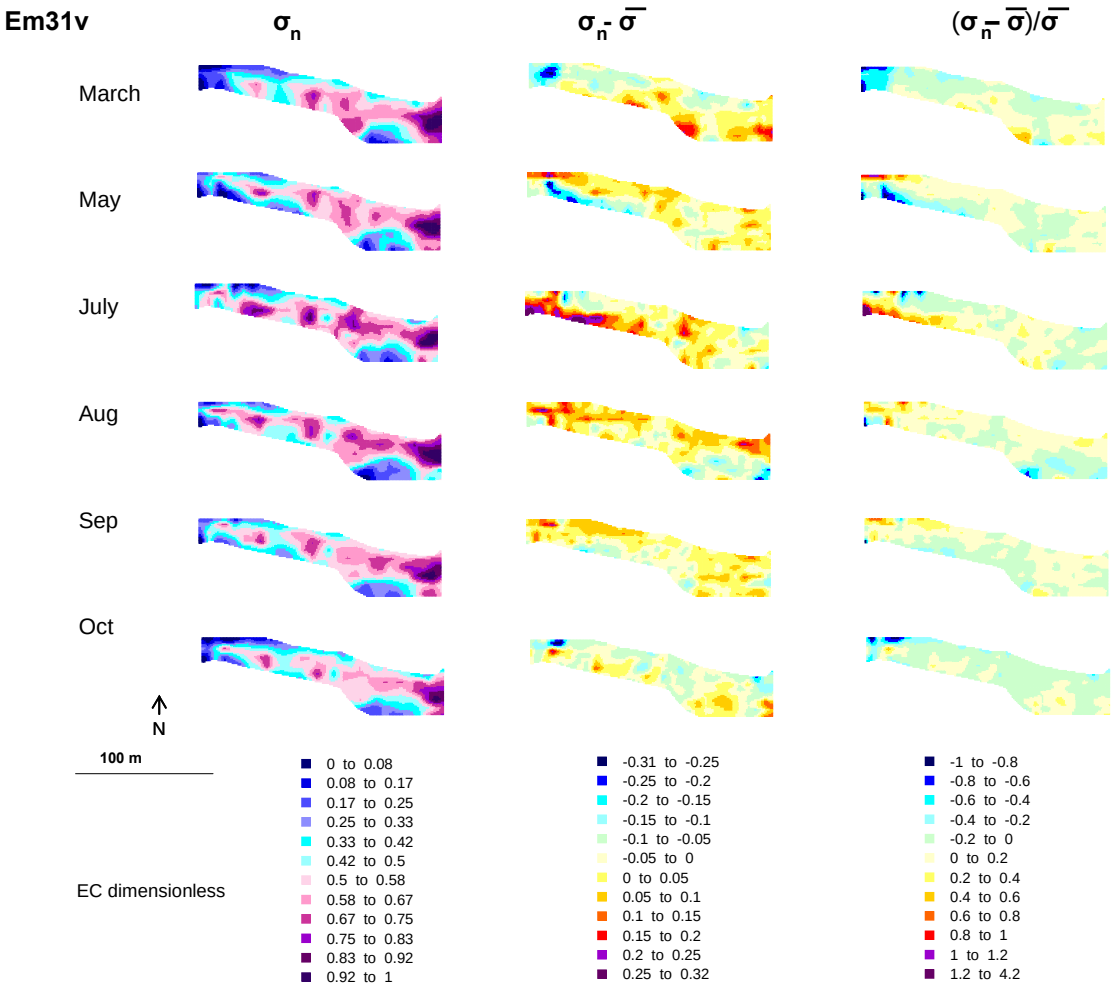

Figure8: Em31v (PD 6m) A - temporal data (dimensionless), B – seasonal change, and C – relative changes

In comparison to the top distribution, the lower data shows a more N-S oriented structure with a characteristic peak in the eastern part. Although the maps look similar, Figure 8b displays significant areas of higher and lower dynamic seasonal change. In this figure, the N-S orientation is even more remarkable, partly because of an accurate 90° front, especially in warmer months – note high contrast between the May and July data, note that the sharp contrast is not an artificial item. Regarding the altitude increasing of the region in south, we interpret the seasonal changes in the Em31v data as a movement of moisture pattern toward north, different than the upper dynamic layer. While the upper layer is more affected by the altitude of the test site (W-E), the lower patterns are predominant influenced by an N-E direction, from the broader topographical settings. The predominant flow direction of the entire part of the hill is assumedly toward north as result from the ascent of hill in south, the second direction is toward east. This situation is similar to the hill slope creeping; here the subsurface pressure is generated toward N-E and the movements react towards S-E (Lindenmaier et al. 2005).

The last column in Figure 8 shows the relatively change. As expected from the similarity of the EC maps, the relative changes in Figure8c are marginal in comparison to the upper layer in Figure7c. Conspicuous by their absence in these maps are the northernmost part in the West and the southernmost part in the West in particular at the comparison of May / July. This area is obviously the most dynamic region of the lower layer.

4. Conclusion

We derived the soil moisture dynamic from temporal and spatial EC maps. The normalization of EC values allowed a comparison of temporary maps and subsequent further calculation to take place. This study thereby shows normalization of discrete EC data as a potential opportunity for the common calibration problems and shifts in absolute data and ranges. The separation of the dynamic moisture signals from the geological stationary background by subtraction of the temporal values from the mean values delineated relative changes of each investigation depth. A two-layer system could be identified; one upper more dynamic layer (PD 1,50m) with an E/W structure and a deeper, more inactive layer (PD 6m) with a N/S oriented structure.
We demonstrated that the soil pattern within the upper layer is associated with the test site altitude, whilst the pattern within the deeper layer is by its N-S structure obviously more related to the broad topographical and geological settings. Spatial distribution within the test site as well as temporal changes of moisture patterns, are strongly influenced by altitude; the other variables slope and aspect do not significantly affect the data at either depth. However, the plotting method is probably inadequate to consider all complex relations in this special case due to the lack of spatial information. It can be said, that slope will assuredly play a role in moisture distribution, but to reveal this, the investigation has to focus on much smaller scales.
An analysis of the influence of precipitation upon the measured data was not feasible due to continual rain events and its high variability during the monitoring period, as well as the highly heterogeneous and cohesive soil of the test site. A reasonable investigation of dependencies between precipitation and EC values requires precise knowledge about the moisture content of a reference day or temporary high resolution monitoring. If rain events and EC data are monitored daily, they will probably establish a reasonable dependency.
Soil moisture measurement by FDR probes was not successful at this site, presumably due to the very high clay content. Alternatively, a validation of soil moisture from the upper horizon could be made using other methods, e.g. by gravimetric water content. However, validation of lower patterns up to 6 m by representative soil probes at different measurement days will impose a technical effort, potentially to an unrealistic degree, and work against any advantages gained from utilizing EMI.
Regarding the results, this applied approach was able to successfully identify moisture dynamics at larger scales and for test sites with complex accessibility problems, whilst also yielding the advantage of portability. In terms of landslide process understanding and forecast, the approach can provide information of higher dynamic regions as an indication for its changing wetness and consequently for its vulnerability – by means of the Em34 device up to a depth of 30m and more. Accordingly, the demonstrated procedure is able to generate dynamic maps from the whole hill slope with short data acquisition time and low operational costs. Thus, the EMI moisture monitoring should accompany landslide investigations, preferably at the start of research for the

selection of areas needing further intensive and higher resolution investigation (e.g. DGPS / inclinometer monitoring stations). The study also shows that the practice of EMI monitoring is not limited by areas with heterogeneous topography and / or complex accessibility nor by high clay content, in comparison to other investigation methods like ground-penetrating radar (GPR), an advantage for the majority of landslide affected hill slopes.
The method applied in this study is a useful process for the separation of temporal changes from stationary background. In addition, it allows for the visualization of temporal changes in three-dimensional subsurface data.

Acknowledgement

The authors would like to offer thanks to David Sauer, Dr. Steffen Popp for support during field operations, as well as the students from the Universities of Potsdam for soil sampling and Munich for FDR data supply. The authors also acknowledge the DFG research project 581 *Coupling of Flow and Deformation Processes for Modeling the Movement of Natural Slopes* and the Helmholtz research platform MOSAIC for furnishing the technical equipment. Special thanks to John Mosquera and Colby Steelman from the University of Waterloo, Canada, for editing the manuscript.

5. References

Abdu, H., D. A. Robinson, et al. 2008. Geophysical imaging of watershed subsurface patterns and prediction of soil texture and water holding capacity. Water Resources Research 44.

Amt der Vorarlberger Landesregierung 2010. Stadt Dornbirn NS Daten: Rohdaten der Messstation Ebnit.

Bittelli, M. F. Salvatorelli and P.R. Pisa. 2008. Correction of TDR-based soil water content measurements inconductive soils. Geoderma 143 133–142

Blonquist Jr J.M.. S.B. Jones and D.A. Robinson. 2005. A time domain transmission sensor with TDR performance characteristics. Journal of Hydrology 314 235–245

Bogaard, T.A. and Th.W.J van Asch 2002. The role of the soil moisture balance in the unsaturated zone on movement and stability of the Beline landslide, France. Earth Surf. Process. Landforms 27: 1177–1188.

Bogena H.R., J.A. Huisman et al. 2007. Evaluation of a low-cost soil water content sensor for wireless network applications. Journal of Hydrology (2007) 344, 32– 42

Brevik, E.C., T.E. Fenton, and A. Lazari 2006. Soil electrical conductivity as a function of soil water content and implications for soil mapping. Precision Agriculture 7(6): 393-404.

Brocca, L., F. Melone , et. al. 2009. Soil moisture temporal stability over experimental areas in Central Italy. Geoderma. Volume 148, Issues 3-4, 364-374

Brocca, L., F. Melone, et al. 2010 Spatial-temporal variability of soil moisture and its estimation across scales. Water Resources Research 46. W02516, 14 PP

Buchanan, S., and J. Triantafilis. 2009. Mapping water table depth using geophysical and environmental variables. Ground Water 47:80-96.

CEN - European Committee for Standardization. 2010. Best Practice Approach for electromagnetic induction measurements of the near surface, Approved Business Plan, CEN Workshop 59

Chambers, J.E., P.B. Wilkinson, et al. 2010. Three-dimensional geophysical anatomy of an active landslide in Lias Group mudrocks, Cleveland basin, UK. Geomorphology.

Crave, E., and C. Gascuel-Odoux 1997. The influence of topography on time and space distribution of soil surface water content. Hydrological Processes 11:203–210.

Dietrich, P. 1999. Konzeption und Auswertung gleichstromgeoelektrischer Tracerversuche unter Verwendung von Sensitivitätskoeffizienten. Tübinger Geowissenschaftliche Arbeiten. 130 S.

Domsch, H., A. Giebel, 2004. Estimation of Soil Textural Features from Soil Electrical Conductivity Recorded Using the EM38. Precision Agriculture 5: 389-409

Dos Santos, V.R.N., and J.L. Porsani, 2011. Comparing performance of instrumental drift correction by linear and quadratic adjusting in inductive electromagnetic data. Journal of Applied Geophysics 73: 1–7.

Famiglietti J.S., J.W. Rudnicki, and M. Rodell. 1998. Variability in surface moisture content along a hillslope transect: Rattlesnake Hill, Texas. Journal of Hydrology 210: 259–281.

Flageollet, J.C., O. Maquaire, B. Martin, and D. Weber. 1999. Landslides and climatic conditions in the Bracelonnette and Vars basins (southern French Alps, France). Geomorphology 30:65–78.

Hayley K, L. R. Bentley 2007. Low temperature dependence of electrical resistivity: Implications for near surface geophysical monitoring GEOPHYSICAL RESEARCH LETTERS, VOL. 34, L18402, 5 PP.,:10.1029/ GL03112

Hedley, C.B., I.Y. Yule, et al. 2004. Rapid identification of soil textural and management zones using electromagnetic induction sensing of soils. Australian Journal of Soil Research 42:389-400.

Huth N.I., and P.L. Poulton 2007. An electromagnetic induction method for monitoring variation in soil moisture in agroforestry systems. Australian Journal of Soil Research 45: 63–72.

Iverson , I.M. 2005. Regulation of landslide motion by dilitancy and pore pressure feedback. Journal of Geophysical Research 110.

Jones S.B., Blonquist, Jr J.M. et al. 2005. Standardizing Characterization of Electromagnetic Water Content Sensors: Part 1. Methodology Vadose Zone Journal 4:1048–1058

Kampf, S.K.2011. Variability and persistence of hillslope initial conditions: A continuous perspective on subsurface flow response to rain events. Journal of Hydrology 404 176–185

Lindenmaier, F., E. Zehe, et al. 2005. Process identification at a slow-moving landslide in the Vorarlberg Alps. Hydrological Processes 19(8): 1635–1651.

Malet J.-P., O. Maquaire et al.2004, Assessing debris flow hazards associated with slow moving landslides: methodology and numerical analyses. Landslides Vol 1, No 1, 83-90,

Martinez G., K. Vanderlinden, et al. 2010. Field-scale soil moisture patter mapping using electromagnetic induction. Vadose Zone J. 9: 871–881.

McNeill, J. D. 1980a. Electrical conductivity of soils and rocks (Geonics Ltd., Mississauga, ... soil textural class using electro-magnetic induction

Mojid, M.A., D.A. Rose, et al. 2007. A model incorporating the diffuse double layer to predict the electrical conductivity of bulk soil. European Journal of Soil Science 58:560-572.

Nyberg, L. 1996. Spatial variability of soil water content in the covered catchment at Gardsjon, Sweden. Hydrological Processes 10: 89-103.#

Parajka , V. Naeimi et al. 2006. Assimilating scatterometer soil moisture data into conceptual hydrologic models at the regional scale, Hydrol. Earth Syst. Sci., 10, 353–368, 2006

Pellerin, L., and P.E. Wannamaker. 2005. Multi-dimensional electromagnetic modeling and inversion with application to near-surface earth investigations. Computers and Electronics in Agriculture 46:71-102.

Price A.G. and B.O. Bauer. 1984. Small-scale heterogeneity and soil moisture variability in the unsaturated zone. Journal of Hydrology, 70 (1984) 277--293

Rein A., R. Hoffmann, P. Dietrich 2004. Influence of natural time-dependent variations of electrical conductivity on DC resistivity measurements. Journal of Hydrology 285 215–232

Robinson, N.J., P.C. Rampant, et al. 2009. Advances in precision agriculture in south-eastern australia. Ii. Spatio-temporal prediction of crop yield using terrain derivatives and proximally sensed data. Crop & Pasture Science 60:859-869.

Santos, R.N.S. and J.L. Porsani 2011. Comparing performance of instrumental drift correction by linear and quadratic adjusting in inductive electromagnetic data Journal of Applied Geophysics 73 1–7

Schneider, U.1999. Geotechnische Untersuchungen, satellitengestützte (GPS) Bewegungsanalysen und Standsicherheitsüberlegungen an einem Kriechhang in EBNIT, Vorarlberg. University of Karlsruhe.

Takagi K., H.S. Lin 2011. Temporal Dynamics of Soil MoistureSpatial Variability in the Shale Hills Critical Zone Observatory. Vadose Zone J. 10:832–842

Talebi, A., R. Uijlenhoet, and P.A. Troch. 2007. Soil moisture storage and hillslope stability. Nat. Hazards Earth Syst. Sci. 7:523–534.

Triantafilis, J., and S.M. Lesch. 2005. Mapping clay content variation using electromagnetic induction techniques. Computers and Electronics in Agriculture 46:203-237.

Van Asch, Th.W.J., S.J.E. van Dijck and M.R. Hendriks 2001. The role of overland flow and subsurface flow on the spatial distribution of soil moisture in the topsoil. Hydrological Processes 15: 2325–2340.

Van Asch Th.W.J., J.P. Malet, and T.A. Bogaard 2009. The effect of groundwater fluctuations on the velocity pattern of slow-moving landslides . Nat. Hazards Earth Syst. Sci., 9: 739–749.

Wagner W., C. Pathe, et al. 2008. Temporal Stability of Soil Moisture and Radar Backscatter Observed by the Advanced Synthetic Aperture Radar (ASAR). Sensors 8: 1174-1197.

Wienhöfer J., K. Germer et al. 2009, Applied tracers for the observation of subsurface stormflow at the hillslope scale.Hydrol. Earth Syst. Sci., 13, 1145–1161

Wienhöfer, J., and F. Lindenmaier 2010. Challenges in Understanding the Hydrologic Controls on the Mobility of Slow-Moving Landslides. Vadose Zone J. 9

Wong, M.T.F., S. Asseng, et al. 2006. A flexible approach to managing variability in grain yield and nitrate leaching at within-field to farm scales. Precision Agriculture 7:405-417.

Wong, M.T.F., Y.M. Oliver, et al. 2009. Gamma-radiometric assessment of soil depth across a landscape not measurable using electromagnetic surveys. Soil Science Society of America Journal 73:1261-1267.

PART II

Combination of electromagnetic induction (EMI) and gamma-spectrometry using K-means clustering: A study for evaluation of site partitioning

Daniel Altdorff[1] *& Peter Dietrich*[1]*,*

[1] *UFZ Leipzig, Departement Monitoring- and Exploration Technologies, Permoserstraße 15, 04318 Leipzig, Germany*

Accepted: 09/12/2011

Article published online: 2012/03/07

DOI: 10.1002/jpln.201100262

Combination of electromagnetic induction (EMI) and gamma-spectrometry using K-means clustering: A study for evaluation of site partitioning

Daniel Altdorff[1] and Peter Dietrich[1],

[1] Helmholtz Centre for Environmental Research – UFZ / Departement Monitoring- and Exploration Technologies / 04318 Leipzig Germany

Abstract

Today rapid survey methods of proximal soil sensing (PSS) provide an increasing number of different and highly resolved data. These multidimensional data sets can lead to multilayered and complex maps of parameters which are only indirectly related to soil properties and soil functions. However, in applications usually just one clear elementary map is required. It is increasing importance is to tackle this problem utilizing a cluster algorithm for the synthesis and reduction of multidimensional input variables. The cluster algorithm provides a partitioning of the investigated site whereby the units are characterized by the statistics of the PSS data. Therefore, the question that arises is how suitable is the suggested partitioning in terms of the delineation of different soil units.

In this study we investigate the suitability of cluster partitioning through a case study at a medium scale test site (approx. 50,000 m²). Two common PSS methods: electromagnetic induction (EMI) and gamma spectrometry (GS) will be employed to create a data set for partitioning by a K-means cluster. The result of the cluster analysis is a delineation of three different parts. In contrast to previous studies, we evaluate the generated partitions by independent soil properties such as grain size, horizon thickness and color of stratified randomly taken soil samples. The analyses of the soil properties show that one of three clusters significantly differs from the others in terms of grain size distribution and horizon thickness. The partitioning of the other two clusters could not confirmed by the considered parameters of the soil samples. Nevertheless, the case study demonstrates the combination of different PSS data by K-means clustering as a potential approach for site partitioning. However an evaluation of the results of the cluster analysis through the collection and analysis of soil samples is highly recommended.

Keyword: site partitioning, proximal soil sensing, rapid soil survey, cluster analysis, EMI, gamma-spectrometry, site-specific crop management (SSCM),

1. Introduction

The demand for reliable high-precision partitioning of test sites has increased over the past several years. Hence, the investigation of soil properties becomes increasingly important (Lin 2004, Vitharana et al. 2008, Behrens et al 2009, Zacharias et al. 2009, Minasny et al 2010). Adaptive land use management, e.g. agricultural site-specific crop management (SSCM) demands reliable maps which include significant information of relevant criteria from the subsurface (Moral et al. 2010, Twarakavi et al 2010). To address these requirements, several direct and indirect survey methods can provide an increasing number of different and highly resolved data. In particular, the number of proximal soil sensing techniques (PSS) has increased in recent time due to the advantages of non-invasive techniques being time and cost efficient. Common PSS survey methods are for example electromagnetic induction (EMI) (McNeil 1980, Triantafilis and Lesch 2005, Robinson et al. 2009) ground penetrating radar (GPR) (Huisman et al. 2003, Lambot et al 2006, Steelman & Endres 2009), electrical resistivity tomography (ERT) (Pellegrin and Wannemaker 2005; Becht et al. 2006) as well as gamma spectrometry (Pracilio et al.2006,Viscarra Rossel et al. 2006a). Also near infrared (NIR) and far infrared (FIR) (Minasny et al. 2008, Viscarra Rossel et al 2011, McBratney et al. 2011), or chlorophyll fluorescence (Buschmann and Lichtenthaler 1998, Lichtenthaler et al 2005, Hura et al. 2011) have become more popular in the last years.

However, all of these methods response only indirectly to the relevant soil properties for land use and management. In addition, the measured proxies could be affected by several soil properties and leads usually to plurivalent results. Thus a combination of different survey methods improves the quality of the test site map (Kvamme 2006, Paasche et al 2007, Ernenwein 2009). On the other hand, while the development of survey methods and its combination delivers more precise and multidimensional results, also the interpretation becomes often more complicated and usually requires the output of multilayered maps. But the real world application of land use and further investigation approaches, like site-specific crop management (SSCM) (Pringle et al. 2003, Green et al. 2007, Moral et al. 2010) and sampling strategies, usually requires a clear and elementary partitioning of the surface and therefore the synthesis and simplification of characteristics from multilayered result maps. A general challenge is therefore the inclusion of various highly resolved field data to improve the result map according to its natural soil conditions as well as the synthesis and simplification of the essential characteristics from its primary data. Thus users must find a balance between a multiplicity of soil information and the demand for simplification.

The application of a mathematical cluster algorithm is a useful method to tackle this problem. It is based on the minimization of the total sum of squared deviations within a cluster group and has gained increasingly popularity in the geosciences. Through which different sources of soil information are used for the partitioning, synthesis and simplification of different test sites. The majority of authors work predominantly with topographical data (Irvin et al. 1997, Theocharopoulos et al. 1997, Burrough et al. 2000, Bragato 2004, Bakhsh et al. 2007, Etzelmüller et al. 2007), while others use chemical soil properties for partitioning (Søvik & Aagaard 2003, Spijker et al. 2005, Vašát et al 2010), soil texture (e.g. Twarakavi et al 2010), work with theoretical data sets (e.g. Simbahan and Dobermann 2006), use geophysical data as input towards partitioning of subsoil (e.g. Dietrich et al. 1998, Tronicke et al. 2004, Paasche et al. 2007,

Dietrich & Tronicke 2009, Paasche et al. 2010) or use texture and geophysical data (Moral et al. 2010). Li et al (2007) use interdisciplinary input data, e.g. vegetation index, EC, total nitrogen, organic matter and cation exchange for clustering towards the delineation of site-specific management zones.

Since the cluster algorithm was established, the generated partitioning maps have been getting more and more acceptable as means for a valid distinction of soil, e.g. for further management applications. However, clustering is an abstract mathematical tool that works only with discrete values. Thus, the results do not necessarily lead to a reasonable partitioning of the test site, e.g. the number of partitions is inadequate for further purposes. Hence, a critical question is: do the generated cluster partitions really reflect the main characteristics of soil properties?

In this study we evaluate a cluster partitioning approach for the upper horizon of a medium scale test site (approx. 50,000 m²). Thereby two common proximal soil sensing methods, electromagnetic induction (EMI) and gamma spectrometry (GS) were used, and data simplification and synthesis through the use of the common K-means clustering. We discuss the partitioning with respect to the properties of the single clusters. In comparison to previous studies we evaluate the cluster parts by stratified randomly taken soil samples from the upper 60 cm, considering the soil properties grain size, horizon thickness and color of the samples as independent parameters.

If the generated cluster partitioning reflects the main characteristics of the soil, the chosen properties should significantly correlate with the cluster allocation.

2. Materials and Methods

2.1 Test Site

The test site Löbnitz / Saxony, Germany, is situated along the bank of the Mulde River in northern Saxony at around 80 m above sea level with no significant alteration. Located on a flat floodplain in a glacially and periglacially modeled landscape, the subsurface of the site is characterized by unconsolidated sediments with varying proportions of clay, silt, sand and gravel. The cultivation of the area is limited to grassland, which has been left unaltered for several years. Field measurements focused on a 50,000 m² sector between the riverbank and the levee.

2.2 Applied Field Methods

2.2.1 EMI

EMI has been an established tool for subsurface characterization for several decades (McNeil 1980, Triantafilis and Lesch 2005, Robinson et al. 2009, Wong et al 2009). It provides the possibility of cost and time efficiently noninvasive mapping of larger areas. The method is easy to apply and can be automated to collect georeferenced data. We use EMI data due to its potential dependency on several central soil properties, e.g. clay content, porosity, bulk density and moisture content for a rapid currently characterizing of our test field (Rein et al. 2004, Mojid 2007).

In this study we used the ground conductivity meters EM38-DD (Geonics Limited, Mississauga, Ontario Canada) in both horizontal and vertical dipole configurations. Thereby we obtained maps

for integral values related to pseudo depths (PD) of 0.75 m - EM38-DD horizontal (Em38h) and 1.5 m - EM38-DD vertical mode (Em38v. The PD explain the predominate regions of signal origin – see details in McNeil 1980. The EM38DD were used with a connected GPS system, fixed on top of sled at heights of approx. 0.2 m and pulled by an all-terrain vehicle. Accuracy of the GPS was <0.1m. The recording frequencies were 5 Hz at a measuring speed of at most 10 km/h and a track pitch of 5 m.

2.2.2 GS

In addition to the EMI survey we use GS as a rapid indicator of the upper soil due to its dependency on the mineral content. Mineral content could allow us to draw conclusions from the genesis of the soil as well as from distribution processes therein (Taylor et al. 2002, Pracilio et al.2006, Viscarra Rossel et al. 2006a).

In this study we use a GSCar gamma spectrometer (GF Instruments / Czech Republic) with 512 5.66 keV channels and a total measuring range from 100 keV to 3 MeV. In a gamma spectrometer natural γ–radiation emitted from the elements in the upper soil hit a sodium iodine crystal that triggers an electric impulse depending on the energy of the impact (see details in IAEA 2003.). The technical setup of the gamma survey in our study is similar to the EMI measurements, in that a sled was pulled with the GSCar instrument. We use a recording frequency of 0.2 Hz. After recording, we extract the signals related to potassium from the whole recorded energy spectrum (range of 1.370–1.570 MeV), uranium (range of 1.660–1.860 MeV) and thorium (range of 2.410–2.810 MeV) as well as the sum of these three signals, in the following called dose rate (DR) as the common gamma unit. These chemical elements (K, U, Th) can offer insight to soil properties, e.g. to the clay content (Wong and Harper 1999, Taylor et al. 2002, Wong et al. 2008). However these dependencies mostly vary with test site, thus a generalization is not appropriate. Nevertheless, the γdata normally relates to the grain size and can therewith give an insight in sediment distribution of the test site.

Soil sampling for evaluation

In relation to the generated cluster map, we take soil samples by stratified random distribution in the test field (Figure 2). The samples were taken by a Pürckhauer soil probe up to a depth of 0.60 m. We collected 21 soil samples in total and characterized the sediments based on grain size, horizon thickness and color by field designation according to the German soil mapping legislation (BGR 2005), colors were defined according to the Munsell Soil Color Chart ® (e.g Viscarra Rossel et al. 2006b).

2.3 Data analysis and preparation

We recorded two EMI and four gamma data sets. Evident outliers of the EMI were removed by hand, that is single highly exposed unnatural high and low data (< 0.5% of the total raw data). To remove other outliers all recorded raw data sets were filtered with approx. 5 – 95 % from whole data range. Subsequently we interpolated all data sets according to its variogram by block Kriging to obtain separate EC maps for both investigation depth and gamma maps for the three elements potassium, uranium, and thorium (for details see Isaaks and Srivastava 1989, Webster et al. 2001). As common unit we also interpolated the DR data (Fig 1).

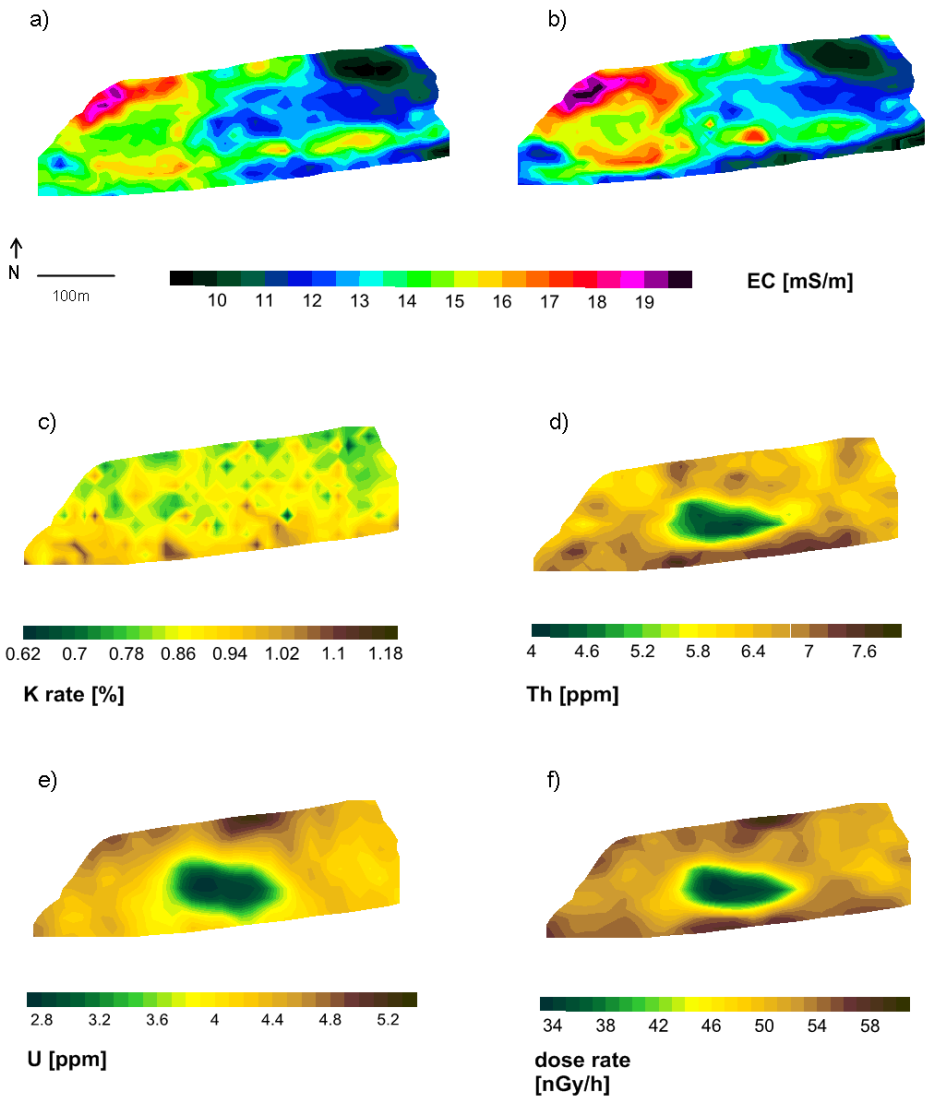

Figure 1: Contour maps of electromagnetic induction (EMI) and gamma-spectrometry (GS): a) Em38h, b) Em38v, c) K, d) Th, e) and f) Dose rate (DR)

For cluster analysis identical coordinates are needed for the discrete variables. Therefore, the same grid was applied to all maps. Regarding the different spatial resolution of the raw data and the size of the test site, we chose a grid size of 4x4 m. Then we combined all grid data to a collective matrix with identical coordinates (*x; y*) and their corresponding values of *p* valid variables.

2.3 Cluster analysis

We mentioned the problem of synthesis and simplification of multivariable data in the introduction. In this study we tackle that problem by mathematical cluster partitioning.

A cluster analysis groups data according to their similarities and reduces the data to its significant characteristics. This method is a functional tool for the allocation of multidimensional data sets and has been becoming common in the geosciences for more than a decade (Irvin et al. 1997, Dietrich et al. 1998, Burrough et al. 2000, Moral et al 2010. Paasche et al. 2010). In this study we use the partitioning clustering of K-means (Dietrich and Tronicke 2009, Twarakavi et al. 2010). It partitions *n* observations into *k* clusters. Thereby, the set of variable values assigned to one spatial point is considered as one observation. The K-means clustering assigns an observation to only one cluster. The mathematic principle of a K-means cluster algorithm is to minimize the total sum Φ of squared deviations from the cluster mean for all considered variables for a predefined number of clusters (MacQueen, 1967):

$$\Phi = \sum_{j=1}^{p} \sum_{i=1}^{k} \sum_{m=1}^{n_i} (x_{i,m,j} - \overline{x_{i,j}})^2 \quad , \qquad (1)$$

where p is the number of variables, k the number of clusters and n_i the number of observations assigned to cluster i. The value $\overline{x_{i,j}}$ is the arithmetic mean for the variable j over all observations assigned to cluster I and $x_{i,m,j}$ is the value of the variable j of the m^{th} observation in the i^{th} cluster. Note that no spatial coordinates are considered in the calculation of Φ.

This study should evaluate the usual praxis of cluster partitioning. The Euclidean distance is the most common distance function, usually the default setting in cluster programs and capable for multi-dimensional data sets (Munkres 2000, Søvik and Aagaard 2003). Thus, from the plurality of possible distances we choose the Euclidean distance. The Euclidean distance needs normalized variables to avoid an overweighting of higher values. Therefore we normalized all variables (v) to a comparable data range with 0.00 as the smallest value to 1 as the biggest value with:

$$v' = (v - min) \cdot \frac{max_{\mathrm{norm}} - min_{\mathrm{norm}}}{max - min} + min_{\mathrm{norm}} \qquad (2)$$

A precondition for reasonable clustering is the independence of input variables to avoid overweighting. Therefore we analyze the data relationships in step B 1). The simplest method for the consideration of data relationships is the plotting of each variable against another. However, often dependencies are more complex and will not become obvious by simple plotting. In this study we work with a principal component analysis (PCA) as a common tool for the discovery of hidden dependencies (Jolliffe 2002, Backhaus et. al 2003, Miranda et al. 2008). The basic principle of PCA is a mathematical transformation of contingently correlated variables into a smaller number of uncorrelated variables, the principal components. The position of the variables

to the coordinates shows their dependencies; same or similar positions indicate a dependency (for details see Backhaus et. al 2003).
Despite its independence, in respect to the quality and the origin of the investigation depth, not all of the recorded data have the same relevance for the aspired partitioning of a test site. Thus for effective cluster partitioning a critical selection of input variables is necessary.
At the start of the cluster analysis, the number of desired clusters has to be appointed. In this study we based the number of suitable clusters on the elbow criterion (Backhaus et al. 2003, Dietrich and Tronicke 2009, Twarakavi et al. 2010). For this purpose, we plot the total sum of squared deviations *s* as a definition of variance vs. the number of clusters *n* . For each cluster the squared deviations of its variables vary with respect to the fitting of data point assortment and usually decrease with increasing of cluster numbers (Simbahan et al. 2006). According to the elbow criterion, the optimal number of clusters is reached when an addition of further clusters yields no more sufficient information:. the break point in this function (see Fig 3)

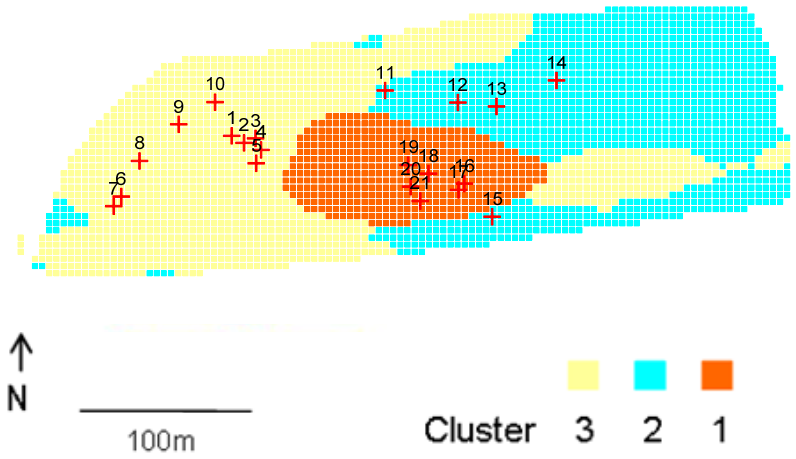

Figure 2 Result map of the demonstrated example including the soil sample locations: the map merge the signals from thorium, uranium and the uppermost EMI data (Em38h). The cluster describes the gamma-depression (cluster 1) as well as the clear E-W division with northern branches (cluster 3) as respect to the Em38h data

For cluster assignment we used the software SYSTAT 12 (Systat Inc. 2007).

3. Results and Discussion

3.1 EMI and gamma results

During the survey we recorded a data setof approx. 30,000-point EMI-data (15,000 for each investigation depth) and approx. 2000-point γ–data. The maps of EM38-DD horizontal (PD 0.75m) and vertical (PD 1.50m) vary only marginally (Figure1). The deeper vertical EM38-DD values are greater than the very near-surface signal from Em38h, possibly a result of drying-out processes towards the surface. In all investigation depths an E-W subdivision is visible with a higher conductive western oval and a southern branch towards the east (Fig 1). The EC increases in the oval by approximately 5 mS/m in both maps. This feature presumably points to local quaternary clay or silt layers with higher electrical conductivity.

The interpolated maps of the γ–spectrometry are shown in Figures 1(c-f). The potassium signal slightly increases towards the south but its spatial distribution scatters intensively as result of a high nugget effect of the data. This indicates a marginal contingent of potassium for the majority of the test field. The thorium and uranium maps show a distinct area of lower concentrations in the middle of the test site. This area could possibly be the result of anthropogenic back filling with significant low gamma-concentration material, e.g. sand that did not affect the EMI signal in the same intensity. Apart from this obvious depression, the spatial characteristics of the single data sets differ from each other. While the rate of thorium increases towards the south similar to the potassium map, the uranium values increase more to the north. The DR is normally used to distinguish the general gamma counts. Consequently DR reflects the signals of all three values, in particular the increase of counts towards the south and the north. In addition to that, the gamma depression in the center is more pronounced in this map (Figure 1f).

Because of the petrophysical properties of soil, apparent electrical conductivity and γ–decay are related, however it is not a simple relationship and depends on several variables (Triantafilis and Lesch 2005, Buchanan and Triantafilis 2009, Robinson et al. 2009, Wong et al 2009). In general, both signals could be affected by similar soil properties. EC could be affected by clay and mineral content, porosity, bulk density and moisture content (Rein et al. 2004, Mojid 2007). Gamma decay also responds to mineral content and could be affected by soil moisture (IAEA 2003). Specifically, both signals are usually affected by clay mineral. Some authors postulate a mostly positive correlation of clay with the EC signal (Hedley et al. 2004, Caroll et al. 2007, Mojid et al. 2007, Weller et al 2007), and others suggest a correlation of clay with the γ–signal (Bierwirth et al. 1996, Wong and Harper 1999, Taylor et al. 2002, Pracilio et al.2006, Viscarra Rossel et al. 2006a). Accordingly, a similar trend in apparent conductivity, in particular the very near-surface values (Em38h) and γ–values, had been expected but did not occur at our test field. The gamma depression for example is indiscernible in the EMI data.

The data from EMI and gamma surveys lead to different resulting maps and illustrate the complexity of interpreting geophysical data from different survey methods. Choosing either map as generally valid excludes some useful information present in the second.

A combination of recorded information of both survey methods is needed. Therefore we use the K-means clustering to prepare a map of the characteristics from the topsoil up to a depth of approx 0.5 m.

3.2 Cluster partitioning and final resulting maps

A reasonable clustering function needs independent input variables. Thus, in this study we did not use the dose rate (DR) due to its function as gamma sum parameter.

By means of the PCA, 94.8 % of the available variables can be described by three components (table 1).

Table 1 Results of the PCA. The Component loadings show the variance of each variable explained by three factors, *e.g.,* factor 1 explains 98.6% of the EM38H signal, factor 2–92.8% of the TH signal, and factor 3–97.6% of the K signal; below the total variance, three factors explain 94.47% of the total variance.

Component Loadings			
	1	2	3
EM38H	0.986	-0.018	0.069
EM38V	0.970	-0.181	-0.079
K	0.062	0.113	0.976
TH	0.040	0.928	0.190
U	0.171	0.867	-0.345

Percent of Total Variance Explained		
1	2	3
38,92	33,18	22,37

Concerning the results of the PCA, a clear fractionation between EMI data and among gamma data is visible. While the EMI data lies more on the first component, the thorium and uranium data correspond with the second component and the third component almost only describes the potassium value. The directions of the EMI vectors in component 1 show once again similarities in the EM38h and EM38v values. Hence, we exclude the EM38v signal also due to its deeper investigation depth. Besides the depression, thorium and uranium differ in its component allocation, so we use both of them in order to bring additional information about the whole test field. The independency of potassium at component 3 would seem most appropriate for further processing. However due to the noisy and insignificant signal, the information of this variable is marginal, thus we drop it out from further proceeding. Regarding the desired partitioning of the upper decimeter, the data from EM38h, Th, and U contains potential information. Consequently we further cluster with these variables.

Now we define the number of appropriate clusters. The plot of the total sum of squared deviations *s* vs. the number of clusters clearly shows the breakpoint at $n = 3$ (see Figure3).

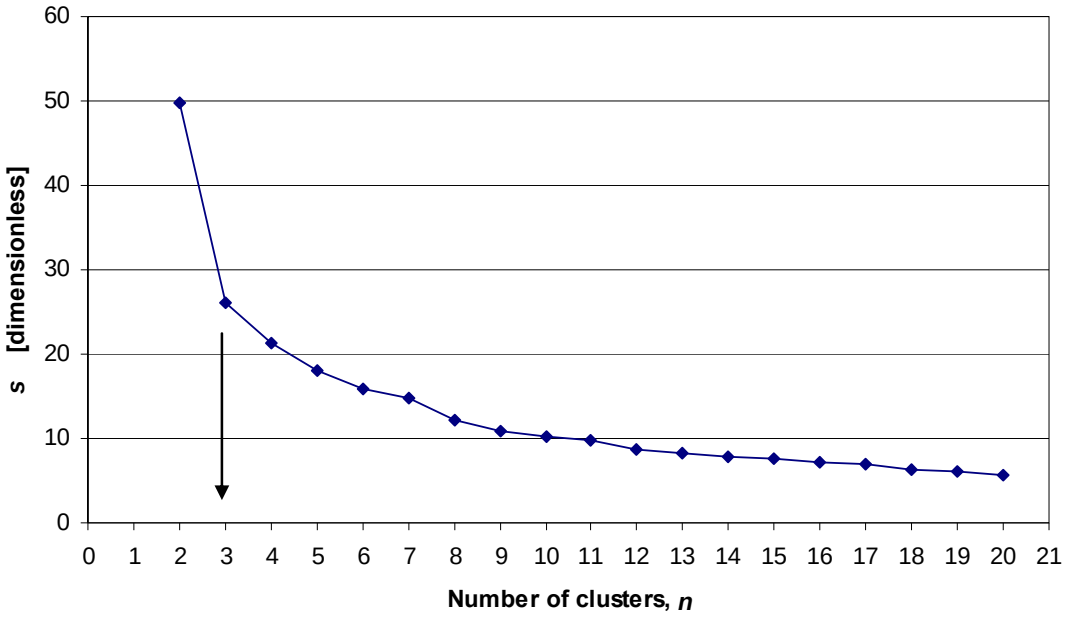

Figure 3: Elbow criteria for selection of appropriated number of cluster , which plots the total sum of squared deviations *s* vs. the number of clusters. The breakpoint is located at $n = 3$

The result map combined the significant distinctions of the gamma and the upper EMI survey (Figure 2). Thereby the partitioning describes the γ–depression (cluster 1) as well as the clear E-W division with southern branches (cluster 3) with respect to the Em38h data.
A closer examination of the cluster properties displays the distinct differences of the three partitions. Figure 4 shows the dimensionless plots of the used variables with its allocation to the corresponding cluster.

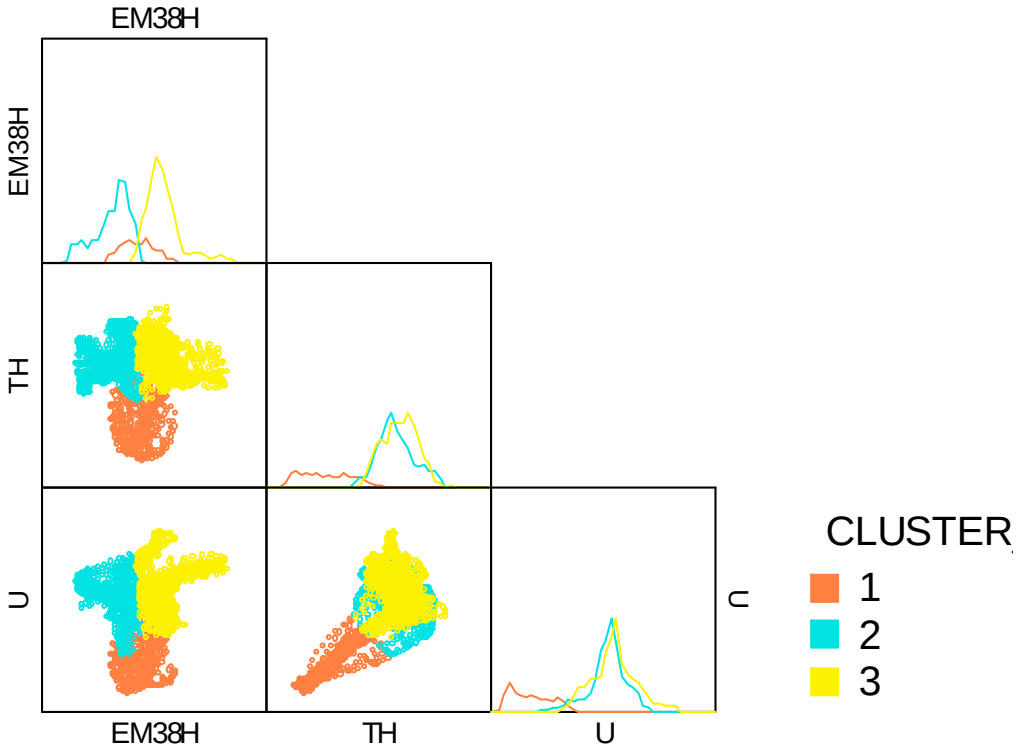

Figure 4: Dimensionless scatter plots for the demonstrated example with its allocation to the corresponding cluster. The lines in the topmost boxes show the data ranges of each variable with its cluster identification by related color; e.g. Em38h values shows a bimodal distribution whereof the higher values belongs to the cluster 3 (yellow line)

The lines in the topmost boxes are histograms of the respective variables and show what data was assigned to the respective clusters. The cluster algorithm splits multimodal data ranges: the bimodal histogram in Em38h was separated by clustering as well as the plateaus from the peak in gamma data. Therewith cluster 1 (orange line) contains low γ–rate (the depression) and medium EC values, cluster 2 (blue line) comprises of medium γ-rate with lower EC values corresponding to the lower Em38h values in the east (compare with Figure 1a) and cluster 3 (yellow line) contains higher Th and U data and the high EC values from the western part in particular. The box and whisker plots in Figure 5 shows the properties of the three clusters in its real units; cluster two and three are differ in its EC values while cluster 1 is characterized by significantly low gamma data.

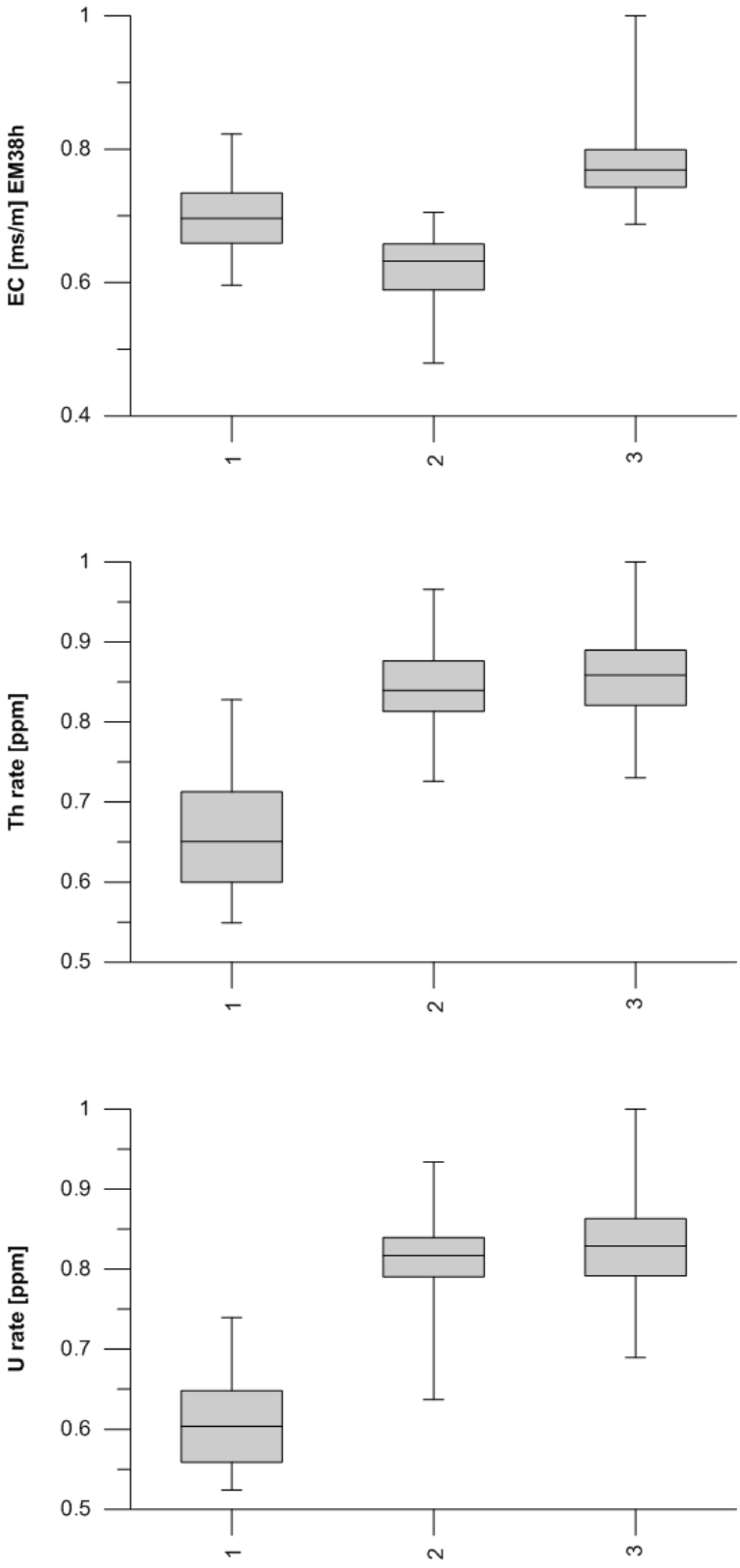

Figure 5 Soil properties of the defined three clusters (x-axe): above EM38h, in the middle the Th and below the U values of each cluster; whiskers indicate the total range, top and the bottom of the box show the 25th and 75th percentiles, and the line inside the box is the median value

3.3 Evaluation of generated cluster map

For the independent evaluation of the generated cluster map, soil samples were taken up to a depth of 0.60 m. 21 soil samples were obtained distributed over all cluster partitions (Figure 2). According to the floodplain, the main grain size of all samples is silt and clay, nevertheless the considered properties vary (table 2).

Cluster 1 (the gamma depression) shows significant dissimilarities to cluster 2 and 3 (Table 2).

Table 2 Properties of the soil samples; number, grain size (cy – clay, si – silt, s – sand, g – gravel), A horizon thickness from surface, color from 1st and 2nd layer (after Munsell Soil Color Chart ®) and cluster allocation

Sample #	Grain size 1th Layer	Grain size 2nd Layer	A horizon [cm]	Soil Color 1th Layer [YR/Value/Chroma]	Soil Color 2nd Layer [YR/Value/Chroma]	Cluster allocation
1	Si si cy	Si cy	25	10 YR 4 4	7.5YR 5 5	3
2	Si si cy	Si cy	25	10 YR 4 5	7.5YR 4 4	3
3	Si si cy	Si cy	29	10 YR 5 3	10 YR 5 4	3
4	Si si cy	Si cy	26	10 YR 4 3	10 YR 4 4	3
5	Si si cy	Si cy	30	10 YR 4 4	7.5YR 4 4	3
6	Si si cy	Si cy	30	10 YR 5 4	10 YR 4 4	3
7	Si si cy	Si cy	38	10 YR 4 3	10 YR 4 4	3
8	Si si cy	Si cy	40	10 YR 4 3	10 YR 5 4	3
9	Si si cy	Si cy	36	10 YR 5 3	10 YR 4 4	3
10	Si si cy	Si cy	32	10 YR 5 4	10 YR 4 4	3
11	Si si cy	Si cy	22	10 YR 4 3	10 YR 4 4	2
12	Si si cy	Si cy	26	10 YR 4 3	10 YR 5 4	2
13	Si si cy	Si cy	35	10 YR 4 3	10 YR 5 4	2
14	Si si cy	Si cy	28	10 YR 4 3	10 YR 5 4	2
15	Si si cy	Si cy	28	10 YR 5 4	7.5YR 5 4	2
16	Si s cy g	Si cy s	41	10 YR 5 4	10 YR 4 4	1
17	Si s cy g	Si cy s	43	10 YR 5 4	10 YR 4 4	1
18	Si s cy g	Si cy s	48	10 YR 5 4	10 YR 4 4	1
19	Si s cy g	Si cy s g	41	10 YR 5 4	10 YR 4 4	1
20	Si s cy g	Si s cy	42	7.5YR 5 3	7.5YR 43	1
21	Si s cy g	Si cy s	50	10 YR 5 3	10 YR 4 2	1

It is characterized by the presence of sand and gravel in the soil with a gravel size up to 2 cm, no other sample contains sand or grain, also the clay content was slightly lower than in cluster 2 and 3. Also the thickness of the first layer (see also Figure 6) is in a completely other range then cluster 2 and 3 with no overlapping.

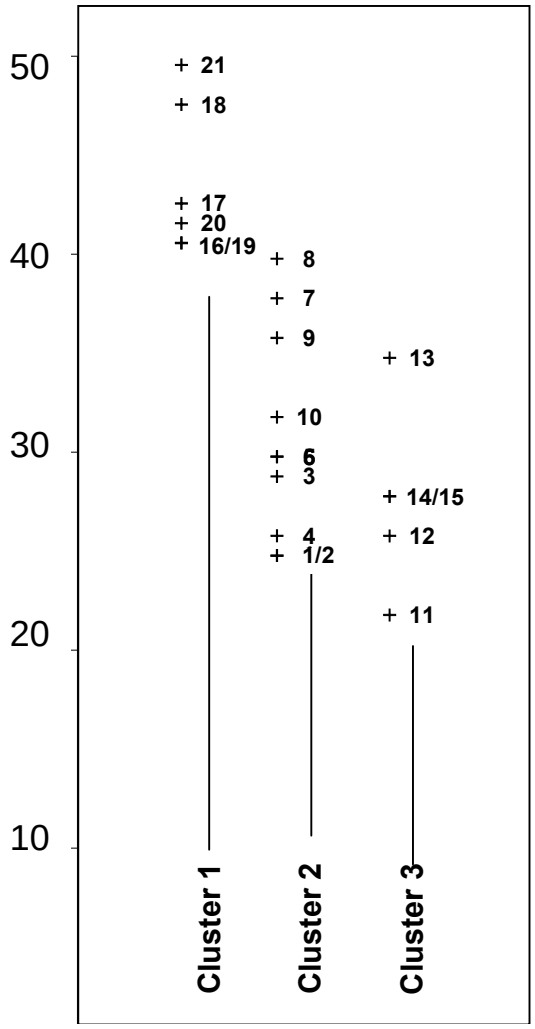

Figure 6: Custer allocation (x-axe) vs. thickness of the A layer / y axe [cm], the thickness of the A layer variation corresponds with cluster 1 only, distinction between 2 and 3 are not significant

In addition, the colors within cluster 1 are mostly consistent.

The relative high content of sand and gravel at this part is a probable explanation for the relatively low gamma values due to the potential negative correlation of sand and gamma counts (Taylor et al 2002). Probably this part is an anthropogenic relic from the riverbank building; maybe by refilling soil, it may also explain the significant deeper first horizon. Regarding these results, the cluster partitioning for this part was successful.

The distinction between cluster 2 and 3 is not clear and only marginal; grain size and horizon thickness are similar, only the color allocation in cluster 2 is more homogeneous but not sufficiently significant. The considered properties of cluster 2 and 3 did not lead to the cluster allocation. In this respect the suggested partitioning does not fit the main characteristics. Regarding this fact, the distinction between them comes from differences in the EC value, which cannot be explained by the grain size or horizon thickness. Differences in EC possibly originate from changes in soil moisture that could affect the EC signal significantly (Dietrich 1999, Rein et

al. 2004, Buchanan & Triantafilis 2009). However, to consider the soil moisture distribution by EMI, a much more complex monitoring strategy is needed. Also, the soil moisture was not a part of the study aim due to its variability.
Regarding the demonstrated three cluster solution only one of the three defined parts could be successfully validated. Concerning the chosen number of clusters, this example shows that the appropriated number of clusters cannot necessarily be defined by technical estimation (e.g. elbow criteria) and also needs the sense of proportion. For this test site probably a two cluster solution could be more adequate with a distinction between the gamma depression and its surroundings.

4. Conclusion

This study combines EMI and gamma spectrometry surveys towards the evaluation of test site partitioning. The EMI and gamma data describe different soil pattern and consequently lead to different resulting maps. We apply a common K-means cluster algorithm for synthesis and simplification of various input data and generate a map for the upper soil. This approach leads to an integral map that reduces and comprises the essential characteristics of the used input variables. The 3 cluster map contains the E-W partitioning from EMI as well as the prominent gamma depression in the center of the test site and reflects the fundamental characteristics of the input data.
However, an independent evaluation of the suggested clusters shows that not all three partitions can be confirmed by independent soil samples. The analysis of the soil properties shows that one of three clusters significantly differs from the others in terms of grain size distribution and horizon thickness The partitioning of the other two clusters could not confirmed by the considered parameters of the soil samples. A potential reason for the difficulties by the sample allocation to these clusters is maybe the influence of several factors on the measured EC, such as soil moisture, that have not been focused on in this study.
Nevertheless, one partition describes the main character of soil properties, grain size and horizon thickness without any ground truthing. Thus, the demonstrated combination of high resolute PSS data and K-means clustering is a potential approach for cost and time efficient site partitioning. However a critical evaluation of resulting final map by soil sampling is nevertheless recommended. Thereby the cluster partitions allow for stratified randomly taken soil samples, a decreasing of sample numbers, and thus decreased time, effort and cost.

Acknowledgement

The authors thank Steffen Popp for his support during the field work and Steffen Zacharias for his constructive help with statistical questions. The authors also acknowledge the EU project iSOIL and the Helmholtz research platform MOSAIC for providing the technical equipment. Special thanks to John Mosquera from the University of Waterloo, Canada, for editing the manuscript.

References

Backhaus, K., B. Erichson, et al. 2003. Multivariante Analysemethoden. Springer ISBN 3-540-00491-2

Becht, A., Appel, E., Dietrich, P. 2006. Analysis of multi-offset GPR data: a case study in a coarse-grained gravel aquifer Near Surface Geophysics 4 (4), 227 – 240

Behrens T., O. Schneider, et al. 2009. Analysis on pedodiversity and spatial subset representativity - the German soil map 1:1,000,000. J. Plant Nutr. Soil Sci.: 172, 91–100.

Bierwirth, P. Gessler P et al. 1996. Empirical investigation of airborne gamma-ray images as an indicator of soil properties Wagga Wagga, NSW. AGSO Record

Bohling G.C. 1997. GSLIB-style programs for discriminant analysis and regionalized classification. Computers & Geosciences Volume 23, Issue 7, August 1997, Pages 739-761

Bohling, G.C. Davis, J.C. et al. 1998. Singularity and Nonnormality in the Classification of Compositional Data. Mathematical Geology, Vol. 30, No. 1

Bragato, G. 2004. Fuzzy continuous classification and spatial interpolation in conventional soil survey for soil mapping of the lower piave plain. Geoderma 118:1-16.

Buchanan, S., and J. Triantafilis. 2009. Mapping water table depth using geophysical and environmental variables. Ground Water 47:80-96.

Bundesanstalt für Geowissenschaften und Rohstoffe (BGR) 2005, Bodenkundliche Kartieranleitung. Schweizerbart'Sche Verlagsbuchhandlung; ISBN-10: 3510959205

Buschmann C, Lichtenthaler H.K. 1998. Principles and characteristics of multi-colour fluorescence imaging of plants JOURNAL OF PLANT PHYSIOLOGY Volume: 152 Issue: 2-3 Pages: 297-314

Burrough, P.A., P.F.M. van Gaans, et al. 2000. High-resolution landform classification using fuzzy k-means. Fuzzy Sets and Systems 113:37-52.

Caroll, Z.L and. Oliver M.A. 2005. Exploring the spatial relations between soil physical properties and apparent electrical conductivity. Geoderma Volume 128, Issues 3-4, Pages 354-374

Dietrich, P. Fechner, T., et al. 1998. A intergated hydrogeophysical approach to sufsurface characterizon. in: Herbert, M and Kovar, K. Groundwater Quality: Remediation and Protection, IAHS Publication No. 250, ISSN 0144-7815:513-520.

Dietrich, P., Tronicke, J., 2009. Integrated analysis and interpretation of cross-hole P- and S-wave tomograms: a case study. Near Geophysics 7, Issue 2, 101-109.

Etzelmüller, B., Romstad, B., Fjellanger, J., 2007. Automatic regional classification of topography. Norwegian Journal of Geology 87, 167- 180.

Ernenwein, E.G. 2009. Integration of multidimensional archaeogeophysical data using supervised and unsupervised classification. Near Surface Geophysics 7:147-158.

Green T. R, J. D. Salas, A. Martinez and R. H. Erskinea. 2007. Relating cropnext term yield to topographic attributes using Spatial Analysis Neural Networks and regression. Geoderma Volume 139, Issues 1-2, 15 Pages 23-37

Hedley, C.B., I.Y. Yule, et al. 2004. Rapid identification of soil textural and management zones using electromagnetic induction sensing of soils. Australian Journal of Soil Research 42:389-400.

Huisman, J. A., S. S. Hubbard, J. D. Redman, et al 2003, Measuring Soil Water Content with Ground Penetrating Radar: A Review, Vadose Zone Journal 2:476–491

Hura T, Hura K, Grzesiak M. 2011. Soil Drought Applied During the Vegetative Growth of Triticale Modifies the Physiological and Biochemical Adaptation to Drought During the Generative Development. Journal of Agronomy and Crop Science Volume: 197 Issue: 2 Pages: 113-123

Internatrional Atomic Energy Agency 2003. Guidelines for radioelement mapping using gamma ray spectrometry data ISBN 92–0–108303–3

Irvin, B.J., S.J. Ventura, et al. 1997. Fuzzy and isodata classification of landform elements from digital terrain data in Pleasant Valley, Wisconsin. Geoderma 77:137-154.

Isaaks E. H., and Srivastava R. M. 1989. An Introduction to Applied Geostatistics, New York Oxford OXFORD UNIVERSITY PRESS

Kvamme, K.L. 2006. Integrating multidimensional geophysical data. Archeological Prospection 13:57-72

Lambot, S., Weihermüller, L., Huisman J.A., et al. 2006, Analysis of air-launched ground-penetrating radar techniques to measure the soil surface water content WATER RESOURCES RESEARCH, VOL. 42, W11403, doi:10.1029/2006WR005097

Li, Y., Y. Shi, F. Li, H-Y. Li. Delineation of site-specific management zones using fuzzy clustering analysis in a coastal saline land. Computers and Electronics in Agriculture, Volume 56, Issue 2, April 2007, Pages 174-186

Lichtenthaler HK, Langsdorf G, Lenk S, et al. 2005. Chlorophyll fluorescence imaging of photosynthetic activity with the flash-lamp fluorescence imaging syste Photosyntetica Volume: 43 Issue: 3 Pages: 355-369 Published: 2005

Lin, H.S. 2004. Hydropedology. Geotimes 49:28-29.

MacQueen, J., 1967. Some methods for classification and analysis of multivariate observations. Pp. 281-297 in: L. M. Le Cam and J. Neyman. Proceedings of the fifth Berkeley symposium on mathematical statistics and probability, Vol. 1.

McBratney A.B., B. Minasny, et al. Removing the effect of soil moisture from NIR diffuse reflectance spectra for prediction of soil carbon. The Second Global Workshop on Proximal Soil Sensing – Montreal 2011 / 108

McNeil, J. D. 1980. Electromagnetic terrain conductivity measurment at low induction numbers.Geonics. Ltd., Technical Note TN-6.

Minasny, B, A.B. McBratney and A.E. Hartemink 2010 Global pedodiversity, taxonomic distance, and the World Reference Base. Geoderma 155: 132-139

Minasny, B., McBratney, A.B., Tranter, G., Murphy, B. 2008. Using soil knowledge for the evaluation of mid-infrared diffuse reflectance spectroscopy for predicting soil physical and mechanical properties. European Journal of Soil Science 59, 960-971.

Mojid, M.A., D.A. Rose, et al. 2007. A model incorporating the diffuse double layer to predict the electrical conductivity of bulk soil. European Journal of Soil Science 58:560-572.

Moral F.J., J.M. Terron, J.R. et al. 2010. Partitioning of management zones using mobile measurements of soil apparent electrical conductivity and multivariate geostatistical techniques. Soil and Tillage Research 106 (2010) 335–343

Moral F.J., J.M. Terrón and F.J. Rebollo. 2011. Site-specific managementnext term zones

based on the Rasch model and geostatistical techniques. Computers and Electronics in Agriculture Volume 75, Issue 2, Pages 223-230

Munkres, J.R. 2000. Typology. Prenticent Hall Inc. ISBN:0-13-181629-2

Paasche, H., J. Tronicke, P. Dietrich 2007, Cooperative inversion based on fuzzy c-means cluster analysis - application to field data, 13th European Meeting of Environmental and Engineering Geophysics

Paasche, H., J. Tronicke, P. Dietrich, 2010. Automated integration of partially colocated models: Subsurface zonation using a modified fuzzy c-means cluster analysis algorithm, Geophysics. 75(3). p.P11

Pellerin, L., Wannamaker P. E., 2005, Multi-dimensional electromagnetic modeling and inversion with application to near-surface earth investigations. Computers and Electronics in Agriculture 46 71–102

Pracilio, G., M.L. Adams, et al. 2006. Determination of spatial distribution patterns of clay and plant available potassium contents in surface soils at the farm scale using high resolution gamma ray spectrometry. Plant and Soil 282:67-82.

Pringle M.J., A.B. McBratney, B.M. Whelana and J.A. Taylora. 2003. A preliminary approach to assessing the opportunity for site-specific crop managementnext term in a field, using yield monitor data. Agricultural Systems Vol. 76, Issue 1, Pages 273-292

Rein, A., R. Hoffmann, P. Dietrich 2004. Influence of natural time-dependent variations of electrical conductivity on DC resistivity measurements Journal of Hydrology 285 215–232

Robinson, N.J., P.C. Rampant, et al. 2009. Advances in precision agriculture in south-eastern australia. Ii. Spatio-temporal prediction of crop yield using terrain derivatives and proximally sensed data. Crop and Pasture Science 60:859-869.

Søvik, A.K., and P. Aagaard. 2003. Spatial variability of a solid porous framework with regard to chemical and physical properties. Geoderma 113:47-76.

Spijker, J., S.P. Vriend, et al. 2005. Natural and anthropogenic patterns of covariance and spatial variability of minor and trace elements in agricultural topsoil. Geoderma 127:24-35.

Steelman, C M., Endres, A. L. 2009, Evolution of high-frequency ground-penetrating radar direct ground wave propagation during thin frozen soil layer development Cold Regions Science and Technology 57 116–122

Simbahan, G.C., and A. Dobermann. 2006. An algorithm for spatially constrained classification of categorical and continuous soil properties. Geoderma 136:504-523.

SYSTAT Software . 2007. Product information. San Jose SYSTAT Software, Inc. www. systat.com

Taylor, M.J., Smettem K. 2002. Relationships between soil properties and high-resolution radiometrics, central eastern Wheatbelt, Western Australia. Exploration Geophysics 33(2) 95 - 102

Theocharopoulos, S.P., P.V. Petrakis, et al. 1997. Multivariate analysis of soil grid data as a soil classification and mapping tool: The case study of a homogeneous plain in vagia, viotia, greece. Geoderma 77:63-79.

Triantafilis, J., and S.M. Lesch. 2005. Mapping clay content variation using electromagnetic induction techniques. Computers and Electronics in Agriculture 46:203-237.

Twarakavi, N.K.C. J. Simunek, et al. 2010. Can texture-based classification optimally classify

soils with respect to soil hydraulics? Water Resources Research 46:W01501

Vitharana U.W.A, T. Saey a, et al. 2008. Upgrading a 1/20,000 soil map with an apparent electrical conductivity survey. Geoderma 148: 107–112.

Viscarra Rossel R.A., H. J. Taylor et al. 2006a. Multivariate calibration of hyperspectral γ-ray energy spectra for proximal soil sensing. European Journal of Soil Science, Volume 58, Issue 1, pages 343–353

Viscarra Rossel R.A., B. Minasny, et al. 2006b. Colour space models for soil science. Geoderma, Volume 133, Issues 3-4

Viscarra Rossel R.A., Chappell, A. et al. 2011. On the soil information content of visible–near infrared reflectance spectra European Journal of Soil Science Special Issue: Pedometrics Volume 62, Issue 3, pages 442–453

Webster, R., A. Margaret, et al. 2001. Geostatistics for Environmental Scientists. John Wiley and Sons Ltd. Chichester. 271 p.

Weller, U., M. Zipprich, et al. 2007. Mapping clay content across boundaries at the landscape scale with electromagnetic induction. Soil Science Society of America Journal 71:1740-1747.

Wong, M.T.F., and R.J. Harper. 1999. Use of on-ground gamma-ray spectrometry to measure plant-available potassium and other topsoil attributes. Australian Journal of Soil Research 37:267-277.

Wong, M.T.F., S. Asseng, et al. 2008. Mapping subsoil acidity and shallow soil across a field with information from yield maps, geophysical sensing and the grower. Precision Agriculture 9:3-15.

Wong, M.T.F., Y.M. Oliver, et al. 2009. Gamma-radiometric assessment of soil depth across a landscape not measurable using electromagnetic surveys. Soil Science Society of America Journal 73:1261-1267.

Zacharias, S., D. Altdorff et al. 2009. Hydropedology and Pedotransfer Functions. in E.J. van Henten, D. Goense et al: Precision agriculture ´09. Wageningen Academic Publishers, pp. 545-550

PART III

Detection of ancient active channel zones using hydrogeophysical methods: An approach to more effective channel restoration

Daniel Altdorff1, Peter Dietrich1, Jannis Epting2, Peter Huggenberger2

[1] UFZ Leipzig, Departement Monitoring- and Exploration Technologies, Germany; [2] Applied and Environmental Geology / Department of Environmental Sciences / University of Basel

Prepared manusrcibt for subbmition to Geomorphology
Expected submitting date: Dezember 2011 / January 2012

Detection of ancient active channel zones using hydrogeophysical methods: An approach to more effective channel restoration

Daniel Altdorff[1], Peter Dietrich[1], Jannis Epting[2], Peter Huggenberger[2]

[1] Helmholtz Centre for Environmental Research – UFZ / Departement Monitoring- and Exploration Technologies [2] Applied and Environmental Geology / Department of Environmental Sciences / University of Basel

Abstract

River restoration and applied restoration measures are of increasing importance for integrated water resources management (IWRM) as well as for ecosystem services including water storage and purification, habitat provision and climate regulation. However, often river restoration is planned and realized by engineering and constructing aspects only and hydrogeological settings and ancient stream channels are neglected. As a result, desired outcomes of restoration projects are reduced with no significant alteration of stream conditions by simultaneously increasing costs. An opportunity to reach the full restoration potential is to investigate ancient active stream courses by applying hydrogeophysical methods as basis for targeted restoration measures.

In this study, we investigate the ancient active channel zone in a floodplain of a heavyly modified low-mountain river in Switzerland by means of hydrogeophysical data with two different approaches. In the first approach we use data from electromagnetic induction (EMI) with four different integral depths (0.75 to 6m) and gamma-spectrometry (GS) to generate a geological structure model (GSM) iteratively by means of various electric conductivity (EC) forward models. This geological structure model allows a 3D delineation of potential ancient stream courses. In the iterative modelling process we vary the geological input parameters based on the measured data until the synthetic EC maps fit to the real EC values. Subsequently, we use the best fitted input data for generation of final GSM as basis for active reconstruction measurements.

In a second approach we generate a K-means cluster map for the floodplain surface that combines the main characteristics from multilayered subsurface data by synthesis and simplification. The obtained cluster delineates parts of significant different soil conditions and therewith provides an indication for areas of potential ancient active channel zones. Hence, the map distinguishes between areas of higher and lower flood vulnerability as well as higher and lower possible river affection as basis for land use recommendation.

A comparison with independent Ground Penetrating Radar (GPR) data has confirmed the obtained structures of both results. Thus, both demonstrated approaches are appropriate tools for the characterization of test sites with no additional subsurface information and with the capacity for detecting ancient active channel zones.

Keyword: river restoration, ancient stream course, EMI, gamma-spectrometry, EC forward modelling, cluster analysis, GPR

1. Introduction

Intact river conditions gain significance due to their positive effects on several environmental processes and their corresponding management relations, e.g. integrated water resources management (IWRM), flood and drought prevention as well as for ecological issues, like habitat protection and revegetation (Rohde et al 2004). Since this relation has become apparent, several legislation frameworks now require river protection and rehabilitation to preserve the river systems and to avoid negative effects of anthropogenic chances, e.g. the 'Water and Rivers Commission Act' (1995) in Australia, the ´Water Framework Direction´ (WFD) (EC 2000) and the Swiss ´Gewässerschutzverordnung´ (Swiss Government 2011) in Europe. The WFD for example requires a ´good ecological status´ for all water bodies until 2015, which means *"the biological quality […] show low levels of distortion resulting from human activity but deviate only slightly from […] undisturbed conditions."* Nevertheless, the majority of rivers in the industrialized countries remain anthropogenicly modified - in Central and Western Europe approximately 15 - 30% of them heavily according to the WFD (EEA 2011).

An opportunity to upgrade the river and floodplain status is to attempt a (partial) restoration of the natural river conditions. River restoration can increase flow storage and energy dissipation of passing flood waves. These measures include increased widening, remeandering of the river channel, increasing channel length relative to the floodplain; restoring channel-floodplain connectivity; and revegetating banks and the floodplain (Sholtes and Doyle 2011). Although channel and floodplain restoration is generally accepted as forward-looking prospect for flood attenuation and habitat protection, studies about its efficiency are still seldom and numerous restoration efforts remain without the desired functional effects (Sivirichi et al. 2011). A possible explanation for the failure of restoration success is that in applications usually standardized common reconstruction measures are applied instead of individually adjusted and best optimized measures. Also, river restoration is usually planned and realized in consideration of engineering and constructing aspects only and hydrogeological settings and ancient stream morphology are neglected. As a result, desired outcomes of restoration projects are reduced with no significant alteration of stream conditions by simultaneously increasing costs (Lennox et al. 2011). In Switzerland, where the demonstrated approach took place, the current ´Gewässerschutzverordnung´ from August 1st 2011 defines several requirements for the purpose of river revitalization . For the river wideness spatial conditions dependent on the depth of the channel bottom exist. For channels deeper than 1m a width of 11m is required; 1-5m depth require a width of six times the depth plus 5m and rivers deeper than 5m require a width of depth plus 30m (capture 7, part 1). Also, the width of the anthropogenicly affected rivers is defined. But do these standardized common reconstruction recommendations really reflect the natural conditions of rivers? The key element in terms of river restoration is the estimation of its natural character.

An opportunity for obtaining the natural river conditions and thus for individually adjusted restoration measurements is given by the investigation of ancient active stream channels (AAC). The AAC represents the area of the morphological and depositional features generated in the transition between high and low flows. Within this area a dynamic interaction between groundwater and surface water takes place. Thereby, the accumulated morphological patterns, e.g. gravel banks act as drainage as well as buffer depending on the current discharge (Figure 1).

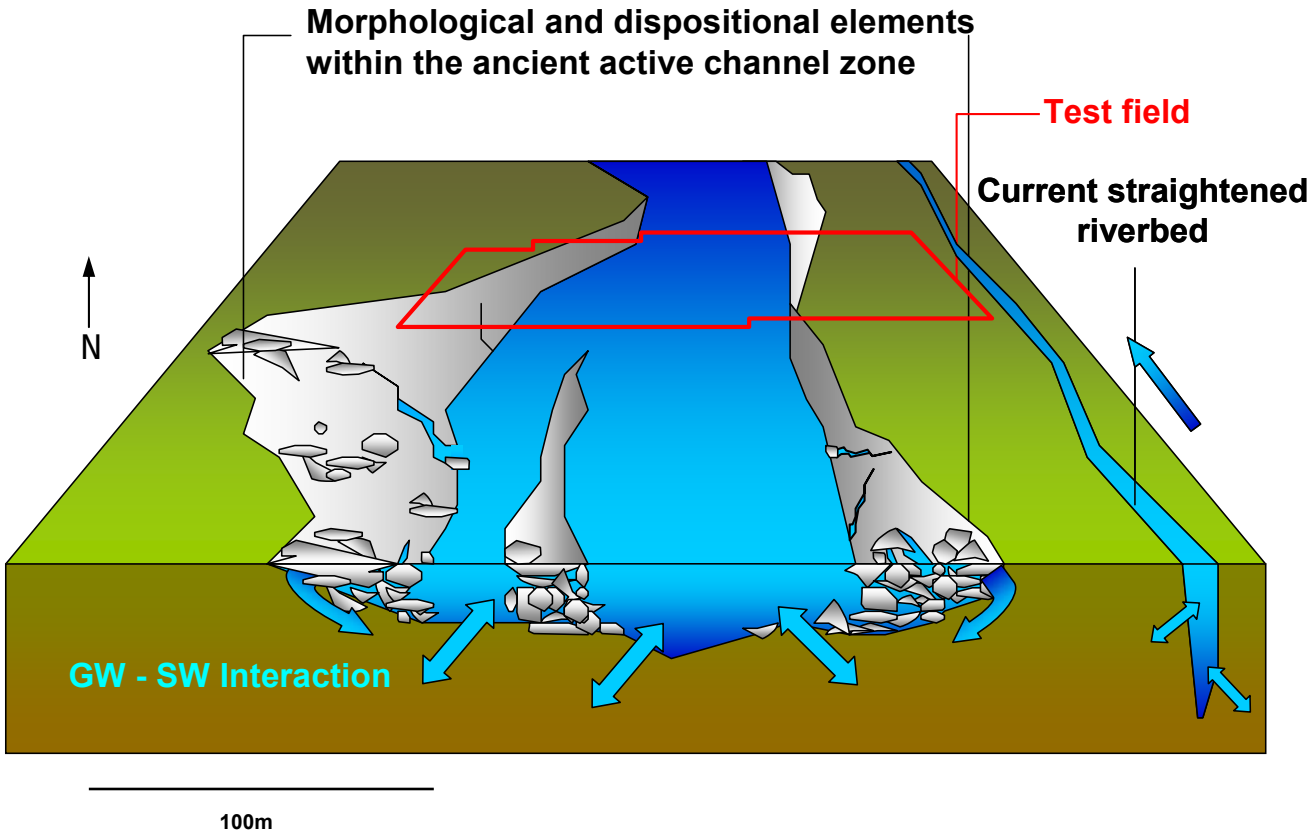

Figure 1 Sketch of the investigated floodplain: possible location of ancient active channel (AAC) with geomorphological elements developed in the transition between high and low flow conditions (middle), the current straightened riverbed rigtht (flow direction toward north) and location of the test field (red line)

A connection between these permeable units of the ancient river and the present river could lead to the best restoration potential. In addition, due to the AAC system information of the dimension from the morphological units could be estimated, that provides an assessment of the process scale involved (square meter or square kilometre) as basis for flood prevention management.
However, an investigation of the AAC system demands a consideration of rivers in context of its spatial and temporal character in past, present, and future (Larsen & Harvey 2011). The description of the status of rivers in the most valid legislation frameworks, e.g. in Europe the WFD as well as the analogue Swiss legislation, does not consider the ancient active channel zones. Therefore, in the past decade Brierley and Fryirs have developed a method for assessment of key attributes of river styles framework as an integrative river classification scheme (Brierley and Fryirs 2000, 2005, 2008). This method includes the stages of (1) river character and behavior, (2) geomorphic river condition, (3) its recovering potential and (4) possible management applications. Considering the workflow of this process one main challenge is the investigation of

geomorphic river conditions in respect of the recovering potential and its possible implementation. In respect of the budget of the corresponding communes / landowner methods for characterizing of subsurface structures are demanded that delineate potential AAC zones by non invasive, cost and time efficient methods.

Ideally, the detected AAC area is reconstructed or a connection of the present river to the AAC is established, e.g. by excavation to reroute parts of the stream to the AAC. However, in most cases a restoration of the ancient river course is practically unfeasible due to limitations of funding and/or other limitations like land use conflicts with the agriculture industry. If the theoretical restoration potential due to these limitations can not be realized, a partitioning of the surface should allow the communes to distinguish between areas inside and outside the AAC. Hydrologically higher connected and highly flood-prone areas can thus be distinguished from less endangered parts. However, this surface partitioning demands a synthesis and simplification of characteristics from multilayered subsurface data. The surface partitioning should reflect the natural conditions of different layers in the subsurface regarding the ancient river streams. If the location of the ancient river stream is known, selective management options reduce potentially adverse effects on anthropogenic use. For example, application of fertilizers should significantly vary between regions of ancient active channel zones and their corresponding alluvial clay. Also potential overflow areas have to be identified.

Regardless of type and extent of a reconstruction or protection measure, the knowledge the characteristic of the ancient river stream is essential for all effective management options. The knowledge about the existence of an AAC can be derived from hydro-geophysical measurements. Hydro-geophysical methods are non-invasive techniques providing time and cost efficient surveys. Common hydro-geophysical methods are electromagnetic induction (EMI) (McNeil 1980, Triantafilis and Lesch 2005, Robinson et al. 2009), electrical resistivity tomography (ERT) (Pellegrin and Wannemaker 2005; Becht et al. 2006), ground penetrating radar (GPR) (Huisman et al. 2003, Lambot et al 2006, Steelman & Endres 2009) or gamma spectrometry (Pracilio et al.2006, Viscarra Rossel et al. 2006). These methods have been successfully applied in hydrogeological research for several years. Buchanan and Triantafilis (2009) have investigated the water table with EMI and gamma spectrometry and Abu et al (2008) have derived the water holding capacity from an EMI signal. Nyquist et al. (2008) have used ERT on river stream bottoms to map groundwater discharge and assess groundwater-surface water interactions within streams. Huggenberger and Meier (1993) have used GPR to investigate fluvial sediments, Chem et al (2001) have attempted the investigation of hydrological conductivity with GPR and Truss et al. (2007) have derived high resolution hydrological soil properties.

In this study, we investigate a part of a floodplain of a heavily modified (see definition in WFD) low-mountain river in Switzerland with different noninvasive hydrogeophysical methods in order to delineate the AAC for further restoration and management measures. The part of the floodplain under investigation comprises the region of the ancient active river channel. We combine data from electromagnetic induction (EMI), gamma-spectrometry (GS) and ground penetrating radar (GPR) to investigate the subsurface of the ancient stream courses. We apply and compare two different approaches. In a first approach we generate a 3D model of the subsurface. The obtained data are used for an EMI forward modelling and inversion to compare the predicted EMI maps with the measuredones. Thereby, the input parameters of the best fitted model are being used for a geological structure model. This model describes different layers and therewith possible ancient

active channels as basis for active reconstruction measurements. In the second approach we generate a K-means cluster map of the floodplain surface (2D) that combines the main characteristics of multilayered subsurface data. The obtained cluster delineates parts of significantly different soil conditions and thus provides an indication for areas of potential ancient active channel zones. Hence, the map distinguishes between areas of high and low flood vulnerability as well as areas of possibly high and low river affection as a basis for land use recommendations.
Both approaches above should delineate the main characteristics of AACs at test sites with no additional subsurface information.

2. Field methods and data base

2.1 Test site

The investigated floodplain is part of the low mountain river Enziwigger two kilometres north of Hergiswill in Canton Luzern, Switzerland. The Enziwigger generally runs from South to North and has a catchment of approx. 38 km² and a precipitation average of 1055 mm (2000 to 2010). The water retention and the corresponding storage capacity of the catchment soils are marginal. Thus precipitation events dominate the flow rate. Average flow rate is 2 m³/s (City of Willisau, 2008). The aquitard consist of cohesive conglomerate und sandstone of the upper molasses and is overlayed with highly hydraulic conductive alluvial gravel (Geological Map Switzerland 1994). The river has been straightened twice, first in the early 19th century (Geographical Dictionary Switzerland 1910) and second in the early 1970´s. Altogether approx. 60% of the whole stream is currently modified. The test site is situated in a quaternary valley with altitude decreasing slightly towards the North and comprises an area of approx. 3500 m² currently used for agricultural issues (Figure 1 and 2).

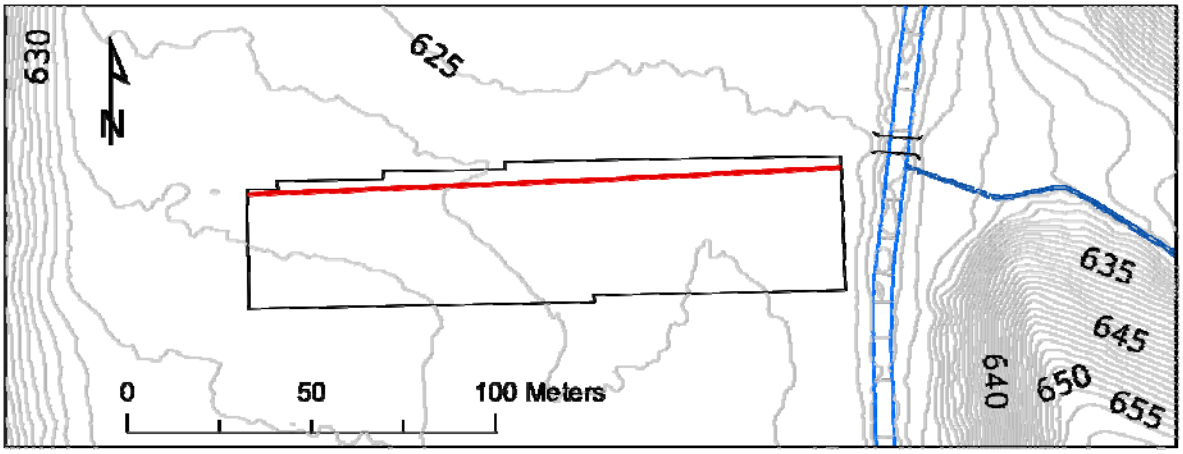

Figure 2 Investigated part of the floodplain: Enziwigger (blue double line) with tributary (blue line), test field (black framed) and location of GPR profile (red line) as well as contour lines of the surface topography [m above sea level]

The corresponding river part was relocated from its original meandering position to the easternmost valley during the second modification. This segment is characterized by both riverbank block constrictions and riverbed steps, which should control the stream velocity. Between the steps the river bed increases due to barring of water and lose therewith partly the contact to the floodplain, a general problem at constructed rivers.
At the time of this study no geological borehole information on this region of the Enziwigger was available.

2.2 EMI

EMI has been an established tool for subsurface characterization for several decades due to its feature of quick and noninvasive mapping of large areas (McNeil 1980, Triantafilis and Lesch 2005, Robinson et al. 2009). For the car-borne EMI survey we used EM38DD and EM31MK2 devices (Geonics Limited, Mississauga, Ontario Canada) in horizontal and vertical dipole coil configurations. Thereby we obtained the following integral values related to 0.75 m - EM38 horizontal (EM38h), 1.5 m - EM38vertical mode (EM38v), 3 m - EM31vertical mode (EM31h) and 6 m - EM31vertical mode (EM31v). The pseudo depth PD means approx. three-quater of the response signal originate from the soil above – see details in McNeil 1980. Both EMI units were used in conjunction with a GPS system and were fixed on top of sledges at heights of 0.4 m and 0.1 m above ground, respectively and pulled by an all-terrain vehicle. The recording frequency in this study was 5 Hz, track pitch approx. 3 m and the vehicle drove with a speed of at most 10 km/h. Accuracy of the GPS was <0.1m.
Despite proper device calibration according to the manual negative signal values were obtained in the EM38h signal. Negative values can occur if the calibration point, the point where the instrument is set to zero, has a higher conductivity than other parts of the test site. This limits the scope of the informational absolute value of the results, in particular for monitoring studies, because further calculations with absolute values will not lead to useful results. These drawbacks are well known in the geosciences community and are still in discussion. The European Committee for Standardization has currently devised a schedule for standardization of EMI near-surface survey information and investigation (CEN 2010). Owing to these problems we consider relative EC values for revealing structural information only. Figure 3 shows interpolated EC maps with a clear N/E- S/W structure and variable depth profile of electric conductivity (EC) with relatively lower values in the near surface and higher values in the deeper areas.

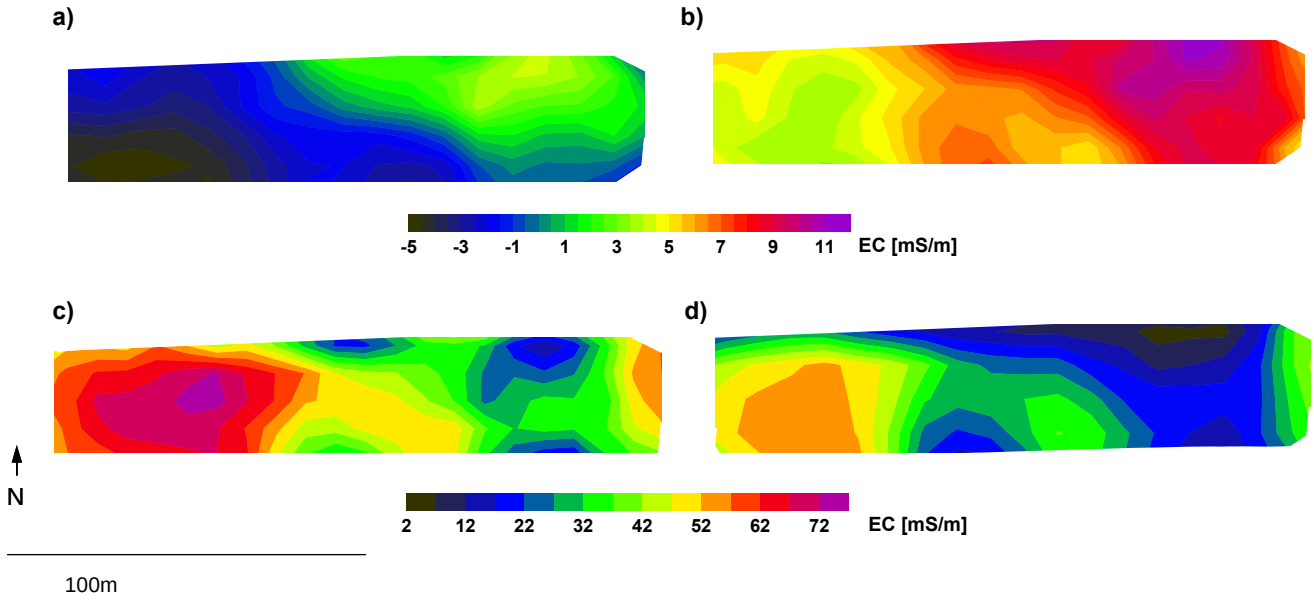

Figure 3 Contour maps of electromagnetic induction (EMI): a) EM38h, b) EM38v, c) EM31h, d) EM31va clear N/E-S/W structures and variable depth profile of electric conductivity (EC) with relatively lower values in the near surface and higher values in the deeper areas (note the differs scales).

2.3 Gamma-spectrometry (GS)

Gamma-spectrometry (GS) is a method to measure upper soil composition due to its dependency on the mineral content (Pracilio et al.2006, Viscarra Rossel et al. 2006). In a gamma spectrometer natural γ–radiation emitted from elements in the upper soil hits a sodium iodine crystal that triggers an electric impulse depending on the energy of the impact (see details in IAEA 2003.) The technical setup of the gamma survey in our study was similar to the EMI measurements. We used a GSCar gamma spectrometer with 512 5.66 keV channels and a total measuring range from 100 keV to 3 MeV and a recording frequency of 0.2 Hz. From the recorded energy spectrum we extracted the signals related to potassium (K) (range of 1.370–1.570 MeV), uranium (U) (range of 1.660–1.860 MeV) and thorium (Th) (range of 2.410–2.810 MeV) as well as the sum of these three signals, in the following called dose rate (DR) as the common gamma unit. These chemical elements (K, U, Th) can offer insight into soil properties, e.g. clay content (Wong & Harper 1999, Taylor et al. 2002, Wong et al. 2008). Figure 4 shows the interpolated result maps with clear distribution structures.

In general the γ–values increase in the western part with lowest values in the northeastern edge – see the sum signal DR in Figure 4d). However, while the K and Th maps show a higher peak in the middle of the test site, the U values increase considerably towards the South.

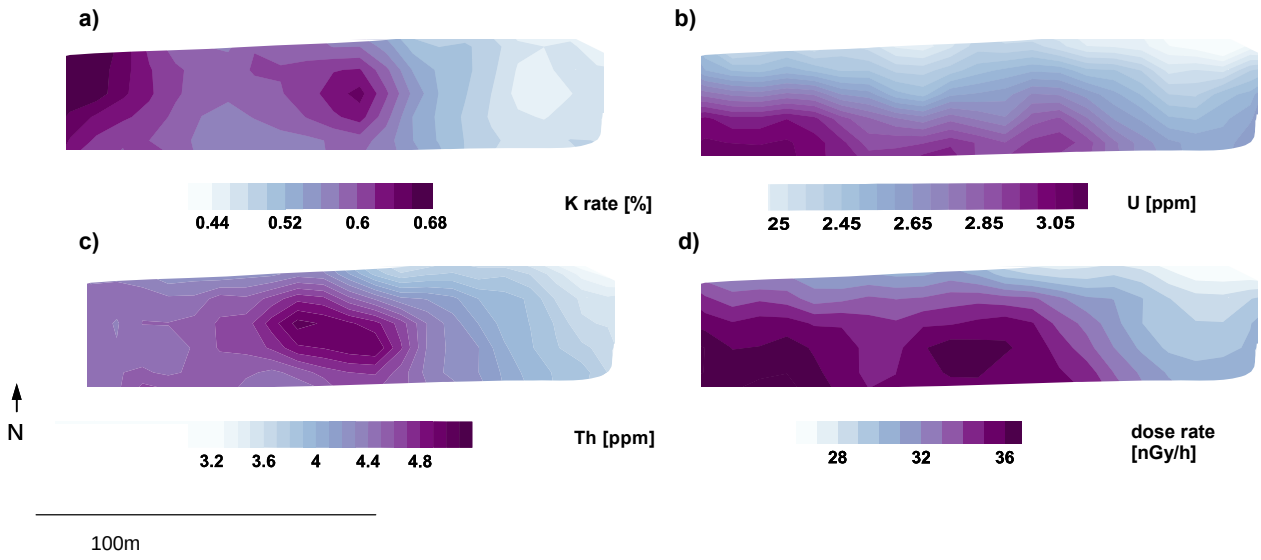

Figure 4 Contour maps of gamma-spectrometry (GS): a) K, b) Th, c) and d) Dose rate (DR), In generally the γ–values increases in the western part with lowest values in the north-eastern edge – see the sum signal DR in Figure 4d)

3. Computer based methods

3.1 Modelling approach

We derive the geological structure model (GSM) model iteratively by means of an EC modelling approach. Thereby, we use the geophysical survey data for generation of different synthetic geological input data for an EC forward modelling program. The input parameters were varied until the predicted EC maps fit the measured EC values. The geological input settings of the best fitted map were used for the generation of the final geological structure model.

For EC forward modelling we use a modified version of the 1.5D program SYNDATA (University of Technology Delft / NL 1995, Van der Krug 2000). SYNDATA is based on the response function of EMI devices (McNeil 1980) and can predict resistivity at a point on the surface of a horizontally stratified half-space based on multilayered resistivity values below. Fixed parameters in the modelling process are coil distance, measuring frequency and mode (vertical or horizontal) of the EMI metre. As input data SYNDATA requires information about the subsurface layers. These free parameters are number, thickness, and resistivity of the subsurface layers and are being iteratively changed during the modelling process.

For generation of multi-layered (3D) EC predictions we modify the SYNDATA program in a way that allows the modelling of unlimited 1.5D input data and its subsequent allocation to spatial coordinates and various pseudo depths (PD). In doing so, we obtain predicted EC values of four different 2.5D maps equivalent to the PD maps of the measured data. Now we compare the structure of the predicted with the measured EC map and adjust iteratively the input data until

the best fit is reached. The input parameters of the best fitted EC model were used in the final geological structure model for a 3D delineation of potential ancient active channel zones.
The modelling workflow can be divided into the following items: (*i*) definition of measuring device(s) (*ii*) definition of number of layers, (*iii*) definition of layer thickness, (*iv*) definition of layer EC condition, (*v*) evaluation of synthetic EC maps by iteration, and (*vi*) generation of the GSM.

3.2 Cluster approach

A cluster analysis groups data according to their similarities and reduces the data to its significant characteristics. This method is a functional tool for the allocation of multidimensional data sets and has been in use in the geosciences for more than a decade (Irvin et al. 1997, Dietrich et al. 1998, Paasche et al. 2010). In this study we use K-means clustering with Euclidean distance (Dietrich and Tronicke 2009, Altdorff and Dietrich 2011). It partitions *n* observations into *k* clusters. The mathematic principle of a K-means cluster algorithm is to minimize the total sum Φ of squared deviations from the cluster mean for all considered variables for a predefined number of clusters (MacQueen, 1967). The Euclidean distance is the most common distance function, usually the default setting in cluster programs and practical for multi-dimensional data sets (Munkres 2000, Søvik and Aagaard 2003). The Euclidean distance needs normalized variables to avoid an overweighting of higher values. Therefore we normalize all variables *v* to a comparable data range with 0.00 as the smallest value and 1 as the biggest value.
After normalizing we use all available hydro-geophysical field data as well as the topographic altitude (Topo) as input for the cluster algorithm towards a partitioning of the floodplain surface.
For cluster assignment we use the software SYSTAT 12 (Systat Inc. 2007).

4. Results and discussion

4.1 Modelling approach

We defined the coil space and the frequency (*i*) according our EMI devices with 1 m, 17000 Hz (horizontal) / 14000 Hz (vertical) for the EM38DD and 3.66 m, 9600 Hz for the EM31MK2. Regarding the unknown subsurface situation we reduce the geological units to three (*ii*) in order to keep the calculated results manageable.
The definition of layer thickness (*iii*) and layer EC condition (*iv*) are crucial for the EC results and therewith for the deduced geological model and demands a sense of possible proportions. Given that no geological information was available for the test site, we first estimate the depth of the layers from the measured EMI information by assuming the measured EC signal corresponds to the thickness of the corresponding layer only. This certainly does not reflect the natural conditions for all test site regions. However a simplification is necessary for the initial model. In doing so, we derive the depth of the first layer from the EM38v signal and analogously the second layer from the lager EM31 signal. As potential thickness we define a range between approx. 0.5 and 1.80 m for the first layer and 1.3 and 2m for the second (its adequate to a depth of approx. 1.75 to 4m). These depths corresponds approximately to the investigation depths of the

respective EMI devices and their measuring configuations. We also use in addition to the EM31 all gamma results for generation of model parameterization towards similar layer thicknesses.
After defining the layer thickness (*iii*), the definition of layer EC condition (*iv*) was concerned. As basis for the adjustment of the EC conditions we strongly simplify conductivity of the layer as quasi-homogeneous, it means we determine just one EC value for the whole layer. Then we successively manually change the EC value in steps of 2 and 5 mS/m from low (2 mS/m) to high (70 mS/) for each layer. Each model was used for the prediction of all four different EC integrals according to the real measured data of EM38h, EM38v, EM31h, and EM31v. Regarding the effort of manual input changes, we optimize the adjustment of input parameters in respect to the obtained results towards the best fitting. We run SYNDATA with approx. 120 different geological input properties.
During the evaluation of synthetic EC maps by iteration (*v*) the predicted maps were compared with the measured maps. The best fit was reached, if the synthetic EC maps show the best structure approximation to the measured EC data. Thereby the main characteristics of the measured EC maps should be described by the synthetic EC maps. Regarding the difficulties of measuring absolute EC values and their comparability, in particular with data of different EMI devices, reproducibility of the measured absolute data was not aimed for.
In addition to the structure adjustment, the coefficient of determination (R^2) was estimated. In respect to the shifts between estimated and measured EC values we regulate the model results by normalization of the predicted values to the data range of the corresponding measured data.
The following input variables show the best fitting: 1st layer thickness generated by the EM38v signal* 0.16 with EC 10 mS/m; 2nd layer thickness generated by the potassium signal* 3.0 with EC 2 mS/m and the 3rd layer (no thickness limitation needed) with EC 30 mS/m.
Figure 5 and 6 show the comparison of predicted and measured EC distribution.

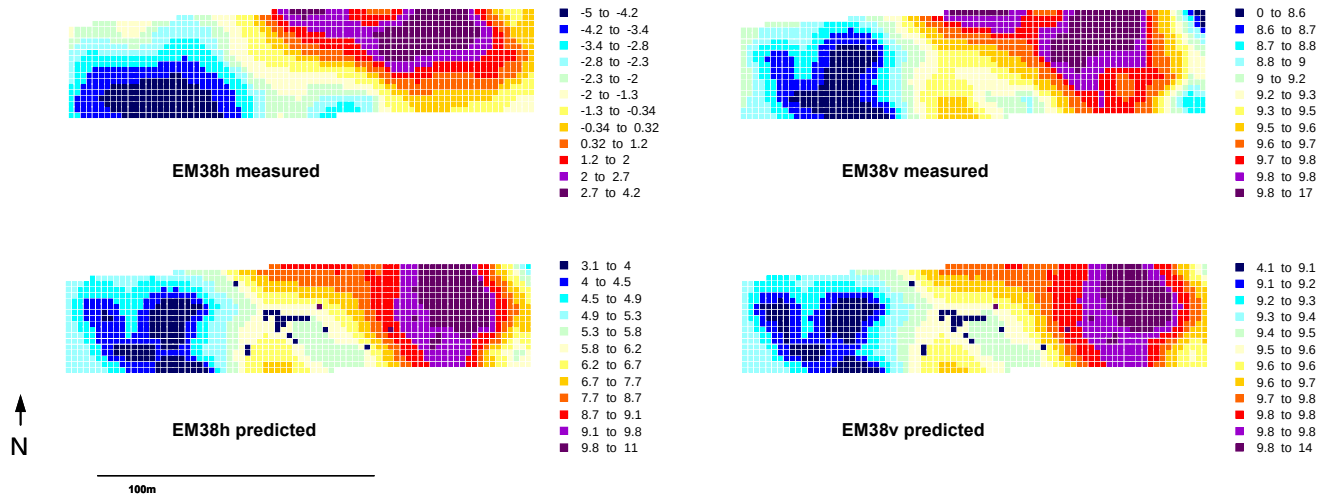

Figure 5 comparison measured vs. predicted EM38 maps, above the measured data, below the corresponding prediction; note that each color scale is different and shows equal numbers in order to allow a visualisation of structural information

Although the data range clearly deviates from the measured values, all four estimated maps reflect the main characteristics of the survey maps (except some technically caused outliers).
The EM38 predictions in Figure 5 fit the measured maps better, probably due to the deriving of the upper soil parameters from the measured EM38v signal. Both predicted maps only vary marginally in their structure. However, considering the data ranges the predicted EM38h map is slightly lower than the EM38v and follows the trend of the measured maps. For all predictions in this model the coefficient of determination (R^2) between measured vs. prediction is much higher than in any other model, in case of EM38 0.795 - EM38h and 0.814 - EM38v.

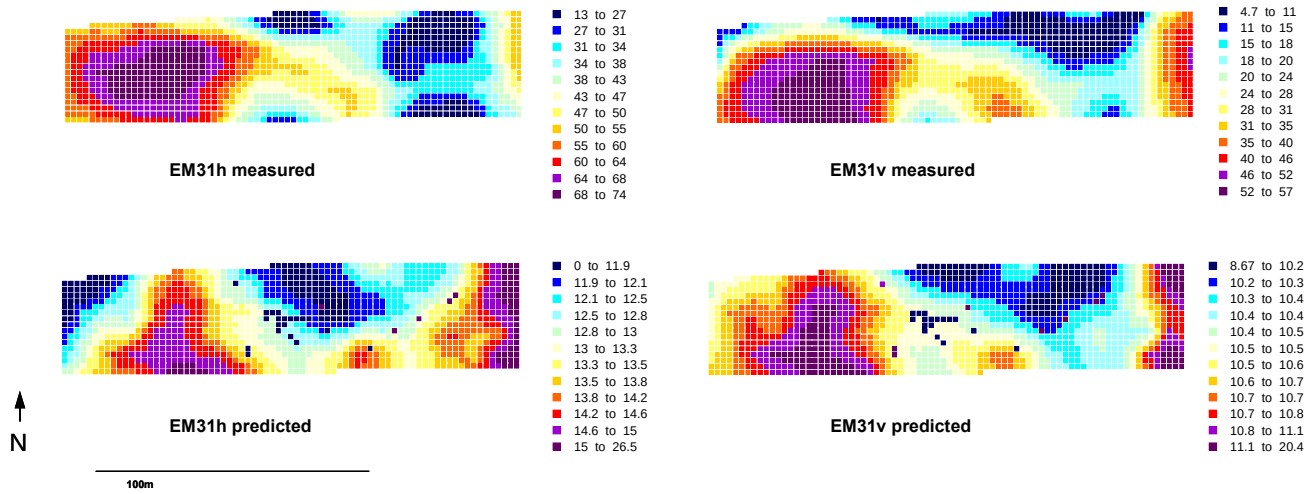

Figure 6 comparison measured vs. predicted EM31 maps, above the measured data, below the corresponding prediction; each color scale is different analogue to Figure 4

Concerning the EM31 maps in Figure 6 the deviation of the structure prediction is evidently higher; in particular in the south-western part the oval higher area is deformed. Nevertheless, the main characteristics agree in both predictions as well as the trend of the data ranges; the EM31h data range is higher in the measured and modelled map. The coefficient of determination (R^2) for the EM31 maps are 0.642 - EM31h and 0.783- Em31v.
The input properties from this model are used for the final geological structure model (*vi*). Basis for the topography of the surface (Topo) interpolation builds the GPS data from the field surveys. From the interpolated surface altitude (in m above sea level) the first and second layer was subtracted and its surface interpolated analogue to the altitude. The thickness of the third layer in SYNDATA is infinite and does not need a limitation. Finally the layers were overlapped for the 3D structure model, as basis for profiles and further visualisation (Figure 7)
Regarding the electrical properties of the model we assume the 1st layer (10mS/m) consists of silt and sand as well as clay; the 2nd layer (2 mS/m) of sand and gravel and the 3rd layer (30 mS/m) consists of clay and silt.

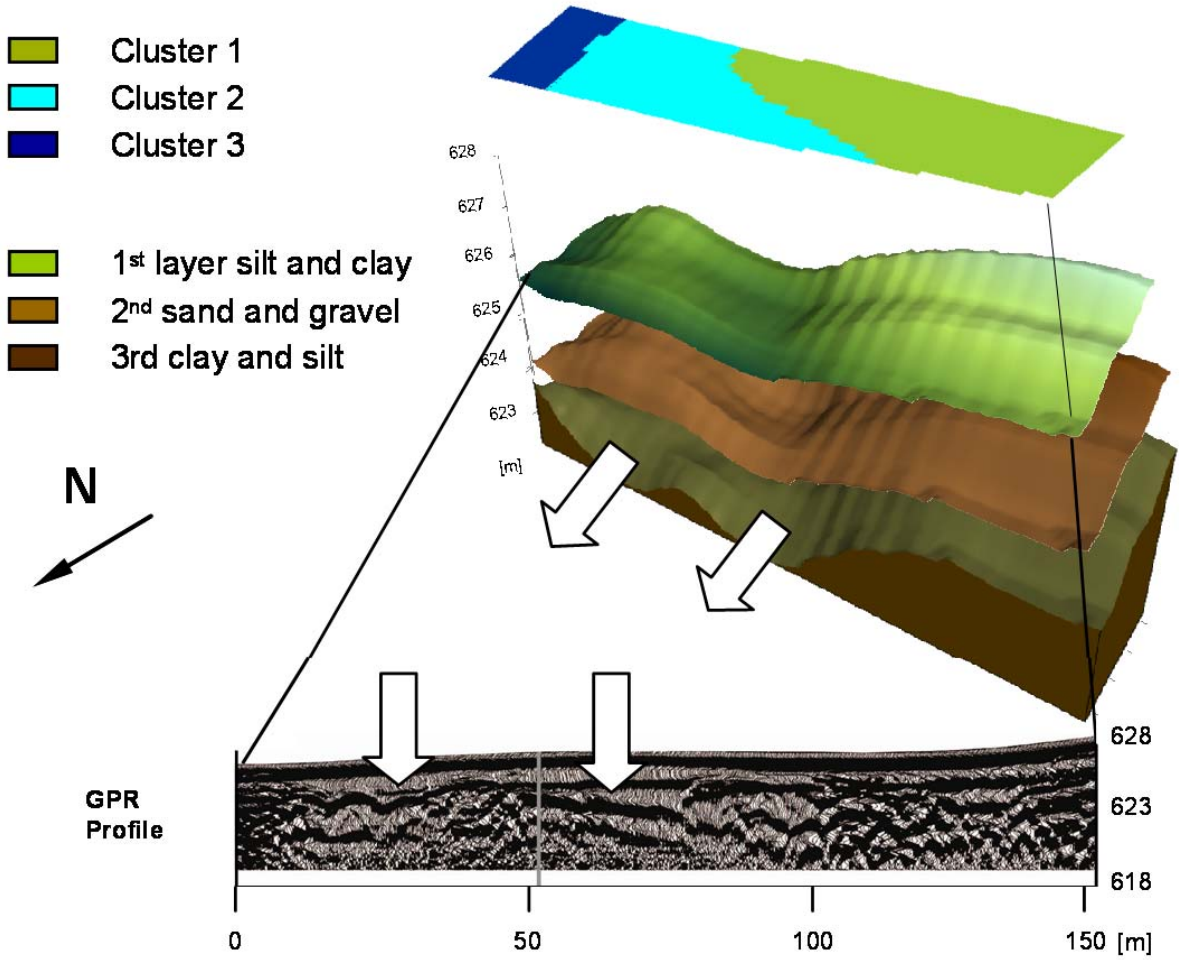

Figure7: Results of the iterative procedure of floodplain modelling by synthetic EC maps and a GPR-profile: Simplified three layer GSM, upper layer (1st) silt and clay, middle layer (2nd) sand and gravel, and lower layer (3rd) clay and silt; the GPR shows following a relatively homogeneous upper layer two significant depressions which correspond with the 3rd layer depression of the GSM; and potential AAC zones (white arrows); above the cluster map with 3 partitions.

4.2. Cluster approach

Purpose of the second approach is to combine the main characteristics of multilayered subsurface data to a simplified 2D surface partitioning map (Altdorff and Dietrich 2011). This map should distinguish zones of potential LAP and zones outside of it. For clustering we use the following input variables, EM38h and v, EM31h and v, K, U, Th and topography. Although we obtain four partitions according to the elbow criterion we decide to limit the cluster map to three clusters. As a consequence, we obtain a clear and reasonably partitioned map with significant distinctions that is also appropriate with respect to manageable land use recommendations.

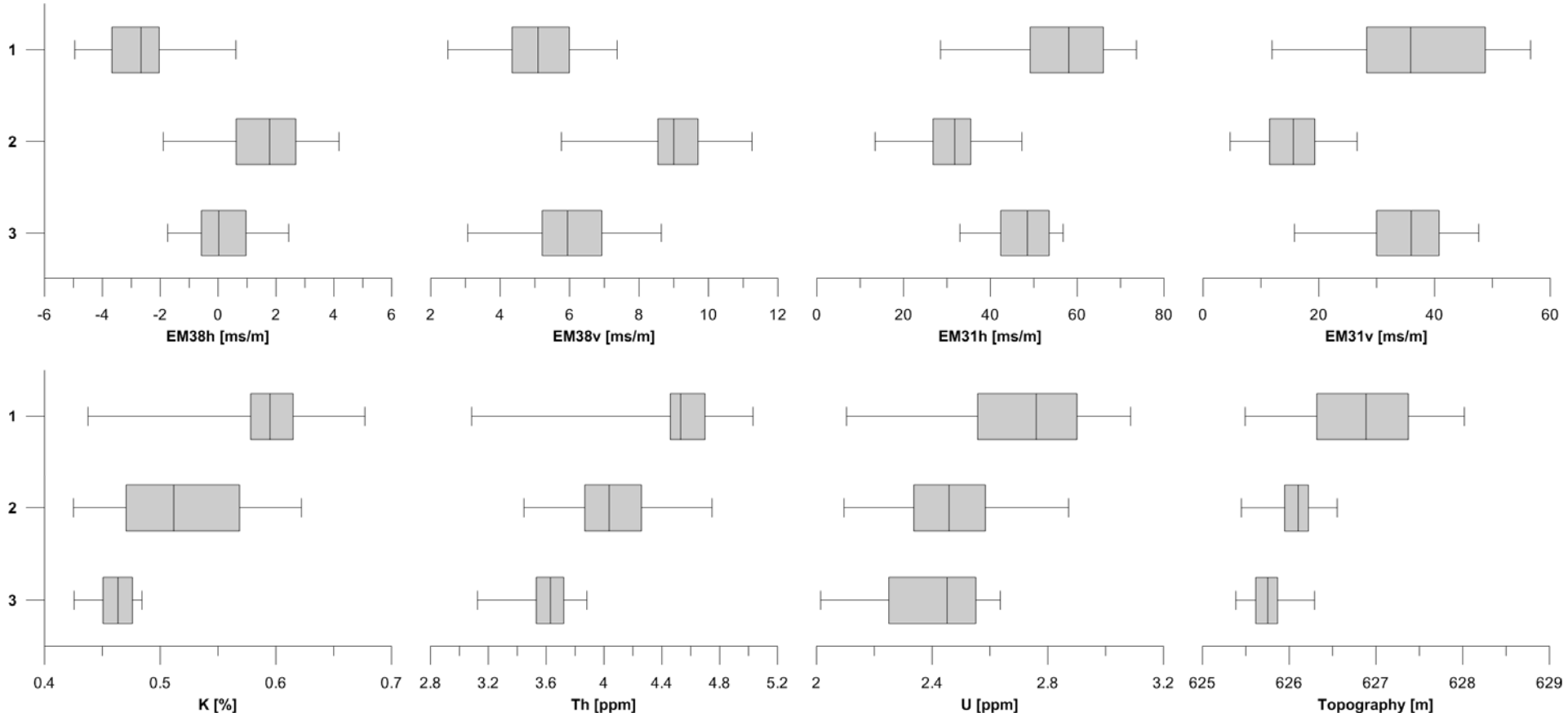

Figure 8 Soil properties of the defined three clusters (y-axes): above the EC of EM38h, v, EM31h and v, below the Gamma values as well as topography (m above sea level); whiskers indicate the total range, top and the bottom of the box show the 25th and 75th percentiles, and the line inside the box is the median val

Figure 8 shows the box-and-whisker plots of the estimated cluster and its corresponding variables. Cluster 1 dominates by the lowermost EM38 and highest EM31 data, highest K, U and Topo values and the majority of upper Th values. Cluster 2 contains the highest EM38, lowest EM31 data and medium gamma values as well as the majority of the lowest Topo data. The characteristics of cluster 3 are not as distinguished as cluster 1 and 2, it contains the lowermost Topo and gamma values, the contingent on other variables are proportionately low.
Concerning the result map Figure 7, a clear deviation with continuous clusters is visible, cluster 1 comprises the area afar from the current river stream (in this view the right side), cluster 2 the middle part and cluster 3 the riverside. Regarding the corresponding properties cluster 1 might descript a lesser hydrologically active area that probably little related to the ancient active channel zone. Indication therefore is e.g. the high EM31 values as potential result of a thicker fine grainy layer in the deeper subsoil. Opposite to that, cluster 2 could describes an area with higher likelihood of an ancient active channel zone. Here, high EM38 values can be a result of a re-sedimentation and lowest EM31 data an indicator of a lower conductive layer in the deeper subsoil probably caused by a thicker sand and grain layer. Cluster 2 also comprises the majority of minor Topo data. We interpret this part as a possible ancient active channel zone with higher potential hydrological connection. Finally, cluster 3 describes the riverside with lowermost Topo and gamma values. This part could be artificially affected by replacing of the river. An assessment of the hydrological relation for this cluster is not certain from the available data. However the striking distance to the river gives reason to the assumption of good hydrological connection.
Regarding selective management options for a reduction of the anthropogenic effect a distinction between cluster 1 and 2 is recommended. Due to the assumption of a potential LAP at cluster 2, this obviously more connected subsurface is more flood-prone and not recommended for house building. In addition, this part should as little as possible be treated with fertilizers and pesticides. Area of cluster 1 in contrast seems more flood robust and is rather acceptable for agriculture applications. The part of cluster 3 is very close to the current river and from this point improper for intensive use or house building

4.3 Validation of results

For an independent validation of the results we use a ground penetrating radar (GPR) profile that crosses the whole test field. We use the georadar system pulseEKKO Pro with a transmitter (Sensors & Software Inc.) for three 2D reflexion profiles and one common mid point (CMP). The profile comprises a length of 190 m and was measured by a 50 Hz antenna with 1 m distance. We situated it in the northern border of the test site. The data was processed and elevation corrected by the program Reflex-Win (Sandmeier Software 2010).
The comparison of the geological structure model with the GPR profile shows considerable similarities (Figure 8). The GPR profile shows two significant depressions with nadirs at approx. 25 m and 65 m corresponding to the depressions of the structure model. In relation to the electrical properties of the model layers we interpret these depressions in the lowermost layer as indication for a potential ancient active channel zone filled with sand and gravel (2^{nd} layer). Also the increas of the thickness of the 3^{rd} layer towards west (in Figure 7 the right side) is confirmed in the GPR profile by the decreasing trend of reflex horizon. Thus we assume the GSM delineates the main characteristics of the floodplain subsurface.

The GPR profile also verifies the partitions of the cluster map. As can be seen in Figure 7 the channel structure of the profile is described by cluster 2 (pale blue) bordered by clusters 1 and 3 as potential ancient riversides. Therewith also the partitioning of the 2D cluster map can be confirmed.

5. Conclusion

Purpose of this study was the exploration of the natural characteristic of part of a relocated low mountain river. We investigated the subsurface of a part of the floodplain above the potential ancient active channel region (AAC). Thereby we used non-invasive hydro-geophysical methods towards the delineation of the AAC zones as the crucial area for further restoration and management issues. A connection between the AAC and the present river could lead to the best restoration potential. In addition, reliable information about the AAC and its involved morphological units provided an assessment of the dimension of the potentially effected process scale. We employed two approaches. In the first approach we obtained a 3D structure model by means of an iteratively EC forward modelling which distinguishes three layers with different properties. The form and dimension of the layers as well as the related EC values gave indication for more hydrological active parts and so consequently for the ancient active channel zone.
In the second approach we partitioned the floodplain surface according to the multilayered subsurface to distinguish areas of different hydrological properties by a K-means clustering. We obtained a map of three different partitions. These partitions were characterized by significant differences of soil properties between and similarities within them and reflected parts of different hydrological properties. Therewith areas of higher and lower flood vulnerability as well as higher and lower river affection were distinguished for land use recommendation.
Both approaches could be confirmed by a validation of independent GPR data. The comparison of the results with the GPR profile showed significant similarities. Thus we assumed that both approaches lead to reliable results. While the modelling approaches provided a 3D delineation of structure information the cluster approach lead to a 2D map with clear distinction of areas above the potential ancient active channel zone. In addition to the 2D partitioning, the 3D model had the advantage of providing depth information and could therefore be used as a basis for a relocation of the modified river to its original channel.
In this study we derived the layer thickness from survey data of a snap-shot situation. Thus a distinction between temporal and average signal was not feasible. A monitoring under different weather conditions will help to distinguish the temporal, e.g. moisture signals from the geological (average) signal. Average data should increase the quality of the derived layers and hence the resolution of the structure model. However for the purpose of this study the model resolution is adequate.
Regarding the manual adjustment of input parameters during the modelling, a computer controlled automatism for best fitting, e.g. Model-Independent Parameter Estimation (PEST) could decrease the effort as well as increase the quality of the predicted maps and consequently of the final structural model. Thus upcoming software development and further studies at different test sites are desirable for the advancement of the demonstrated modelling approach.

Regarding the completely unknown subsurface both approaches discussed provide opportunities for delineating the main characteristics of soil from the near subsurface up to several meters depth.

Acknowledgements

The authors thank Jan Van der Krug for providing the program SYNDATA and Marek Mahn for the technical help during the modification, Simon Kögler for his support during the field work and Steffen Zacharias for his constructive help with statistical questions. The authors also acknowledge the Helmholtz research platform MOSAIC for providing the technical equipment. (Special thanks to John Mosquera from the University of Waterloo, Canada, for editing the manuscript.)

References

Altdorff, D., Dietrich, P., 2011. Combination of electromagnetic induction (EMI) and gamma-spectrometry using K-means clustering: A study for evaluation of site partitioning. Journal of Plant Nutrition and Soil Science, in press.

Becht, A., Appel, E., Dietrich, P., 2006. Analysis of multi-offset GPR data: a case study in a coarse-grained gravel aquifer. Near Surface Geophysics, 4(4):227 – 240.

Brierley, G. J., Frvirs, K., 2000. River Styles, a Geomorphic Approach to Catchment Characterization: Implications for River Rehabilitation in Bega Catchment, New South Wales, Australia. Environmental Management, 25(6):661 – 679.

Brierley, G. J., Frvirs, K., 2005. Geomorphology and River Management: Applications of the River Styles Framework. Blackwell Publishing: Oxford, UK, 398pp.

Brierley, G. J., Frvirs, K., 2008. River Futures: An Integrative Scientific Approach to River Repair. Island Press: Washington, USA, 328pp.

Buchanan, S., Triantafilis, J., 2009. Mapping water table depth using geophysical and environmental variables. Ground Water, 47:80-96.

Chen, J., Hubbard, S., Rubin, Y., 2001. Estimating the Hydraulic Conductivity at the South Oyster Site from Geophysical Tomographic Data Using Bayesian Techniques Based on the Normal Linear Regression Model. Water Resources Research, 37(6):1603 – 1613.

City of Willisau, 2008. Averaging flow rate measured on 13th November 2008 during a construction project in Willisau / Canton Luzern / Switzerland

Dietrich, P., Fechner, T. et al., 1998. A intergated hydrogeophysical approach to sufsurface characterizon. in: Herbert, M and Kovar, K. Groundwater Quality: Remediation and Protection, IAHS Publication, 250, ISSN 0144-7815:513-520.

Dietrich, P., Tronicke, J., 2009. Integrated analysis and interpretation of cross-hole P- and S-wave tomograms: a case study. Near Geophysics, 7(2):101-109.

European Environment Agency 2011. http://www.eea.europa.eu/themes/water [Accessed August 2011].

Gerber, M. E., Kopp, J., eds., 1994. Landeshydrologie und –geologie, Geologischer Atlas der Schweiz, map sheet 1129: Sursee.

Gewässerschutzverordnung (GSchV) 1998, Bern: Swiss Federal Council.

Huggenberger, P., Meier, E., 1993. Anwendung des Georadars in der Hydrogeologie: Erkennung von Inhomogenitäten im Hinblick auf eine quantitative Beschreibung von Stofftransportprozessen. Wasser, Energie, Luft, 5-6:119 – 123.

Huisman, J. A., Hubbard, S. S., Redman, J. D., et al., 2003. Measuring Soil Water Content with Ground Penetrating Radar: A Review. Vadose Zone Journal, 2:476–491.

Internatrional Atomic Energy Agency, 2003. Guidelines for radioelement mapping using gamma ray spectrometry data. ISBN: 92–0–108303–3.

Irvin, B.J., Ventura, S. J., et al., 1997. Fuzzy and isodata classification of landform elements from digital terrain data in Pleasant Valley, Wisconsin. Geoderma, 77:137-154.

Knapp, C., Borel, M., Attinger, V., eds., 1910. Geographisches Lexikon der Schweiz, 6th ed. Neuenburg: Gebrüder Attinger, pp. 632.

Lambot, S., Weihermüller, L., Huisman, J. A., et al., 2006. Analysis of air-launched ground-penetrating radar techniques to measure the soil surface water content. Water Resources Research, 42, W11403, doi:10.1029/2006WR005097.

Larsen, L. G., Harvey, J. W., 2011. Modeling of hydroecological feedbacks predicts distinct classes of landscape pattern, process, and restoration potential in shallow aquatic ecosystems. Geomorphology, 126(3-4):279 – 296.

Lennox, M. S. et al., 2011. Development of vegetation and aquatic habitat in restored riparian sites of California's north coast rangelands. Restoration Ecology, 19(2):225 – 233.

MacQueen, J., 1967. Some methods for classification and analysis of multivariate observations: 281-297, in: L. M. Le Cam and J. Neyman. Proceedings of the fifth Berkeley symposium on mathematical statistics and probability, Vol. 1.

McNeil, J. D. 1980. Electromagnetic terrain conductivity measurment at low induction numbers.Geonics. Ltd., Technical Note TN-6.

Munkres, J. R. 2000. Typology. Prenticent Hall Inc. ISBN: 0-13-181629-2.

Nyquist J. E., Freyer, P. A., Toran L., 2008. Stream Bottom Resistivity Tomography to Map Ground Water Discharge. Ground Water, 46(4):561 – 569.

Paasche, H., Tronicke, J., Dietrich, P., 2010. Automated integration of partially colocated models: Subsurface zonation using a modified fuzzy c-means cluster analysis algorithm, Geophysics. 75(3):11 – 22.

Pracilio, G., M.L. Adams, et al., 2006. Determination of spatial distribution patterns of clay and plant available potassium contents in surface soils at the farm scale using high resolution gamma ray spectrometry. Plant and Soil, 282:67 – 82.

Robinson, N.J., Rampant, P. C., et al., 2009. Advances in precision agriculture in south-eastern australia. Ii. Spatio-temporal prediction of crop yield using terrain derivatives and proximally sensed data. Crop and Pasture Science, 60:859 – 869.

Rohde, S., Kienast, F., Bürgi, M., 2004. Assessing the restoration success of river windenings: a landscape approach. Environmental Management 34(4):574 – 589.

Sholtes, J. S., Doyle, M. W., 2011. Effect of Channel Restoration on Flood Wave Attenuation. Journal of Hydraulic Engineering, 137(2):196 – 208.

Sivirichi, G. M., et al., 2011. Longitudinal variability in streamwater chemistry and carbon and nitrogen fluxes in restored and degraded urban stream networks. Journal of Environmental Monitoring, 13:288 – 303.

Søvik, A.K., Aagaard, P., 2003. Spatial variability of a solid porous framework with regard to chemical and physical properties. Geoderma, 113:47 – 76.

Steelman, C. M., Endres, A. L., 2009. Evolution of high-frequency ground-penetrating radar direct ground wave propagation during thin frozen soil layer development Cold Regions Science and Technology, 57:116 – 122.

SYSTAT Software . 2007. Product information. San Jose SYSTAT Software, Inc. www. systat.com [Accessed July 2011].

Taylor, M.J., Smettem K., 2002. Relationships between soil properties and high-resolution radiometrics, central eastern Wheatbelt, Western Australia. Exploration Geophysics, 33(2):95 – 102.

Triantafilis, J., Lesch, S. M., 2005. Mapping clay content variation using electromagnetic induction techniques. Computers and Electronics in Agriculture 46:203-237.

Truss, S., et al., 2007. Imaging rainfall drainage within the Miami oolitic limestone using high-resolution time-lapse ground-penetrating radar. Water Resources Research, 43(3): doi:10.1029/2005WR004395.

University of Technology Delft / NL 1995, intern technical program development by Jan Van der Krug

Van der Krug, J., et al. 2000. An apparent-resistivity concept for low-frequency electromagnetic soundig techniques. Geophyiscal Prospecting, 48:1033 – 1052.

Viscarra Rossel R.A., Taylor, H. J., et al. 2006a. Multivariate calibration of hyperspectral γ-ray energy spectra for proximal soil sensing. European Journal of Soil Science, 58(1):343 – 353.

Viscarra Rossel R.A., B. Minasny, et al. 2006b. Colour space models for soil science. Geoderma, 133(3-4):320 – 337.

Water and Rivers Comission Act 1995, Perth: Government of Western Australia.

Wong, M. T. F., Harper, R. J., 1999. Use of on-ground gamma-ray spectrometry to measure plant-available potassium and other topsoil attributes. Australian Journal of Soil Research, 37:267 – 277.

Wong, M. T. F., Asseng, S., et al., 2008. Mapping subsoil acidity and shallow soil across a field with information from yield maps, geophysical sensing and the grower. Precision Agriculture, 9:3 – 15.

Wong, M. T. F., Oliver, Y. M., et al., 2009. Gamma-radiometric assessment of soil depth across a landscape not measurable using electromagnetic surveys. Soil Science Society of America Journal, 73:1261 – 1267

Summary and Conclusion

The demand of methods to quantify and best utilize the soil's natural capital is increasing simultaneous with the world's growing population and the corresponding stress on soils (Banwart 2011). Therefore, reliable high-precision information from soil and subsoil properties are needed. An opportunity for the acquisition of reliable high-resolute soil and subsoil data is given by proximal soil sensing methods (PSS). The ability to combine noninvasive survey data with spatial information by GPS decreases the time of data collection and allows thus data acquisition from medium and large scale areas. However, all of these methods are responding only indirectly to the soil properties relevant for land use and management, e. g. soil moisture and grain size. In addition, the measured proxies can be affected by several soil properties, which can lead to ambiguous results. Hence, a recent challenge in soil science is the improvement of the reliability of PSS results towards the solution of specific questions.
The presented thesis has addressed the application and improvement of PSS results at the example of using EMI and GS at three different filed studies with different specific questions.

Part I This part considers the delineation of soil moisture pattern at a landslide affected hill slope in Vorarlberg / Austria. This landslide is triggered by infiltration of precipitation and the corresponding pore pressure changes which is related to changes in vadose zone moisture distribution (Schneider 1999, Lindenmaier et al. 2005, Wienhöfer et al. 2011). Consequently, information of spatial and temporal soil-moisture dynamics are required. The study shows the difficulties in obtaining soil moisture information from larger areas with heterogeneous topography and / or complex accessibility.
A typical approach of obtaining, the soil moisture information is given by Time-Domain-Response (TDR) and / or Frequency-Domain-Response (FDR) due to the contrast of dielectric permittivity of soil water and soil-matrix material (Jones et al. 2005, Bittelli et al. 2008). However, the application of TDR / FDR at this site has not leaded to plausible results (presumably due to the very high clay content). The study therefore uses EMI data as proxy for soil moisture and delineates spatial and temporary moisture patterns over a complex landslide affected slope.
The first study also shows that the practice of EMI monitoring is neither limited to areas with heterogeneous topography and / or complex accessibility nor by high clay contents. This is an clearly advantage in comparison to other investigation methods like ground-penetrating radar

(GPR), which cannot be applied on relative high-conductive ground. The applied EMI monitoring approach in this study is a useful process for the separation of temporal changes from stationary background. In addition, it allows for the visualization of temporal changes in three-dimensional subsurface data.

Part II This part discusses the problem of synthesis and simplification of multidimensional test-site information and its reliability. The study has shown that different survey methods resulted in different pattern of soil classification and consequently to different maps of soil properties. However, land-use management requires usually a clear partition of the ground surface. K-means clustering has been become a common tool in geosciences during the last decade (Irvin et al. 1997, Dietrich et al. 1998, Burrough et al. 2000, Moral et al. 2010, Paasche et al. 2010). *Part II* discusses the K-means clustering approach as common possibility for merging multivariate soil data and its critical validation. Therefore, EMI and gamma data from a Central German floodplain were acquired and compared with each other. Then, the multiple data were merged towards a clear partitioning of surface with a K-means cluster algorithm. The study has demonstrated that the application of K-means result in an integral map of shallow subsurface partitions that reduces and comprises the essential characteristics of the used input variables.
The study has also addressed the reliability of the generated cluster partitions by an independent evaluation. Therefore stratified randomly soil probes were takes and concerned in terms of grain size distribution and horizon thickness. The results show that not all partitions could be confirmed by independent soil samples. One of three clusters significantly differs from the others in terms of grain size distribution and horizon thickness and confirm so the reliability of the corresponding cluster delineation. The partitioning of the other two clusters could not confirmed by the considered parameters of the soil samples. A possible reason for the difficulties is very likely the influence of several factors on the measured EC, such as soil moisture, that has not been taken into account by this study. Nevertheless, one partition describes the main characteristics of soil properties, grain size and horizon thickness without any ground truth data. Thus, the demonstrated combination of PSS data with a high resolution and K-means clustering is a potential approach for cost and time efficient site partitioning. The study has also illustrated that a critical evaluation of the final map by soil sampling is nevertheless recommended. Nevertheless a site partitioning based on cluster analysis enables a selective soil sampling and thus target-orientated and efficient measures at lower time and cost efforts.

Part III has addressed the problem of effective river restoration. Since the relation of intact river conditions and positive effects on several environmental processes and their corresponding management relations have become evident, river restoration has become increasing important. Therefore, several legislation frameworks deal with river protection and rehabilitation in order to preserve the river systems and to avoid negative effects of anthropogenic actions. Nevertheless, river restoration is often planned and realized by standardized engineering and constructing aspects only and hydrogeological settings and ancient stream channels are neglected. As a result, desired outcomes of restoration projects are reduced with no significant alteration of stream conditions by simultaneously increasing costs. The key element in terms of river restoration is the estimation of the river's natural character and, subsequently, the adjustment of restoration measures. The study dealing with this problem has demonstrated the ability of EMI and gamma surveys for investigation of ancient active channel zones (AAC) at a floodplain of a low mountain river in Switzerland. As a result of this study, a connection between the AAC and the present river could have to the best restoration potential.

This part of the thesis was split into two approaches, the first approach has addressed the generation of a 3dimensional geological structure model, and the second approach has proceeded toward the 2dimensional delineation of the 3dimensional subsurface data. This approach offers the land owner or the decision makers an adaptive river protection or restoration concept with respect to the funding budget.

In the first approach the study has obtained a 3dimensional structure model by means of iterative EC forward modelling. The EC forward model requires the thickness and the resistivity of different layers and predicts the electric conductivity (EC) on surface. By comparing the structure of the predicted EC data with the measured EC data, an iterative adjustment of the input data has been possible that has proceeded until the best fit was reached. The input parameters of the best fitted model were then used for the generation of the 3D geological structure model. The model distinguished between three layers with different properties as indication of the potential AAC region. Independent results from ground penetration radar have confirmed the structure of the 3D model. The forward modelling of 3D EMI values was possible due to a modification of the 1.5D model SYNDATA (University of Technology Delft / NL 1995, Van der Krug 2000).

The second approach of *Part III* deals with the partitioning of the floodplain surface by a K-means clustering analogue to the approach described in *Part II* of this thesis. The purpose of segmentation of the multilayered subsurface was to distinguish areas of different hydrological properties. These partitions were characterized by significant differences of soil properties between the clusters and similarities within the clusters. As a result, the obtained clusters reflect

zones of different hydrological properties and are regarded as of areas of higher and lower flood vulnerability as well as areas of higher and lower river adverse effect affection in terms of land-use recommendation.

Scientific achievement

Regarding the initial problems of the thesis, the following conclusions can be drawn:

(1) How can the comparability of the absolute EMI values assured and shifts of data ranges excluded? This question addresses directly the drawback of EMI technology and is discussed in *Part I* of the thesis. As already mentioned, EC data represent integral values, which are highly sensitive to several external influences, such as temperature, solar radiation, and battery voltage. Consequently, the calibration of the EM device is complex and the reproducibility of absolute data is difficult, despite the same calibration procedure (e. g. Domsch 2004, Pellerin and Wannamaker 2005, Hayley et al. 2007, Abdu et al 2008, Santos and Porsani 2011). This fact definitely limits the area of application due to the decreased significance of the EM results, in particular for monitoring studies because for monitoring of EC values, reproducibility is curial to omit changes in EC signals (CEN 2010). *Part I* of the thesis suggests a comparability of the EMI values by normalizing of discrete single values. This has allowed a comparison of temporary soil-structuring maps and subsequent further calculation to take place. Therefore, the study suggested the filtering of the raw data with the limits of 5 – 95 % from whole range, the interpolation and the subsequent rasterization of all maps to the same grid size in order to obtain a matrix with identical coordinates (*x; y*) and their corresponding EC values. After normalization all data including those with shifts are in the same range of scale that allows a visualization with identical scales as well as further calculations even for data sets with negative values.

(2) Is a delineation of soil moisture and its spatial and temporal distribution with EMI possible? The approach in *Part I* demonstrates the delineation of spatial and temporal distribution of soil moisture under the assumption that changes in EC signal are strongly associated to changes in soil moisture. Given the relative temporal stability of properties of the soil matrix, seasonal changes in measured EC signal are caused by changing moisture conditions within the soil. Thus, the comparison of normalized EMI maps presents a potential opportunity to explore changes in soil moisture and to identify hydrological zone of different dynamics in both spatial

and temporal dimensions (see *Part I* Figure 4 as well as *Part I* Figure 7 and 8). Thereby the visualization of the standard deviation (SD) obtained from raster grid data of repeated measurements offers the possibility for identification of areas of higher and lower dynamic soil moisture changes (*Part I* Figure 4). In addition, the separation of the dynamic moisture signals from the stationary geological background by subtraction of the temporal values from the mean values is an opportunity for delineation of relative changes of each of the regarded investigation depths (see *Part I* Figure 7 and 8).
Consecutively, the delineation of spatial and temporal moisture distribution by means of EMI is possible according to the approach described in *Part I*.

(3) Are EMI and GS results able to delineate similar soil characteristics from the same test site?
Part II points out that EMI data and gamma data are basically related to each other, however, it is not a simple relationship and it depends on several variables (Triantafilis and Lesch 2005, Buchanan and Triantafilis 2009, Robinson et al. 2009, Wong et al. 2009). The study in *Part II* has discussed the problems of influence from similar soil properties on the both signals. In general, both signals could be affected by similar soil properties, for example by clay and mineral content as well as moisture content (Cockx et al.1997, IAEA 2003, Rein et al. 2004, Mojid 2007,) In particular, clay mineral can affect both signals. Several studies postulate a general positive correlation between clay content and EC signal (Hedley et al. 2004, Caroll et al. 2007, Mojid et al. 2007, Weller et al 2007), and others suggest a correlation of clay with the γ–signal (Bierwirth et al. 1996, Wong and Harper 1999, Taylor et al. 2002, Pracilio et al. 2006, Viscarra Rossel et al. 2007). In the thesis, GS is applied on two different floodplains with presumablely noticeable clay content. Consequently, similarities between both the EMI and gamma maps are expected. However the results of both studies show that significant similar soil pattern did not occur. The gamma depression shown in Figure 1 of *Part II* is indiscernible in the EMI data while increased EC values in the west are not reflected in the gamma data . Moreover, the obtained maps of EMI and GS results in *Part III* differ in its characteristics of higher and lower values (see *Part III* Figure 3 and 4). In general the γ–values increase in the western part with lowest values in the northeastern edge, inparticular the sum signal DR while the EMI values of the upper EM38h device shows almost an inverse distribution.
Although both methods could be affected by similar soil properties, the resulting maps not imperatively delineates similar soil characteristics.

(4) How can multidimensional subsurface data are combined towards a 2dimensional test site mapping and do the generated partitions really reflect the main characteristics of soil properties? The increasing number of survey methods (e. g. from proximal soil sensing) provides an increasing number of different data in high resolution, which results in multilayered and complex parameters maps . However, for most applications usually just one elementary map is required. *Part II* has discussed the opportunity of merging multidimensional data by a K-means cluster algorithm. A cluster analysis groups data according to their similarities and reduces the data to its significant characteristics. Therewith a synthesis and simplification of multivariable data is possible. Regarding the obtained results (see *Part II* figure 1 and 2) the combination of the relevant characteristics from the input variables are observable. The final map contains the E-W partitioning structure from EMI as well as the prominent gamma depression in the centre of the test site. Analogue to *Part II* in *Part III* the combination of the multidimensional input data by using an K-means clustering leads to plausible results. Figure 7 shows an evident synthesis of the 2D map from the 3D input data below (see *Part III* figure 7). In summary, a K-means clustering is feasible to combine multidimensional subsurface data.

As discussed in *Part II,* the reliability of the generated maps is directly related to the input variables, or in other words: the cluster map is only as good as the input parameters. This fact addresses the question of the reliability of the applied methods. In the presented study, a combination of EMI and GS data is used, however, for validation of the results, the following parameters were available: grain size, soil colour and horizon thickness. A validation of the partitions with EC and GS point measurements could evaluate the probability of significant dissimilarities between the clusters certainly. However, the purpose of the study was practical oriented and should evaluate the typical use of K-means algorithms in soil science. Two of three clusters could nevertheless confirmed by the independent soil properties from soil sampling.The demonstrated combination of EMI, GS data and K-means clustering is a potential approach for cost and time efficient site partitioning. However, a critical evaluation of the resulting map by soil sampling is nevertheless recommended.

(5) Could an EMI forward modeling predict the measured EMI values and the structure of four different investigation depths with just one model? The study in *Part III* shows EMI forward modeling as potential tool for iterative inversion towards subsurface characterization. The demonstrated model has successfully predicted the structure from measured EMI values of four different investigation depths. One model was able to predict the structure of the following

integral values related to 0.75 m - EM38 horizontal (EM38h), 1.5 m - EM38vertical mode (EM38v), 3 m - EM31vertical mode (EM31h) and 6 m - EM31vertical mode (EM31v). However, due to the great dissimilarities in data ranges of the measured data sets, the prediction of measured EMI values was not achieved. This problem is related to the high sensitivity of the EMI devices to influences, such as temperature solar radiation, and battery voltage. The calibration of EM sensors is complex and reproducibility of absolute data is limited, despite regular calibration (Domsch 2004, Pellerin and Wannamaker 2005, Hayley et al. 2007, Abdu et al 2008, Santos and Porsani 2011). This hampers the exact prediction of absolute EC values by means of forward modeling. In contrast to the absolute EC values, the structures of predicted maps confirms the main character of the corresponding maps from all four different investigation depths (see *Part III* Figure 5 and 6), hence EC forward modeling can predict the structures of EC maps of four different investigation depths with one model successfully.

(6) Is a reliable 3dimensional delineation of significant structures in subsurface possible by EMI and GS data only? Conventionally, the answer is no. However, the study in *Part III* demonstrates that a subsurface delineation with EMI and Gamma data is basically possible. Precondition for this is the iterative inversion of EC condition of the geological layers by forward modeling. A 3D structure model was generated that delineates the area of potential ancient active river channel. An independent validation by ground penetration radar (GPR) could confirm the significant structures of the 3D model.

In this study the layer thickness was derived from survey data just one survey day and represents a ´snap-shot situation´. Thus, a distinction between the temporal signal, influenced e.g. by soil moisture and the average signal was not feasible. Repeated measurements under different weather conditions would help to distinguish the temporal signal from the geological (average) signal according the demonstrated approach in *Part I*. The average data should definitely increase the quality of the derived layers and hence the resolution of the structure model because temporal influences on the EMI and GS signals e.g. by soil moisture could be excluded. Thus the deriving of layer thickness by means of EMI and GS signal represents more stationary conditions. However, for the purpose of the delineation of ACC, the model resolution was adequate.

Regarding the manual adjustment of input parameters during the modelling, a computer controlled automatism for best fitting, e. g. Model-Independent Parameter Estimation (PEST) could decrease the effort as well as increase the quality of the predicted maps and consequently the quality of the final structural model. Upcoming software developments and further studies at different test sites are desirable for the advancement of the demonstrated modelling approach.

Regarding the completely unknown subsurface, both approaches discussed in *Part III* provide opportunities for delineating the main characteristics of soil from the near subsurface up to several meters depth.

In summary, this thesis addresses the improvement of data evaluation and interpretation of proximal soil sensing methods electromagnetic induction (EMI) and gamma spectrometry (GS). Therefore three different test sites with three different problems were investigated and concerned. For each problem an individual adjusted approach was develop, applied and critical discussed. All developed evaluation approaches gained the information yield of the measured proxy data. Although developed under specific site conditions all demonstrated approaches offers portability and should be applied in other applications.

References

Abdu, H., D. A. Robinson, et al. 2008. Geophysical imaging of watershed subsurface patterns and prediction of soil texture and water holding capacity. Water Resources Research 44.

Bierwirth, P., S. Hardy, P. Wilson, S. Philip, D. Smith, I. Heiner, and M. Grundy. 1997. Integrating gamma-radiometrics into landscape modelling of soil attributes: Results of an ACLEP exchange. Australian Collaborative Land Evaluation

Bittelli, M. F. Salvatorelli and P.R. Pisa. 2008. Correction of TDR-based soil water content measurements inconductive soils. Geoderma 143 133–142

Buchanan, S., and J. Triantafilis. 2009. Mapping water table depth using geophysical and environmental variables. Ground Water 47:80-96.

Burrough, P.A., P.F.M. van Gaans, et al. 2000. High-resolution landform classification using fuzzy k-means. Fuzzy Sets and Systems 113:37-52.

Caroll, Z.L and. Oliver M.A. 2005. Exploring the spatial relations between soil physical properties and apparent electrical conductivity. Geoderma Volume 128, Issues 3-4, Pages 354-374

CEN - European Committee for Standardization. 2010. Best Practice Approach for electromagnetic induction measurements of the near surface, Approved Business Plan, CEN Workshop 59

Cockx, L., M., Van Meirvenne, and De Vos, B.: Using the EM38DD Soil sensor to delineate clay lenses in a sandy forest soil, Soil Sci Soc Am J, 71(4), 1314-1322, 2007.

Dietrich, P. Fechner, T., et al. 1998. A intergated hydrogeophysical approach to sufsurface characterizon. in: Herbert, M and Kovar, K. Groundwater Quality: Remediation and Protection, IAHS Publication No. 250, ISSN 0144-7815:513-520.

Domsch, H., A. Giebel, 2004. Estimation of Soil Textural Features from Soil Electrical Conductivity Recorded Using the EM38. Precision Agriculture 5: 389-409

Hayley K, L. R. Bentley 2007. Low temperature dependence of electrical resistivity: Implications for near surface geophysical monitoring GEOPHYSICAL RESEARCH LETTERS, VOL. 34, L18402, 5 PP.,:10.1029/ GL03112

Hedley, C.B., I.Y. Yule, et al. 2004. Rapid identification of soil textural and management zones using electromagnetic induction sensing of soils. Australian Journal of Soil Research 42:389-400.

Internatrional Atomic Energy Agency, 2003. Guidelines for radioelement mapping using gamma ray spectrometry data. ISBN: 92–0–108303–3.

Irvin, B.J., S.J. Ventura, et al. 1997. Fuzzy and isodata classification of landform elements from digital terrain data in Pleasant Valley, Wisconsin. Geoderma 77:137-154.

Jones S.B., Blonquist, Jr J.M. et al. 2005. Standardizing Characterization of Electromagnetic Water Content Sensors: Part 1. Methodology Vadose Zone Journal 4:1048–1058

Lindenmaier, F. Zehe, E. et al., 2005. Process identification at a slow-moving landslide in the Voralberg Alps. Hydrological Processess, 19(8):1635 – 1651.

Mojid, M.A., D.A. Rose, et al. 2007. A model incorporating the diffuse double layer to predict the electrical conductivity of bulk soil. European Journal of Soil Science 58:560-572.

Moral F.J., J.M. Terron, J.R. et al. 2010. Partitioning of management zones using mobile measurements of soil apparent electrical conductivity and multivariate geostatistical techniques. Soil and Tillage Research 106 (2010) 335–343

Paasche, H., J. Tronicke, P. Dietrich, 2010. Automated integration of partially colocated models: Subsurface zonation using a modified fuzzy c-means cluster analysis algorithm, Geophysics. 75(3). p.P11

Pracilio, G., Adams, M.L., Smettem, K.R.J., and Harper, R.J. 2006.: Determination of spatial distribution patterns of clay and plant available potassium contents in surface soils at the farm scale using high resolution gamma ray spectrometry, Plant and Soil, 282, 67-82,

Pellerin, L., and P.E. Wannamaker. 2005. Multi-dimensional electromagnetic modeling and inversion with application to near-surface earth investigations. Computers and Electronics in Agriculture 46:71-102.

Rein A., R. Hoffmann, P. Dietrich 2004. Influence of natural time-dependent variations of electrical conductivity on DC resistivity measurements. Journal of Hydrology 285 215–232

Robinson, N.J., Rampant, P. C., et al., 2009. Advances in precision agriculture in south-eastern australia. Ii. Spatio-temporal prediction of crop yield using terrain derivatives and proximally sensed data. Crop and Pasture Science, 60:859 – 869.

Santos, R.N.S. and J.L. Porsani 2011. Comparing performance of instrumental drift correction by linear and quadratic adjusting in inductive electromagnetic data Journal of Applied Geophysics 73 1–7

Schneider, U., 1999. Geotechnische Untersuchungen, satellitengestütze (GPS) Bewegungsanalysen und Standsicherheitsüberlegungen an einem Kriechhang in Ebnit, Voralberg. University of Karlsruhe.

Taylor, M.J., Smettem K., 2002. Relationships between soil properties and high-resolution radiometrics, central eastern Wheatbelt, Western Australia. Exploration Geophysics, 33(2):95 – 102

Triantafilis, J., Lesch, S. M., 2005. Mapping clay content variation using electromagnetic induction techniques. Computers and Electronics in Agriculture 46:203-237.

Viscarra Rossel R.A., H. J. Taylor et al. 2007. Multivariate calibration of hyperspectral γ-ray energy spectra for proximal soil sensing. European Journal of Soil Science, Volume 58, Issue 1, pages 343–353

Weller, U., Zipprich, M., Sommer, M., Castell, W.Z., Wehrhan, M., 2007. Mapping clay content across boundaries at the landscape scale with electromagnetic induction. Soil Science Society of America Journal 71, 1740-1747.

Wienhöfer, J., Lindenmaier, F., 2011. Challenges in Understanding the Hydrologic Controls on the Mobility of Slow-Moving Landslides. Vadose Zone Journal, 10(2):496 – 511.

Wong, M.T.F. & Harper, R.J. 1999. Use of on-ground gammaray spectrometry to measure plant-available potassium and other topsoil attributes. Australian Journal of Soil Research, 37, 267–277.

Wong, M. T. F., Oliver, Y. M., et al., 2009. Gamma-radiometric assessment of soil depth across a landscape not measurable using electromagnetic surveys. Soil Science Society of America Journal, 73:1261 – 1267